OFFICE OF NAVAL RESEARCH
CONTRACT N00014-75-C-1077
Task No. NR 105-832
Technical Report No. 1

A PREDICTION OF RESPONSE OF THE HEAD AND NECK OF THE U. S. ADULT MILITARY POPULATION TO DYNAMIC IMPACT ACCELERATION FROM SELECTED DYNAMIC TEST SUBJECTS

by

L.W. Schneider
B.M. Bowman
R.G. Snyder
L.S. Peck

Highway Safety Research Institute
The University of Michigan
Ann Arbor, Michigan 48109

May 1976

strength. These latter measurements were taken in both the sagittal and lateral planes.

Measurement results were used to establish parameter values for the MVMA-2D Crash Victim Simulator data set in an attempt to reproduce the dynamic response of these volunteers to $-G_x$ sled acceleration at 6 and 15 G's. Procedures used for computing the various parameter values and comparisons between predicted and experimental results are presented. In addition, measurement data for 18-24 year females taken previously have been utilized to predict the dynamic response that would be expected if these subjects were tested at 6 and 15 G's.

Further work in studying the significance and relation of various physiological and biomechanical parameters and of stimulus and experimental test conditions to the dynamic response is planned using both modeling and correlation techniques. Measurement data for other segments of the adult population will be used to extend the NAMRL results to the general adult occupant population.

ACKNOWLEDGEMENTS

The research work reported on herein was supported by the Office of Naval Research, Medical and Dental Division and was conducted with the cooperation and supervision of the Naval Aerospace Medical Research Laboratory (NAMRL), Michoud Station, New Orleans.

The authors would like to acknowledge the professional assistance and advice offered during the past year by Dr. Channing L. Ewing, Dr. Daniel J. Thomas, and Mr. Leonard Lustick of NAMRL and of Dr. Hurley Robbins, Head, Biomathematics Department, HSRI and Dr. Don Chaffin, Professor of Industrial Engineering, The University of Michigan. The authors are also grateful for the professional assistance of Dr. Herbert M. Reynolds, physical anthropologist, HSRI, who took the anthropometry measurements, for the time and effort of those personnel at NAMRL involved with the preparation of the experimental data, and for the expert and unique talents of Dan Golomb, programming analyst, who performed all of the computer programming for data handling and graphical displays of results used in this study and report.

TABLE OF CONTENTS

LIST OF TABLES

LIST OF TABLES (CONTINUED)

LIST OF FIGURES

LIST OF FIGURES (CONTINUED)

LIST OF FIGURES (CONTINUED)

LIST OF FIGURES (CONTINUED)

SUMMARY

Physical characteristics of the head and neck were measured on 18 young adult male Navy volunteers who had previously undergone tests on the NAMRL sled facility in New Orleans. Measurements taken include 55 standard anthropometric measures, 32 anthropometric measures of the seated subject, three dimensional head and neck range of motion, neck muscles reflex times in response to head jerks, and neck muscle voluntary isometric strength. The reflex time and strength tests were performed in both the sagittal and lateral planes. The range of motion results for this group of 18 NAMRL subjects were in good agreement with results for 18-24 year males and females from the general population. In the sagittal plane, the average range of motion angles in extension were 79.0 and 60.5 degrees respectively as measured from the Frankfort Plane position. Reflex times were similar for flexion, extension, and lateral bend, being 53.5, 55.5, and 51.5 msec respectively. In strength, the group of NAMRL subjects was similar to 35-44 year males of the general population. The greatest strengths were in extension where the average is about 33% greater than in flexion or lateral bend.

Where appropriate, these measurement results for 5 of the 18 subjects were utilized in establishing a data set for the MVMA-2D Crash Victim Simulator. Simulations of NAMRL sled tests at -Gx impact accelerations of 6 and 15 G's were made using either the experimental T_1 accelerations as input to the neck or experimental sled acceleration profiles as input to the sled. Simulation results for head angular acceleration, head angular velocity, head angular position, head resultant acceleration, and T_1 resultant acceleration are compared with average experimental results out to 300 msec for the group of five

subjects. Results to date indicate reasonably good agreement between experimental and simulation curves at both 6 and 15 G's. Further work is needed, however, to improve certain aspects of the model such as joint stop characteristics, passive tissue modeling, and restraint system modeling. Effects of changing muscle tension, chest compliance, joint stop stiffness coefficients, and upper torso joint stiffness (i.e., amount of torso flexion) have also been examined using the MVMA-2D model. Results obtained with varying amounts of muscle tension indicate that muscle effects are more predominant at 6 G's than at 15 G's.

Simulations for 18-24 year females at 6 and 15 G's were made using measurement data obtained in previous studies at HSRI. Results were not dramatically different from the NAMRL simulations, the primary difference being an increase in the maximum flexion angle of the head by about 40 and 25 percent at 6 and 15 G's respectively.

Chapter 1

INTRODUCTION AND OBJECTIVES

A. Statement of Project Goal

Measurements of dynamic responses to impact accelerations which have been taken on a selected male military population at the Naval Aerospace Medical Research Laboratory (NAMRL) at Michoud Station, New Orleans, represent the most comprehensive source of information available related to the dynamic response of the human head and neck. To what extent these data represent the total adult U.S. population is unknown, however. In recent studies sponsored by the Insurance Institute for Highway Safety (IIHS) and conducted by the Highway Safety Research Institute (HSRI), basic information which is believed to be representative of neck physical characteristics for the adult U.S. population from 18 to 75 years has been obtained. Included in these data are anthropometry, head/neck range of motion, neck muscle strength, and neck muscle reflex time measurements. The primary purpose of this study is to determine to what extent these data may be used with mathematical modeling techniques in order to extend and project the NAMRL dynamic response results to the general adult U.S. population.

B. Background

Response of the human head and neck to impact accelerations is a matter of major concern in the design

---

The rights, welfare and informed consent of the volunteer subjects who participated in this study were observed under guidelines established by the U.S. Department of Health, Education and Welfare policy on protection of human subjects and accomplished under medical research design protocol standards approved by the Committee to Review Grants for Clinical Research and Investigation Involving Human Beings, Medical School, The University of Michigan.

of biomechanical models, anthropomorphic dummies, and occupant crash protection devices.

There are a large number of studies which have attempted to determine the relationships of head injury and concussion to impact forces, but only recently has attention been given to the respective influences of the effects of head motion upon injury. It is still unclear what the respective effects of rotational and translational forces may be. Results of experiments reported by researchers such as Holbourn (14), Pudenz, et al. (19), Martinez (16), and Ommaya (18) have indicated that rotation alone can cause brain injury and concussion in whiplash. However, Hodgson (13), Gurdjian (12) and others contend that other factors such as resultant intracranial pressure gradients may cause trauma by high shear stress concentration in the brain stem and upper spinal cord. Young, et al. (26) have recently demonstrated concussion to the fixed primate head without translational movement. Clarke (4), studying human volunteers in dynamic tests of adult males at peak sled velocities of 26.2 ft/sec and 7.8 to 10 G, concluded that peak head angular accelerations and linear resultants may have less traumatic consequences than the degree of head-neck hyperextension.

This disagreement among researchers as to the mechanisms of injury in head impact and whiplash is also seen in consideration of critical values of rotational velocity and acceleration at which concussion occurs in man. Recent work by Ewing and Thomas (8) using male human volunteers in dynamic sled tests found no clinically observable effects. due to acceleration on a subject in which the peak mouth angular velocity exceeded 30 rad/sec (at 10 G, 250 G/sec), although this level had been previously considered by Mahone, et al. (15) and Ommaya to be the critical level for human concussion.

Similarly, although there has been considerable effort to realistically simulate the human neck in various versions of an "improved" anthropomorphic dummy, the lack of valid human bioengineering data has remained a major problem and much controversy in this area continues.

Thus the continuing series of impact acceleration tests being conducted by Ewing, et al. (5-10) using human volunteer subjects have been of particular significance since this effort has resulted in an extensive body of kinematic experimental data under dynamic conditions. This work, which has involved precise measurement of the complete input acceleration to the head and neck (measured at the first thoracic vertebra), precise measurement of the dynamic response of the head and neck to the input acceleration, and development of data acquisition and automatic processing systems, must be characterized as producing the most extensive dynamic data using the most sophisticated experimental techniques and precise instrumentation to date for the impact range under study.

Primary objectives of the NAMRL research effort are to acquire data that can be used to 1) develop design criteria for construction of dummies which will closely reproduce man's response to crash acceleration , and 2) define the envelopes of impact acceleration which result in the injury. If these results are to include concern for the total population who may be involved in crash situations in both military and non-military vehicles, then it becomes important to be able to extend these dynamic response data to the general U.S. adult population.

In two studies by Snyder, et al. (22,23) and reported by Foust, et al. (11) and Schneider, et al. (21), basic data concerning physical characteristics of the head and neck were obtained on a sample of subjects designed to represent the adult vehicle occupant population. These

studies were, to our knowledge, the most comprehensive attempt to relate such physical measurements such as muscle isometric strength, muscle reflex time, cervical range of motion, and anthropometry to the age, sex, and stature of a population representative of U.S. adults.

While subjects were tested in both sagittal and lateral planes, the general relationships of the measured physical characteristics to age and sex were the same in both. Cervical range of motion was greatest in the rotational plane and smallest in the lateral plane, and showed an average decrease with age of 20-45 percent from young to elderly subjects. Neck muscle reflex times ranged from about 30 to 75 msec, were generally smaller for lateral head movements, showed an increase with subject age, and were slightly shorter on the average for females. Muscle strength was found to be about 33% greater in extension than in flexion or lateral bend, showed a decrease with age, and was on the average 1-1/2 to 2 times greater in males than in females. No significant correlations between these measurements and subject anthropometric measures were found.

A basic assumption underlying the application of these data to studies on human impact tolerance is that there is a relationship between the differences in physical characteristics of individuals and differences in dynamic response to impact. If this assumption is valid, a potentially productive research program would involve bridging the gap between the dynamic studies of a highly selected population on the one hand, and the essentially static measurements representative of the U.S. adult population on the other. The present study was undertaken out of these considerations.

C. Objectives

In order to accomplish the goals of this study, two principal objectives must be achieved. First, it must be shown that the static measurements can be utilized in a mathematical model to give accurate simulations of experimental impact results, and that this validated model can be used across a range of impact accelerations and conditions. Secondly, it must be demonstrated that reasonable correlations exist between measured physical properties and experimental dynamic response characteristics. In order to attain these objectives, the following tasks were established.

1) Conduct all of the HSRI sagittal plane and lateral plane testing on a group of NAMRL subjects who have previously undergone acceleration impact testing over a range of acceleration levels. Data collected would include standard anthropometry, seated anthropometry, three dimensional voluntary range of motion of the head and neck, neck muscle stretch reflex times and acceleration in response to head jerk, and maximum voluntary neck muscle isometric strength.

2) Compare NAMRL measurement results with results from the U.S. adult population obtained in the IIHS sagittal and lateral plane studies (11, 21).

3) Use the NAMRL measurement results to establish parameter values where appropriate in the data set of the MVMA-2D Crash Victim Simulator.

4) Run the MVMA-2D model with this data set, appropriate initial conditions, and stimulus inputs in an attempt to reproduce the experimental results from NAMRL subjects at several acceleration levels. Adjust or "tune" other parameters for which no data are available in order to obtain optimal matching to experimental curves.

5. Determine if and when any relationships exist between static measurements and dynamic response, and confirm that these relationships are supported by the model by:

a) correlating various static measurements with various peak parameter values in experimental response curves for the group of NAMRL subjects measured.

b) examining changes in response curves for subjects with different physical characteristics and using these different measurements in the model to see if the changes are predicted.

6. Use the measurements obtained in the IIHS studies to predict the dynamic response results that would be obtained if other segments of the population were tested at the NARML sled facility.

7. Use the validated MVMA-2D model to predict the response of occupants subjected to more realistic and practical crash situations.

8. Use the validated MVMA-2D model to predict the response of NAMRL subjects to sled tests where the acceleration vector is of a greater magnitude than can be safely used with volunteer subjects.

At the time of this report, tasks 1 through 3 have been completed for a group of 18 NAMRL subjects who have undergone sled tests up to 15 G's in the -Gx direction. Considerable progress has been made with task 4 although further work and improvements in the model are needed. Measurement procedures and results are presented in Chapter 2 while Chapter 3 describes the procedures and results to date concerned with tasks 3 and 4. Chapter 4 gives the results obtained by using the IIHS data to predict sled test responses at 6 and

15 G's for 18-24 year females (task 6). Chapter 5 contains a brief discussion of the results to date and suggestions for future work on tasks 4 through 8.

Chapter 2

MEASUREMENT OF PHYSICAL CHARACTERISTICS

A. General

Eighteen male Navy personnel who had previously undergone testing on the NAMRL sled facility were brought to the Highway Safety Research Institute (HSRI) for two to three days for measurements of physical characteristics related to the head and neck. The subjects were brought to HSRI in three groups of 7, 6, and 5 over a period of one month. They were assigned subject identification numbers consisting of a prefix code denoting the sex, age, and stature of the individual and a chronological testing number from 1 to 18. Table 2.1 is a list of these HSRI subject codes together with the corresponding NAMRL subject number. The letter N denotes NAMRL male subject (to distinguish from others previously tested); A indicates that the subject was between 18-24 years; while S, M, and T correspond to short, medium, and tall according to the 1-20th, 40-60th, and 80-100th percentiles of stature for this age and sex.

While the immediate concern in this study was to measure those physical characteristics which relate to head and neck movement in the sagittal plane (since NAMRL sled testing is with -Gx acceleration), the capability existed from previous studies to test in lateral bending and these measurements were also taken on each subject for future use. Measurements taken include standard anthropometry, anthropometry of the seated subject, head and neck range of motion, neck muscle stretch reflex times, and neck muscle isometric strength capability. The following sections describe briefly the testing procedures used (these are discussed in detail in references 22 and 23) and also present the measurement results for this group of 18 Navy subjects.

TABLE 2.1

HSRI AND NAMRL SUBJECT NUMBERS FOR 18 NAVY SUBJECTS

HSRI	NAMRL
NAM01	H-39
NAM02	H-46
NAT03	H-49
NAM04	H-42
NAM05	H-48
NAM06	H-44
NAS07	H-38
NAM08	H-32
NAM09	H-52
NAM10	H-47
NAT11	H-51
NAM12	H-50
NAM13	H-53
NAT14	H-43
NAT15	H-35
NAM16	H-33
NAT17	H-40
NAT18	H-37

B. Anthropometry

1. Methods. A total of 87 anthropometric measurements were obtained on each subject during the initial phase of testing. Figure 2.1 is a list of these measurements divided into two groups. Group I contains 55 measurements taken by standard techniques to describe the general body characteristics, the head and neck, location and sizes of body masses, and body somatotypes. Group II contains 32 measurements taken to describe the position of the seated occupant. Of these 32, 7 were taken with standard equipment while 25 are measures taken or derived from orthogonal photogrammetry techniques. The photogrammetry setup consists of a set of three Pentax cameras oriented orthogonally to each other and aimed toward the subject from the front, left side, and top. The cameras are aligned such that the centers of their focal planes intersect at a common origin within the subject. The locations of high contrast markers placed on the subject's head and upper torso and visible in at least two cameras, may be determined in three dimensions by geometric relations and measurements from the films. The films are projected onto a tablet digitizer and the points are digitized in a specified sequence onto paper tape. The tapes are later analyzed by computer programs which compute the 3-dimensional location of the points.

2. Results. Table 2.2 presents the statistics of the anthropometric measurements for the 18 NAMRL subjects measured while Table 2.3 gives the statistics for the three-space location of the head and torso of the seated subject. In many cases, the names of measurements have been abbreviated for compactness and these abbreviations may be cross referenced with a more complete measurement name in Appendix A. Tables B.1 and B.2 in Appendix B contain the individual data for each subject from which these statistics were derived.

GENERAL BODY ANTHROPOMETRY

1. Weight
2. Stature
3. Erect Sitting Height
4. Head Circumference
5. Bennett Ellipse Circumference
6. Bitragion Diameter
7. Head Breadth
8. Head Length
9. Sagittal Arc Length
10. Coronal Arc Length
11. Bitragion - Glabella Arc Length
12. Bitragion - Menton Arc Length
13. Bitragion - Inion Arc Length
14. Facial Height
15. Lateral Neck Breadth
16. Anterior - Posterior Neck Breadth
17. Superior Neck Circumference
18. Inferior Neck Circumference
19. Posterior Neck Length
20. Biacromial Breadth
21. Shoulder Breadth (Bideltoid)
22. Chest Height
23. Chest Breadth
24. Chest Circumference
25. Waist Height
26. Waist Breadth
27. Waist Circumference
28. Hip Height
29. Hip Breadth (Standing Erect)
30. Hip Circumference
31. Acromion - Radiale Length
32. Upper Arm Circumference (at Axilla)
33. Upper Arm Circumference (above Elbow)
34. Biceps Flexed Circumference
35. Radiale - Stylion Length
36. Forearm Circumference
37. Wrist Circumference
38. Hand Length
39. Trochanter - Femoral Condyle Length
40. Upper Thigh Circumference
41. Lower Thigh Circumference
42. Fibula Length
43. Fibular Height
44. Calf Circumference
45. Ankle Circumference
46. Foot Length
47. Ball of Foot Breadth
48. Humeral Biepicondylar Diameter
49. Femoral Biepicondylar Diameter
50. Triceps Skinfold
51. Subscapular Skinfold
52. Suprailiac Skinfold
53. Anterior Superior Iliac Spine (ASIS) Breadth
54. Right ASIS - Symphysion
55. Left ASIS - Symphysion

SEATED ANTHROPOMETRY

56. Normal Sitting Height (Relative to Seat Reference Point)
57. Tragion Height (Rel SRP)
58. Tragion Depth (Rel SRP)
59. Glabella Height (Rel SRP)
60. Glabella Depth (Rel SRP)
61. Eye Ellipse Point Height (Rel SRP)
62. Eye Ellipse Point Depth (Rel SRP)
63. Eye Ellipse Point Width (Rel. Glabella)
64. Cervicale Height (Rel SRP)
65. Cervicale Depth (Rel SRP)
66. Suprasternale Height (Rel SRP)
67. Suprasternale Depth (Rel SRP)
68. Shoulder Height (Rel SRP)
69. Shoulder Depth (Rel SRP)
70. Shoulder Breadth
71. Anterior Superior Iliac Spine Height (Rel SRP)
72. Anterior Superior Iliac Spine Depth (Rel SRP)
73. Bispinous Breadth
74. Trochanterion Height (Rel SRP)
75. Trochanterion Depth (Rel Tragion)
76. Bitrochanterior Diameter
77. Hip Breadth (Seated)
78. Infraorbitale Height (Rel Tragion)
79. Infraorbitale Depth (Rel Tragion)
80. Tragion Height (Rel Cervicale)
81. Tragion Depth (Rel Cervicale)
82. Glabella Height (Rel Tragion)
83. Glabella Depth (Rel Tragion)
84. Eye Ellipse Point Height (Rel Tragion)
85. Eye Ellipse Point Depth (Rel Tragion)
86. Ectocanthus Height (Rel Tragion)
87. Ectocanthus Depth (Rel Tragion)

Figure 2.1 Anthropometry Measurements

TABLE 2.2 ANTHROPOMETRY STATISTICS

VARIABLE	N	MEAN	STD DEV	MINIMUM	MAXIMUM
WT(KG)	18	76.9	12.5	61.1	105.2
WT(LB)	18	169.1	27.6	134.5	231.5
STAT(CM)	18	177.0	4.5	165.5	184.4
PONDINDX	18	32.2	1.6	28.7	34.9
BBSITHT	18	92.9	3.6	85.0	99.8
HEADCIR	18	57.0	1.9	54.6	61.6
HEADBIPS	18	65.6	2.4	62.2	70.5
BITRCDI	18	13.9	0.6	13.0	14.8
HEADBR	18	15.0	0.4	14.4	15.9
HEADLG	18	19.6	0.8	18.0	20.8
SAGARC	17	35.1	1.3	32.1	37.6
CORARC	18	35.2	1.0	33.0	36.7
BITRCGLB	18	29.6	1.0	27.7	31.3
BITRCMEN	18	31.5	1.5	29.4	34.5
BITRCINA	18	28.9	2.0	24.8	32.3
FACEHT	18	13.2	0.8	11.6	14.6
LATNKBR	18	12.3	0.7	11.3	13.8
APNKBR	18	11.4	0.8	10.4	12.9
SUBNKCIR	18	37.9	2.7	34.9	44.3
INFNKCIR	18	39.0	2.5	35.6	43.9
POSTNKLG	18	16.7	1.3	14.9	19.5
BIACRBR	18	40.8	1.7	38.2	44.9
BIDEITBR	18	48.4	2.5	45.3	54.2
CHESTHT	18	132.2	3.8	122.1	138.3
CHESTBR	18	31.0	2.1	28.6	34.7
CHESTCIR	18	95.6	6.1	88.2	111.8
WAISTHT	18	106.7	2.8	99.8	111.5
WAISTBR	18	29.9	3.3	26.5	37.6
WAISTCIR	18	83.9	8.3	73.8	100.0
HIPHT	18	92.7	2.7	86.6	96.7
HIPBRSTL	18	33.6	2.0	31.2	37.5
HIPCIR	18	96.5	6.3	89.2	112.3
ACRRADLG	18	32.8	1.6	30.2	35.8
ARMCIRAX	18	32.9	3.3	27.8	39.6
ARMCIREL	18	26.1	3.7	14.8	32.4
BICEPCIR	18	33.1	3.2	27.8	39.8
RADSTYLG	18	26.1	0.9	24.9	28.2
FRARMCIR	18	28.4	1.8	26.2	32.4
WRISTCIR	18	17.4	0.8	16.3	19.3
HANDLG	18	18.9	0.4	18.1	19.9
IRCREMLG	18	41.2	1.5	38.4	43.4
UPTHICIR	18	57.5	5.9	48.3	69.2
LWTHICIR	18	39.3	3.7	34.1	46.9
FIBULALG	18	40.6	1.6	38.0	43.3
FIBULAHT	18	45.7	1.8	41.6	49.6

TABLE 2.2 (continued)

VARIABLE	N	MEAN	STD DEV	MINIMUM	MAXIMUM
CALFCIR	18	36.7	3.4	30.0	44.0
ANKLECIR	18	22.5	1.4	19.6	25.1
FOOTLG	18	26.6	0.8	25.0	28.2
FOOTBR	18	10.3	0.6	9.1	11.1
HUMDIA	18	7.1	0.3	6.5	7.5
FEMDIA	18	9.8	0.5	9.3	11.2
TRICPSF	18	14.6	7.8	5.7	30.5
SUBSCPSF	18	15.9	8.4	7.0	39.3
SUPILSF	18	16.5	8.3	6.0	38.3
LTIL-SYM	18	13.1	0.9	11.4	14.7
RTIL-SYM	18	13.5	1.0	11.7	14.9
ASISBR	18	21.5	1.7	18.0	23.9
NRMSITHT	18	89.8	3.6	82.5	97.0
TRAGHT S	18	76.4	3.1	70.5	82.3
TRAGDP S	18	-0.7	2.4	-4.9	3.6
GLABLHTS	18	80.3	3.3	73.9	86.1
GLABLDPS	18	9.5	2.5	5.0	14.2
EYELPHTS	18	78.0	3.2	72.0	83.5
EYELPDPS	18	7.8	2.4	3.4	12.0
EYELPWDG	18	3.3	0.3	2.8	3.8
C7HT S	18	65.3	2.8	60.2	70.3
C7DP S	18	-9.1	1.7	-12.6	-7.1
SSTRNHTS	18	57.1	2.4	52.3	60.7
SSTRNDPS	18	2.4	1.8	-1.7	5.2
SHLDRHTS	18	56.9	2.7	52.2	61.3
SHLDRDPS	18	-4.7	1.9	-8.6	-1.2
SHLDRBR	17	41.4	2.1	36.8	47.0
ILCSPHTS	18	19.5	0.9	18.2	21.2
ILCSPDPS	18	10.5	1.0	9.3	12.9
BISPNBR	18	25.3	1.4	23.2	28.2
TROCHHTS	18	9.2	1.3	7.1	11.7
TROCHDPS	18	10.6	1.4	7.8	13.1
BITRCHDI	18	32.1	1.3	29.3	34.2
HIPBRSIT	18	37.7	3.4	33.7	46.0
ORBHT T	18	0.3	0.5	-0.7	1.0
ORBDP T	18	8.2	0.8	7.4	10.7
TRAGHTC7	18	11.1	1.3	8.3	13.7
TRAGDPC7	18	8.4	1.2	6.7	11.1
GLABLHTI	18	3.9	0.7	2.6	5.1
GLABLDPI	18	10.2	0.9	9.1	12.7
EYELPHTI	18	1.5	0.5	0.8	2.5
EYELPDPI	18	8.3	0.8	7.7	11.0
ECTCNHTI	18	1.5	0.5	0.8	2.5
ECTCNDPI	18	7.4	0.8	6.6	10.0

TABLE 2.3 UPPER TORSO AND HEAD LANDMARK COORDINATE STATISTICS (re SRP)

VARIABLE	N	MEAN	STD DEV	MINIMUM	MAXIMUM
SHLDRSX	18	-4.7	1.9	-8.6	-1.2
SHLDRSY	18	19.3	1.7	14.5	21.2
SHLDRSZ	18	56.9	2.7	52.2	61.3
C7 SX	18	-9.1	1.7	-12.6	-7.1
C7 SY	18	-1.4	1.1	-3.3	0.7
C7 SZ	18	65.3	2.8	60.2	70.3
SSTRNSX	18	2.4	1.8	-1.7	5.2
SSTRNSY	18	-1.4	1.1	-3.2	0.7
SSTRNSZ	18	57.1	2.4	52.3	60.7
TRAG SX	18	-0.7	2.4	-4.9	3.6
TRAG SY	18	5.7	1.8	2.7	11.7
TRAG SZ	18	76.4	3.1	70.5	82.3
ORBITSX	18	7.5	2.3	3.1	11.6
ORBITSY	18	2.0	1.2	-1.0	3.9
ORBITSZ	18	76.8	3.2	70.3	82.3
GLABLSX	18	9.5	2.5	5.0	14.2
GLABLSY	18	-1.4	1.2	-4.8	0.6
GLABLSZ	18	80.3	3.3	73.9	86.1
EYELPSX	18	7.8	2.4	3.4	12.0
EYELPSY	18	1.9	1.2	-1.2	3.7
EYELPSZ	18	78.0	3.2	72.0	83.5
ECCANSX	18	6.7	2.4	2.3	11.2
ECCANSY	18	3.2	1.2	0.2	4.9
ECCANSZ	18	77.9	3.2	72.0	83.4

C. Range of Motion

1. Methods. As described in references 21 and 22, orthogonal photogrammetry was also used to determine the subject's head and neck range of motion. Immediately following the seated anthropometry measurements the subjects were asked to perform the sequence of head movements shown in Table 2.4. In each position when the subject attained the limit of his voluntary movement, photographs were taken simultaneously by the three cameras. Figure 2.2 shows a subject performing the head and neck extension movement. The Euler angles describing each position

Figure 2.2 NAMRL Subject Performing Range-of-Motion Tests

relative to the Frankfort plane position were computed by digitizing the points on the coordinate system head piece worn by the subject throughout these movements. The vectors describing the orientation of these coordinate axes in space were determined in a manner similar to the seated anthropometric measures and the Euler angles computed by appropriate equations (see appendix E of reference 22).

TABLE 2.4

SEQUENCE OF RANGE-OF-MOTION POSITIONS

1. Frankfort Plane
2. Normal
3. Extension
4. Flexion
5. Right Rotation
6. Left Rotation
7. Right Lateral Bend
8. Left Lateral Bend
9. Left Rotation Plus Bend Toward Left
10. Left Rotation Plus Bend Toward Rear
11. Right Rotation Plus Bend Toward Left

In computing the Euler angles, the order of movements to attain a given position is assumed to be yaw (rotation), pitch (flexion or extension), and then roll (lateral bend) and the Euler angle reference frame axes are as shown in Figure 2.3 where positive x is forward, positive y is toward the right, and positive z is down.

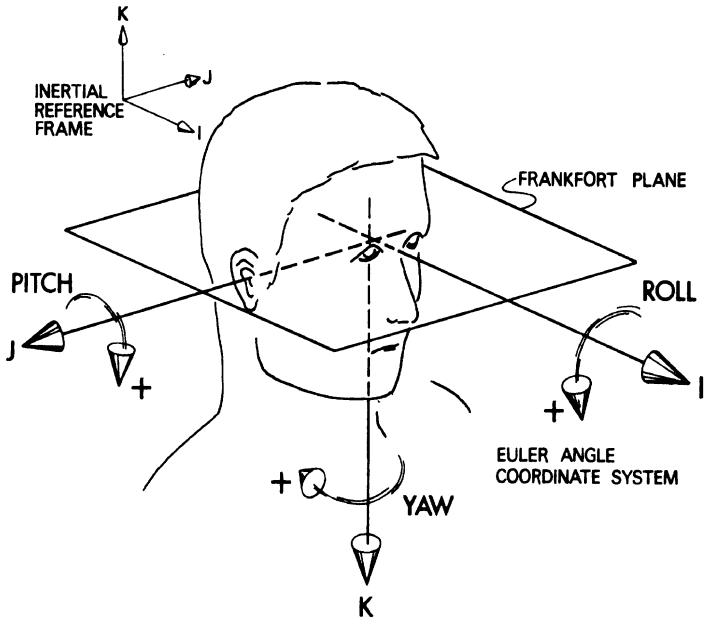

Figure 2.3 Euler Angle Reference Frame and Angle Directions

2. Results. While the measures of sagittal plane range of motion are of primary significance to this study, presentation of all the results is given here for completeness and future reference. Table 2.5 gives the statistical summary for these 18 subjects showing the mean, standard deviation, and minimum and maximum value for each Euler angle at each position. The significant number is the value for the angle related to the plane of primary movement (e.g., the pitch angle in flexion) but the other angles give an indication of the deviations from this plane which might be caused by performing the

TABLE 2.5 RANGE-OF-MOTION STATISTICS

VARIABLE	N	MEAN	STD DEV	MINIMUM	MAXIMUM
P2NEUTY	18	-0.7	2.5	-7.1	3.5
P2NEUTP	18	-2.0	3.4	-6.0	4.5
P2NEUTR	18	0.1	1.2	-1.9	2.4
P3EXTY	0	0.0	0.0	M.D.	M.D.
P3EXTP	18	79.0	6.6	63.0	87.5
P3EXTR	0	0.0	0.0	M.D.	M.D.
P4FLEXY	18	1.2	5.3	-10.9	11.7
P4FLEXP	18	-60.5	5.4	-68.5	-50.6
P4FLEXR	16	-2.1	5.6	-10.3	13.5
P5RTRCTY	18	76.1	5.8	66.3	88.4
P5RTRCTP	18	-2.1	5.8	-9.9	8.6
P5RTRCTR	17	5.9	4.5	-4.9	14.6
P6LTRCTY	18	-77.5	5.9	-83.2	-66.2
P6LTRCTP	17	-2.7	4.7	-11.4	5.3
P6LTRCTR	18	-9.5	4.8	-19.2	-0.2
P7RLBNDY	18	4.1	7.4	-8.1	20.7
P7RLBNDP	18	0.4	5.5	-10.7	10.9
P7RLBNDR	18	45.0	7.5	34.9	67.0
P8LLBNDY	18	-4.6	5.6	-12.7	7.9
P8LLBNDP	18	-0.7	6.2	-11.9	12.5
P8LLBNDR	17	-47.1	6.4	-56.9	-35.8
P9LRCFLY	18	-71.3	6.9	-85.5	-58.4
P9LRCFLP	18	-31.1	6.7	-44.1	-19.4
P9LRCFLR	18	-12.7	10.2	-31.6	12.6
P10LRCBY	18	-73.8	6.9	-88.6	-63.3
P10LRCBP	18	3.5	7.4	-10.7	13.0
P10LRCBR	18	-40.5	10.0	-55.8	-24.4
P11RRCXY	18	77.0	6.7	64.1	89.0
P11RRCXP	18	23.3	9.4	6.9	40.0
P11RRCXR	18	14.8	6.1	4.3	26.1
PSAGROM	18	139.6	8.1	118.3	155.7
PRCTRCM	18	153.6	10.4	136.6	171.6
PLATRCM	17	92.0	12.8	71.3	121.4

movement incorrectly or forcing against the physiological "stops." As with the anthropometry, the abbreviated names can be cross referenced with the list in Appendix A. Table 2.6 is an attempt to simplify these results and shows only the average Euler angles for the group. Individual range-of-motion results can be found in Table B.3 of Appendix B.

D. Reflex Times and Strength

1. Methods.

a. Reflex time. Neck muscle reflex times were measured by recording both head acceleration and neck muscle electromyograph (EMG) signals in response to a head jerk produced by dropping a 1 lb. weight approximately 6 to 8 inches. The set-up for testing of the extensor muscles (splenius capitus) is shown in Figure 2.4. A line attached to a band placed about the subject's

Figure 2.4 NAMRL Subject Ready for Sagittal Reflex Time Test

head is draped over a pulley and threaded through the drop weight which is held in position by an electromagnet. When a switch on a control console is depressed, the weight is released and caught by the small pretension or stop weight

TABLE 2.6

AVERAGE EULER ANGLES FOR 18 NAMRL SUBJECTS

	AVERAGE EULER ANGLE RE FRANKFORT POSITION		
POSITION	YAW	PITCH	ROLL
Normal	-.7	-2.0	.1
Extension	-	79.0	-
Flexion	1.2	-60.5	-2.1
R. Rotation	76.1	-2.1	5.9
L. Rotation	-77.5	-2.7	-9.5
R. Lateral Bend	4.1	.4	45.0
L. Lateral Bend	-4.6	-.7	-47.1
L. Rot. + Flexion	-71.3	-31.1	-12.7
L. Rot. + LLB	-73.8	3.5	-40.5
R. Rot + Extension	77.0	23.3	14.8

producing a "tug" to the subject's head. Two surface electrodes placed over the muscle group of interest (the splenius capitus for extensors, the sternamastoids for flexion and lateral bend) measure the electrical activity resulting from the stretch reflex response of the muscle produced by the jerk. Head acceleration was measured by a set of 4 linear accelerometers which were oriented in the plane of the head jerk in a configuration which allows for calculation of resultant head angular and linear accelerations. These accelerometers are mounted to a bar and fixed to a bite plate held in the subject's mouth during testing. The plate is fitted to each subject using a thermoplastic moldable dental compound.

Each subject was tested in sagittal flexion (extensor muscles), sagittal extension (flexor muscles), and lateral flexion to the left. A series of six or more drops were performed in each position and the average reflex time computed. Prior to each test the subject was instructed to relax and close his eyes, but to attempt to maintain his head erect when the tug was felt.

Figure 2.5 shows a typical result produced by the weight drop where only one accelerometer signal is needed and used to compute the reflex time. The beginning of muscle electrical activity is indicated by a sharp spike in the relaxed EMG signal, followed by intermittent electrical activity. The time from onset of head acceleration to this first spike is called the muscle reflex time. It is not, however, the time required to develop maximum muscle force which must include a contraction time of approximately 100 msec. The total time from initial head movement to maximum muscle force is therefore the sum of the reflex time and the contraction time and could be called a reaction time.

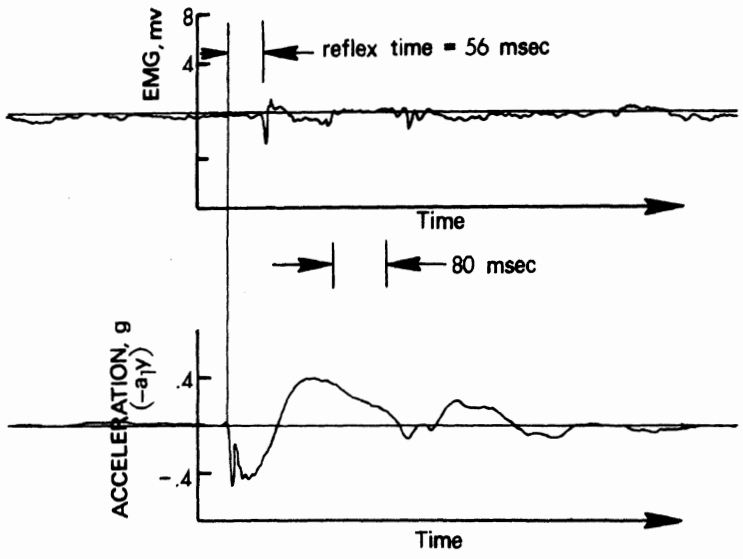

Figure 2.5 Typical EMG and Acceleration Signals in Response to Reflex Test Weight Drop.

b. Strength. Maximum voluntary isometric neck muscle strength was measured on each subject as a measure of the strength capability of the neck muscles for restraining the head during impact. Tests were performed in extension, flexion, and left and right lateral bend exertions with the subject seated in the same test seat as used for range of motion and reflex testing. Figure 2.6 shows a subject being tested for flexor, extensor, and lateral muscle strengths. A band placed about the head is attached by an adjustable length inelastic rope to the rigid test frame via a force transducer (i.e., a strain ring). The subject was instructed to pull on the rope using only his neck muscles, to build rapidly but smoothly to a maximum level, and to hold that level for a count of 4 seconds. The subject's feet were placed flat on the floor and the subject was not allowed to rise up from the seat or use his torso except to maintain his position. Three maximum exertions were made in each of the four

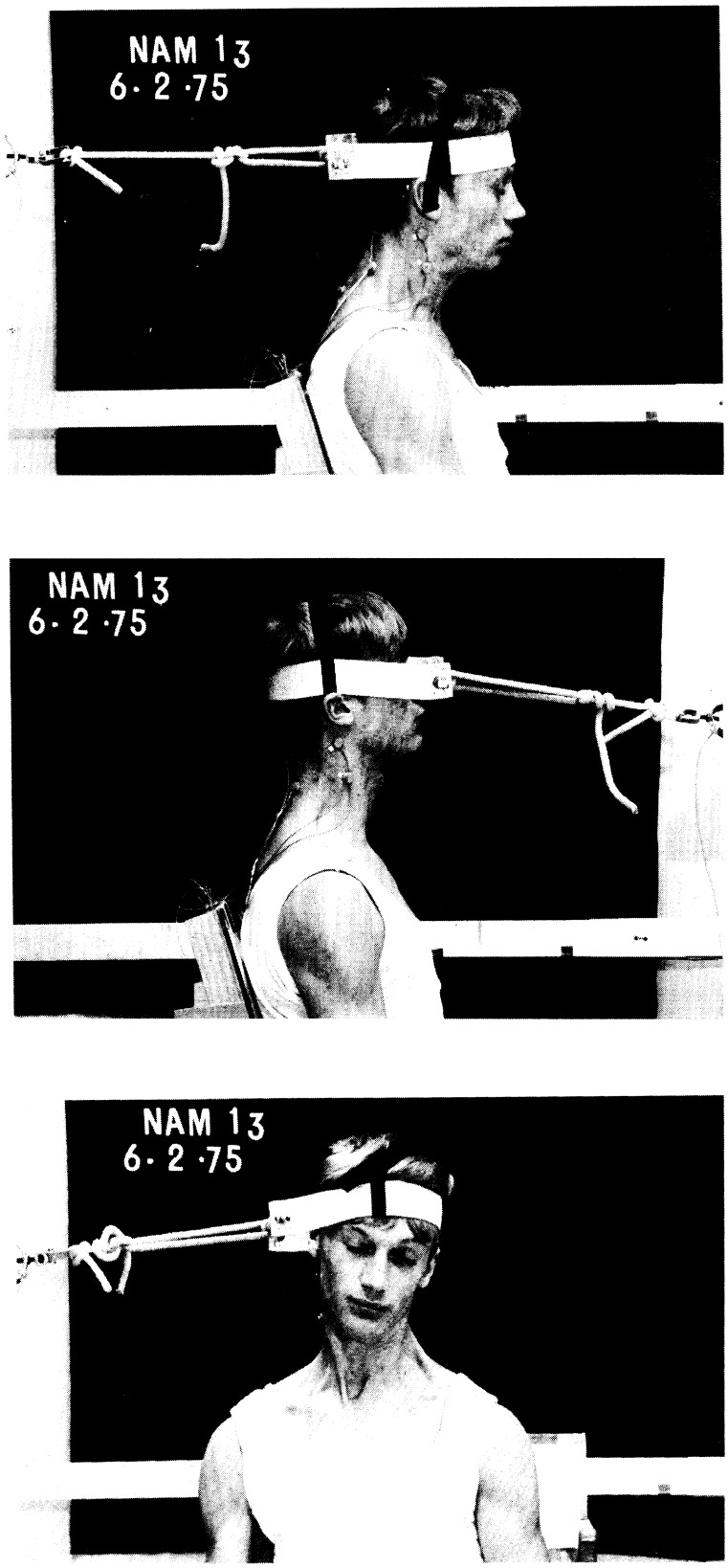

Figure 2.6 NAMRL Subject Performing Isometric Strength Testing in Flexion (Top), Extension (Middle), and Lateral Bending (Bottom).

directions with 2 minutes of rest between trials, and the average force of each set computed. Figure 2.7 shows typical force curves and the EMG signal resulting from these tests.

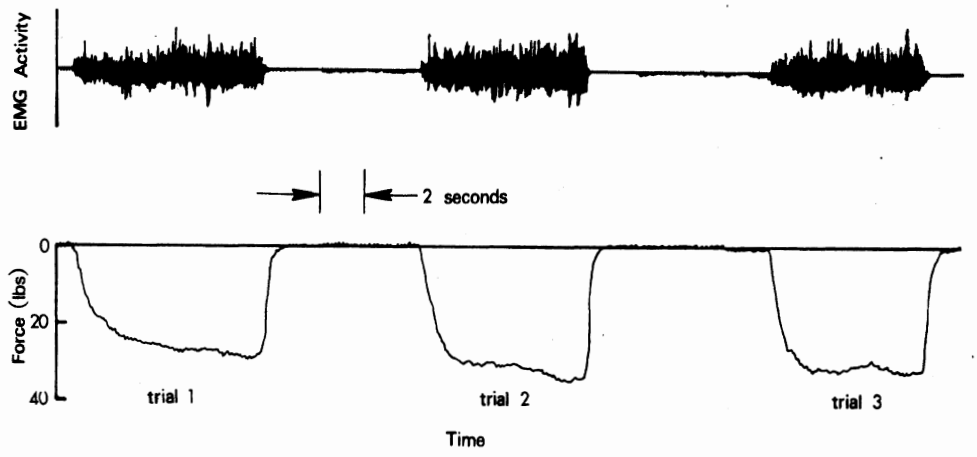

Figure 2.7 EMG and Force Signals Resulting from Isometric Strength Tests

2. Results. Table 2.7 gives the strength and reflex time statistical results for the 18 Navy subjects. The abbreviated variable names may be cross referenced in Appendix A for a more complete title.

TABLE 2.7

REFLEX TIME AND STRENGTH STATISTICS

VARIABLE	N	MEAN	STD DEV	MINIMUM	MAXIMUM
RFL LAT	18	51.5	7.5	37.0	70.0
RFL FLXR	17	55.5	7.6	43.3	68.8
RFL EXTR	18	53.3	8.6	37.6	66.3
RFL AVG	18	53.6	6.1	44.8	63.9
STR RTL	18	35.7	9.9	22.7	56.0
STR LTL	18	35.9	8.4	19.3	53.7
STRLATAV	18	35.8	8.9	21.0	51.7
STR EXTR	18	46.0	9.2	32.3	57.3
STR FLXR	18	34.3	6.7	16.7	42.0
STRSAGAV	18	40.2	7.1	24.8	48.7
SAGLATAV	18	38.0	7.6	22.9	50.0

It will be noted that the average reflex times for the three pull directions are nearly the same, being between 51 and 56 msec, while the range in reflex times is from 37 to 70 msec.This is in contrast to the results of two previous studies (22 and 23) where the data suggested that the reflex times in lateral bending were significantly less than in sagittal bending. The strength results indicate nearly identical values for right and left lateral pulls and these are nearly the same as the results for flexion, although the maximum forces achieved in lateral bending are significantly higher than achieved in flexion (56.0 lbf. to 42.0 lbf.). The greatest strengths were in extension where the average of 46.0 lbf. is about 33% greater than the average in lateral bend or flexion. The maximum strength in extension was similar to that for lateral bend, however. Table B.4 in Appendix B shows the individual strength and reflex values from which these statistics were derived where each strength value is the average of three trials and each reflex time is the average of at least 6 tests.

E. Comparison of Measurement Results with IIHS Study Results

1. Anthropometry. As indicated by the third letter in the prefix code of the HSRI subject numbers (S,M, or T), eleven of the eighteen subjects tested are of medium stature, six are tall, and only one is short according to U.S. population data on stature for 18-24 year males. Thus, the group of subjects used in this study is biased toward tall individuals. The mean stature for the group is 177.0 cm as compared to 174.86 cm and 174.95 cm for young male medium stature subject groups in the sagittal and lateral studies respectively.

2. Range of Motion. Table 2.8 summarizes the average range of motion results for the primary Euler angles in the planar head movements and compares these results with

TABLE 2.8 COMPARISON OF NAMRL AND IIHS STUDY RANGE-OF-MOTION RESULTS

Group	N	Flexion	Extension	Total Sag.	L. Rot	R. Rot	Total Rot.	L. Lat	R. Lat	Total Lat.
Navy	18	60.5	79.0	138.4	77.5	76.1	153.6	47.1	45.0	92.0
18-24 Yr. Females	16	59.3	64.7	124.1	76.5	74.1	150.6	45.6	40.4	86.0
35-44 Yr. Females	16	51.5	52.7	104.6	72.0	71.6	143.6	42.2	31.6	73.9
62-74 Yr. Females	16	40.7	43.5	84.3	63.8	59.7	123.6	33.1	23.1	56.3
18-24 Yr. Males	16	56.2	72.8	129.0	76.2	73.2	149.5	44.6	41.7	86.3
35-44 Yr. Males	16	50.5	52.2	102.7	68.6	68.5	137.1	38.2	34.8	73.0
62-74 Yr. Males	16	38.8	37.8	76.6	56.5	57.3	113.9	25.8	22.2	48.8

average results from the different subject groups in the IIHS lateral plane study. It can be seen that for every position, the average range of motion for the NAMRL subjects is greater than for all other groups and this difference is particularly significant in extension. As expected, the results are most similar to the 18-24 year male and female groups. A t-test for comparison of population means shows the NAMRL results to be not significantly different from the 18-24 year male results at the .10 level of significance. It is interesting, however, that the standard deviation for the Euler angles is consistently and considerably smaller for the NAMRL population than for the IIHS study population. This is illustrated in Table 2.9 which compares the NAMRL results with the results from 18-24 year males from the IIHS lateral study. Perhaps this is due to the difference in subject motivation, level of training, and subject conditioning which results from experience as subjects for human experiments.

Table 2.9

Comparison of Means and Standard Deviations of Range-of-Motion Results for NAMRL Subjects and 18-24 Year Males From IIHS Study.

	Primary Euler Angle (degrees)			
	IIHS Lateral Study		NAMRL	
Position	Mean	S.D.	Mean	S.D.
Extension	72.8	18.2	79.0	6.6
Flexion	56.2	11.6	60.5	5.4
R. Rotation	73.2	9.4	76.1	5.8
L. Rotation	76.2	7.2	77.5	5.9
R. Lateral Bend	41.7	12.6	47.1	6.4
L. Lateral Bend	44.6	11.3	45.0	7.5

3. Reflex Times and Muscle Strength. Table 2.10 compares the average NAMRL results for measured muscle reflex times and isometric pull force with averaged results from the IIHS lateral and sagittal studies. With regard to reflex times, there is no particular group that the NAMRL subjects match particularly well or consistently for all planes. As mentioned previously the NAMRL data show similar reflex times for all directions while IIHS study results show longer times for sagittal movements than for lateral movements. This discrepancy is unexplained at this time. In lateral bending, the NAMRL results match best with the 62-74 year females, the 18-24 year males, and the 35-44 year males. In sagittal bending, NAMRL average reflex times are closest to the young and middle aged females.

Concerning strength results, it is seen that the NAMRL subjects match extremely well with the 35-44 year males. A t-test for comparison of population means for these two groups shows no significant difference at a significance level of .05.

TABLE 2.10 COMPARISON OF NAMRL AND IIHS STUDY REFLEX TIME AND STRENGTH RESULTS

Group	Reflex Time (msec)			Pull Strength (lbf)		
	Lateral	Flexors	Extensors	Lateral	Extensors	Flexors
Navy	51.5	55.5	53.3	35.8	46.0	34.3
18-24 Yr. Females	45.1	62.3	57.0	18.8	27.0	19.4
35-44 Yr. Females	43.6	62.0	58.8	17.3	26.7	16.6
62-74 Yr. Females	53.0	74.7	73.5	11.8	22.8	13.8
18-24 Yr. Males	48.9	68.2	59.0	28.0	37.7	32.4
35-44 Yr. Males	52.8	77.1	62.2	32.1	45.1	34.8
62-74 Yr. Males	58.3	88.1	77.8	18.9	33.9	26.3

Chapter 3

COMPUTER SIMULATIONS OF NAMRL SLED TESTS

This chapter is divided into three major sections. In Section A, a brief description of the characteristics and capabilities of the MVMA-2D model is given. In section B, these characteristics as they apply to this study are developed further in a description of how the measurement data described in Chapter 2 have been used to determine model parameter values and how other parameters for which there are no data available were determined. Section C presents the simulation results for 6 and 15 G sled tests and is divided into two parts. The first part describes simulation results obtained by using experimental T_1 acceleration signals as direct input to T_1. In the second part, results obtained by using sled acceleration data and including restraint system and torso characteristics are presented.

A. The MVMA-2D Crash Victim Simulator

All simulation work in this study has utilized the MVMA-2D Crash Victim Simulator, Version III. This model, in its current form, is a result of HSRI extensions and improvements made upon the original CAL 2-D model (1966), later modified to the ROS (Revised Occupant Simulation) in 1971 and MODROS (Modified Revised Occupant Simulation) in 1972. Pertinent to the modeling in this study is the use of a two-joint extensible neck. The human occupant is constructed of 9 body segments (head, neck, upper torso, middle torso, pelvis or lower torso, upper leg, lower leg, upper arm, and lower arm) divided by 8 pivot joints as shown in Figure 3.1. For each segment except the neck, the mass, location of the center of mass, and mass moment of inertia are specified. For the neck, the mass is distributed as desired at the upper and lower neck pivot points.

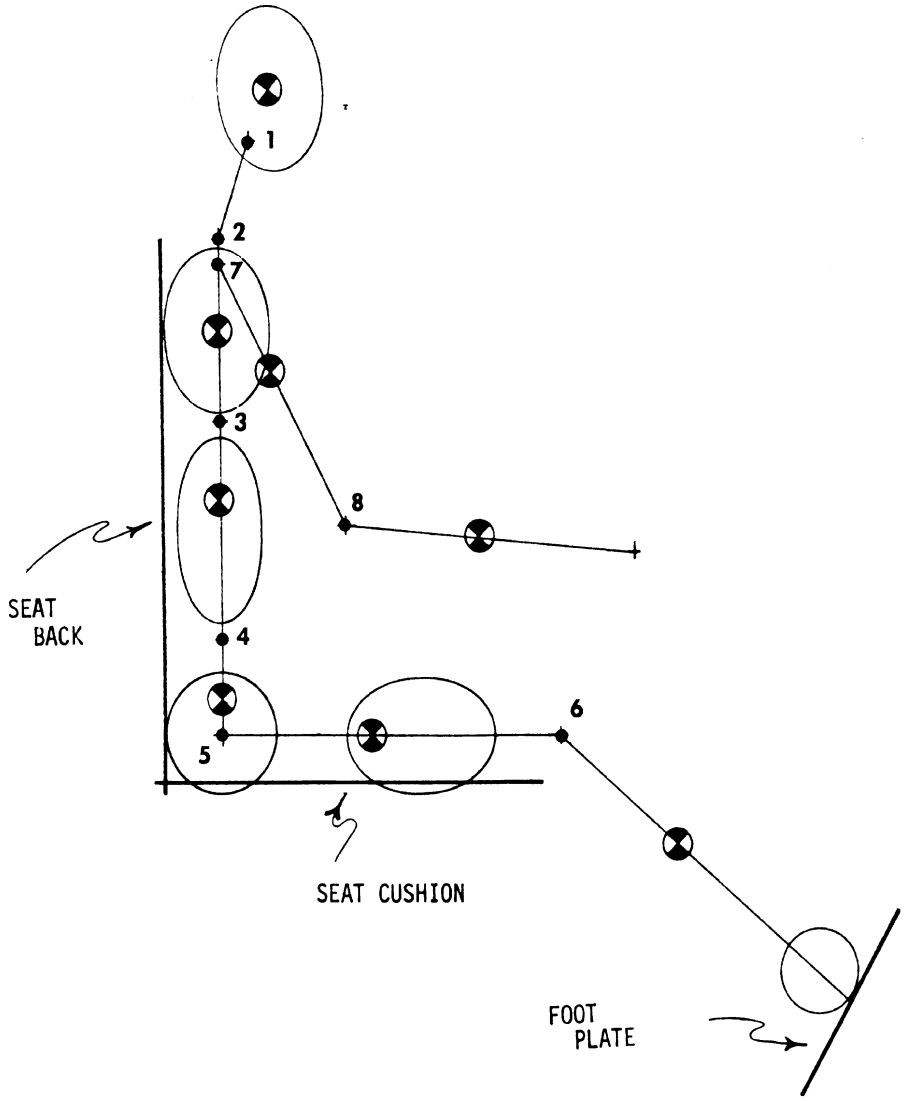

Figure 3.1 MVMA-2D Simulated Sled-Test Subject Showing Approximate Body Segment Lengths and Ellipses, Centers of Masses, and Joint Locations.

The equation of motion describing the dynamic behavior of the articulated occupant were derived using Lagrangian formulations. Energy dissipation at the joints may be through the mechanisms of friction and/or viscosity while the moments acting at each of the simulated joints may be derived from up to five sources including biodynamic muscle tension, elasticity, viscous damping, coulomb friction, and non-linear energy-dissipating motion-restrictive stops. Interaction of the occupant with vehicle structures and restraint systems may be established by specifying contact ellipses with desired material properties (including force deformation and energy absorbing characteristics) and contacting surfaces and belts with specified properties. The restraint system can utilize up to four belts — two attaching to the hip segment, one to the upper torso, and one attaching arbitrarily to any torso segment. In addition, options for free slip between belt pairs (force equalization) or for percentage force limits of one belt relative to another for simulating friction are also available. A more detailed description of these features may be found in references 2 and 20.

B. Determination of Model Parameters

A valuable feature of the MVMA-2D model as it relates to this study is that it has been developed based upon attempts to consider and simulate the individual physical factors which have an influence on the dynamic response of the occupant. For example, instead of lumping all neck properties into a general visco-elastic element with two parameter constants, the model is general enough to allow separation of some of the factors, such as muscle versus passive tissue, which physically act to affect the response. Thus, it is possible to use experimental data where available to simulate these factors and to

gain a better understanding through the model of the relative importance of each.

At the beginning of the modeling phase of the project, it was decided to match simulation results with the sled test results from a closely matched subgroup of the 18 subjects rather than to match with all 18 subjects or with an individual subject. An examination of the anthropometric and strength measurements for those properties judged to have the most significant effects on head and neck dynamic response in sagittal flexion was made and resulted in a selection of 5 subjects (NAM01, NAM04, NAM06, NAM08, and NAT18) whose measurement data would be used for establishing model parameter values and whose sled test results would be used for comparison. Tables 3.1 and 3.2 give the individual data and group statistics for selected measurements used in establishing the data set of the NAMRL simulations. While these results were used to establish model parameter values, the manner in which these data are used depends upon certain modeling assumptions and other non-obvious procedures. In addition, for other parameters used in the model there are no experimental data from which to derive reliable parameter constants. For these reasons, the following subsections are included to document the procedures used to date in this study.

1. Segment specifications — lengths, masses, centers of masses, and moments of inertia.

a. Torso and Extremities. Torso length was computed as the distance from trocanterion height to cervicale height as measured in the seated position. As shown in Figure 3.1, the torso is divided into three segments. Initially, the lengths of these individual segments were determined by proportioning them the same relative to total torso length as is used in the MVMA-2D

TABLE 3.1 SELECTED MEASUREMENTS FOR FIVE NAMRL SUBJECTS

SUBJECT NO	VARIABLES WT (KG)	STAT (CM)	ERSITHT	HEADCIR	FACEHT	APNKBR	SUPNKCIR	INFNKCIR
NAM01 H-39	74.09	174.20	93.50	55.80	13.30	11.10	37.90	38.40
NAM04 H-46	75.45	176.80	91.90	59.10	14.10	11.70	38.70	39.30
NAM06 H-49	65.68	175.80	92.30	54.70	13.80	10.40	35.40	36.50
NAM08 H-42	75.45	176.00	91.80	57.10	11.90	11.10	36.90	37.30
NAI18 H-48	74.09	181.70	94.90	61.60	13.50	10.80	37.30	38.70

SUBJECT NO	VARIABLES ACRRADLG	RADSTYLG	HANDLG	TRCFEMLG	FIBULALG	NRMSITHT	TRAGHT S	GLABLHTS
NAM01 H-39	30.50	25.20	18.30	39.00	39.50	91.40	77.80	82.40
NAM04 H-46	31.90	26.10	18.40	40.60	39.90	87.70	73.90	78.30
NAM06 H-49	31.80	24.90	18.70	40.00	40.00	89.10	76.10	79.60
NAM08 H-42	32.10	26.10	19.10	41.20	40.80	88.80	75.60	79.70
NAI18 H-48	34.10	26.70	19.90	42.80	43.20	90.70	75.70	78.60

TABLE 3.1 (continued)

SUBJECT NO	VARIABLES C7HT S	TRCCHHTS	C7 SX	C7 SZ	TRAG SX	TRAG SZ	REI AVG	STR EXTR
NAM01 H-39	64.10	10.00	-11.40	64.10	-4.70	77.80	50.30	44.70
NAM04 H-46	63.10	8.90	-7.40	63.10	-0.40	73.90	62.90	55.00
NAM06 H-49	63.50	9.40	-12.60	63.50	-4.90	76.10	63.30	37.00
NAM08 H-42	67.30	9.10	-7.60	67.30	1.40	75.60	54.70	50.00
NAT18 H-48	65.00	10.80	-7.10	65.00	2.50	75.70	51.10	54.70

SUBJECT NO	VARIABLES STR FLXB	P2NEUTP	P3EXTP	P4FLEXP	PSAGRCM
NAM01 H-39	39.30	0.80	83.00	-66.00	149.00
NAM04 H-46	36.00	-3.10	87.50	-68.20	155.70
NAM06 H-49	33.30	3.70	85.80	-50.60	136.40
NAM08 H-42	36.70	1.80	76.50	-57.80	134.30
NAT18 H-48	34.70	1.00	82.00	-65.10	147.10

TABLE 3.2

SELECTED MEASUREMENT STATISTICS FOR 5 NAVY SUBJECTS

VARIABLE	N	MEAN	STD DEV	MINIMUM	MAXIMUM
WT(KG)	5	73.0	4.1	65.7	75.5
STAT(CM)	5	176.9	2.9	174.2	181.7
ERSITHT	5	92.9	1.3	91.8	94.9
HEADCIR	5	57.7	2.7	54.7	61.6
FACEHT	5	13.3	0.8	11.9	14.1
AENKBR	5	11.0	0.5	10.4	11.7
SUPNKCIR	5	37.2	1.2	35.4	38.7
INFNKCIR	5	38.0	1.1	36.5	39.3
ACRRADLG	5	32.1	1.3	30.5	34.1
RADSTYLG	5	25.8	0.7	24.9	26.7
HANDLG	5	18.9	0.6	18.3	19.9
TRCFEMLG	5	40.7	1.4	39.0	42.8
FIBULALG	5	40.7	1.5	39.5	43.2
NFMSITHT	5	89.5	1.5	87.7	91.4
IRAGHT S	5	75.8	1.4	73.9	77.8
GLABLHTS	5	79.7	1.6	78.3	82.4
C7HT S	5	64.6	1.7	63.1	67.3
TROCHHTS	5	9.6	0.8	8.9	10.8
C7 SX	5	-9.2	2.6	-12.6	-7.1
C7 SZ	5	64.6	1.7	63.1	67.3
TRAG SX	5	-1.2	3.4	-4.9	2.5
TRAG SZ	5	75.8	1.4	73.9	77.8
RFL AVG	5	56.5	6.3	50.3	63.3
STR EXTR	5	48.3	7.6	37.0	55.0
STR FLXR	5	36.0	2.3	33.3	39.3
P2NEUTP	5	0.8	2.5	-3.1	3.7
P3EXTP	5	83.0	4.2	76.5	87.5
P4FLEXP	5	-61.5	7.3	-68.2	-50.6
PSAGRCM	5	144.5	9.0	134.3	155.7

baseline data set[1] for 50th percentile males. In this data set the lower-most segment corresponds to the pelvic mass and is 20% of the torso length. The middle and upper torso segments are about 25 and 55 percent of the torso length respectively. These proportions are somewhat arbitrary, however, and were later changed in this study to 44 and 36 percent respectively in order to provide for torso bending above the chest restraint belt. In most of the results presented later in this chapter, however, the upper and middle torso joints (joints 3 and 4) have been made essentially rigid so that the torso bends only at the hip joint (see section 7).

Extremity segment lengths were determined directly from the averaged anthropometric measures taken in this study. Initially, trocanter-femoral length was used for upper leg length, fibula length for lower leg, radiale-stylion plus hand length for lower arm, and acromion-radiale for upper arm length. At a later point in the study, the arm segments were removed and one half of the upper arm mass was added to the upper torso mass. This was done when it was realized from the high speed films that the arms were restrained by straps.

Mass and moment of inertia values for the torso were also scaled in proportion to segment values in the baseline data relative to total body mass minus the mass of the head and neck. Segment masses were scaled in direct proportion to segment length while moments of inertia were scaled to the baseline data, by proportions of mass times segment length squared.

Distances from link ends (i.e., joints) to segment centers of mass were scaled to the baseline data proportions. These values were all adjusted appropriately when

---

[1]This baseline date set for the MVMA-2D model has been established and modified over the years from existing and newly acquired data and continues to be updated and improved as the model is used.

the upper torso joint (joint 3) was moved up . The values shown in Table 3.3 are those used in the NAMRL data set for the results of this report.

Table 3.3

Torso and Extremity Segment Specifications For NAMRL Data Set

Segment	Length(cm)	End of Link to Center of Mass(cm)	Mass(kg)	Iyy ($Kg-m^2$)
Upper torso (includes 1/2 upper arm mass)	20.3	10.15	15.3	.1433
Middle torso	23.9	8.8	9.5	.1343
Hip	10.8	4.2	8.4	.1995
Upper leg	40.7	18.5	17.62	.2705
Lower leg	40.7	28.8	9.5	.3412

b. Head and Neck Mass and Moment of Inertia. A correlation of anthropometric dimensions with head mass and moment of inertia measurements on five male cadavers from a study by Chandler, et al., 1975 (3) showed that head mass is highly correlated with head circumference and that moment of inertia is highly correlated with the quantity [(menton to vertex)^2 + (head length)^2] x [head circumference]. Accordingly, these anthropometric measures from the five NAMRL subjects were used with these measures from cadavers to obtain estimates for head mass and head moment of inertia. Neck mass was obtained by scaling to the head mass in proportion to the MVMA base-line data, and was distributed with 33 percent at the condyles and 67 percent at the lower neck joint. To the head mass and moment of inertia were added the mass and moments of inertia due to the instrument packages given as .522 kg and .0075 kg-m^2 respectively by Ewing and Thomas (9). These calculations resulted in the following

values for the NAMRL data set.

Instrumented Head Mass = 4.615 Kg
Instrumented Head Iyy = .024 Kg-m^2
Neck Mass = 1.194 Kg

c. Neck length and location of head c.g. While x-rays of the NAMRL subjects were not available, an estimate of neck length and location of the head center of gravity relative to the occipital condyles was obtained by using x-ray films from young male subjects of the IIHS studies. The X and Z distances from tragion to the condyles were measured and scaled and added to the average distances of tragion to head center of gravity determined by Ewing, et al. (8) (i.e., the head c.g. lies 2.1 cm above and 1.3 cm forward of tragion). To this was added the distance the head c.g. is shifted by the instrumentation package which is given by Ewing and Thomas (9) as .35 cm forward and .2 cm down. Neck length was estimated by using anthropometry results for the five NAMRL subjects in order to locate tragion and cervicale in two dimensions. X-ray measurements from the IIHS young males were utilized in order to locate the condyles and C_7-T_1 relative to these external anatomical points. The neck length was then computed as the straight line distance from C_7-T_1 to the occipital condyles. The results of these measurements and calculations gave the following values:

x distance condyles to head c.g. = 2.47 cm
z distance condyles to head c.g. =-4.16 cm
neck length =11.2 cm

where the positive x axis is forward in the Frankfort plane and positive z is down.

2. Head and Neck Range of Motion. Since the physical situation being simulated involved primarily sagittal plane movements, only the sagittal plane range of motion results need to be considered here. These results give a measure for the maximum head angle forward (flexion) and maximum head angle rearward (extension) from the Frankfort plane position achieved by voluntary effort. While these angles are the cumulative result of bending at several articulations along the length of the neck (i.e., at each cervical disk) and at the condyles, the MVMA-2D model considers only two neck joints connected by a straight-line segment neck. While these joints may be positioned as desired, it was considered most reasonable to initially consider the upper neck joint to be at the occipital condyles and the lower neck joint to be at the C_7-T_1 disk. For range-of-motion input specifications, then, the model requires that joint stop angles for movement of the neck relative to the torso and movement of the head relative to the neck be specified. Figure 3.2 illustrates these required stop angles where the

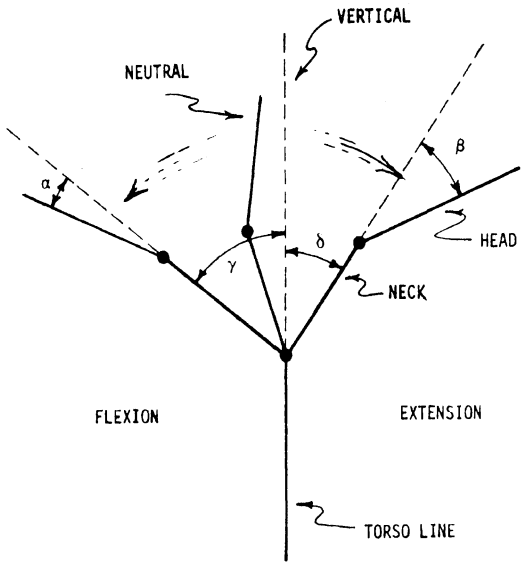

Figure 3.2 Range-of-Motion "Stop" Angles used in MVMA-2D Crash Victim Simulator.

maximum flexion and extension of the neck relative to the torso are labeled γ and δ respectively, and the maximum angle of the head beyond the neck angle in full flexion and extension are α and β respectively. The problem, then, is to determine these angles from the range-of-motion results. Two possible solutions were considered.

The first approach considered was to measure α, β, γ, and δ directly from y-camera photographs. The difficulty, of course, is to locate the condyles and the C_7-T_1 disk. These points were estimated, however, by using average measures of the x and z distances from C_7-T_1 to cervicale and tragion to the condyles obtained from x-rays of young males in the IIHS study. These distances were then scaled appropriately and marked off from cervicale and tragion on the projected NAMRL range-of-motion photographs. In this way, the angle of the neck relative to the torso line (assumed to be vertical) was measured directly in flexion, extension, and Frankfort positions. The angle of the head relative to the neck was measured as the angle between the perpendicular to the Frankfort plane and this neck angle line. While there is some inaccuracy in the measurements due to the difficulty in locating cervicale in extension and the uncertainty of the change in orientation of C_7 during flexion and extension, some consistency in the method was found and average values for α, β, γ, and δ were determined to be:

$$\alpha = -3.5°$$
$$\beta = 64.9°$$
$$\gamma = 64.4°$$
$$\delta = 19.0°$$

The sum of these angles should equal the total sagittal range of motion and is 144.8 degrees compared to 144.5 degrees determined by orthogonal photogrammetry techniques for these five subjects.

When the joint stop angles are determined in this way (where the orientation of the neck is considered to be that of the straight line segment connecting C_7-T_1 to the condyles) some of the range of motion due to articulations at neck joints is attributed to the upper neck joint in the model. While this may be a reasonable way of dividing the range of motion between the two joints, it does have some drawbacks. If the upper neck joint is to represent the occipital condyles, which is an important articulation between the large mass of the head and the relatively small extensible neck, then it is perhaps more important that the joint stop angle specification for this joint be correct even though this means that the lower joint assumes the cumulative range of motion for all other neck joints.

As a result of these considerations, a second approach was used to determine the joint stop angles needed in the model. In the IIHS sagittal study, x-rays were taken while subjects performed full flexion and full extension movements. From these x-rays, the change in angle of C_2 (this is nearly the same as the angle of C_1 and easier to measure) relative to the vertical was used for the lower neck joint range of motion, while the change in head angle (as determined by the Frankfort plane) relative to C_2 was used for the condyle range of motion. The results of these measures gave:

$$\alpha = -5.0°$$
$$\beta = 25.5°$$
$$\gamma = 71.0°$$
$$\delta = 53.3°$$

While these values were not determined from the NAMRL subject data, the total range of motion which is the sum of these angles is 144.3 degrees compared to 144.5 for the five NAMRL subjects. Also, a t-test between the IIHS

sagittal study range-of-motion results and the NAMRL range-of-motion results showed no significant difference at the .10 level of significance.

The primary difference in these angles from those derived by the first method is in extension where the head-neck angle is 25.5° compared to 64.9° and the neck-torso angle is 53.3° compared to 19°. For the first method, the total head flexion from vertical is $\alpha + \gamma = 60.9°$ while for the second it is 66°. In extension, the first method gives $\beta + \delta = 83.9°$ as compared to 78.3° for the second method.

While NAMRL simulations using stop angles determined by both of these techniques have been used, simulations presented in this report use the results of the second approach. Differences in occupant response due to the two sets of data depend upon stiffness values of the joint stops, however. As will be discussed in the next section, the values for joint-stop stiffness being used at this time result in only small differences in the model output from the two sets of data.

3. Passive Joint Torques and Joint Stops. There are virtually no data available from which to determine reasonable estimates for passive joint resistance and joint stop characteristics of the head and neck. While the MVMA-2D model has the capability to simulate these torques by several sources, initially all passive resistance coefficients within the range-of-motion angles were set to zero and torques due to movement beyond the joint stops were represented by a constant times the square of the angular deformation of the stop. Values which have been used previously in the MVMA-2D model for this quadratic angular deflection coefficient are 2.82 and 5.5 $N\text{-}m/deg^2$ for both neck joints at flexion and extension stops respectively. When the model was run

under these conditions (with muscle effects included), however, the results showed sharp peaks of acceleration produced by the joint stops which were clearly not present in the experimental sled test results (see Figure 3.23). It was clear that the joint stops were too stiff but intuitively the values used did not seem excessive for the range-of-motion angles measured on the subjects.

An attempt to remedy this problem was made by reducing the joint stop angular deflection coefficients by a factor of 100 and also adding some appreciable viscous damping to the joints throughout the range of motion. The results were much more reasonable. While little justification can be offered at this time for these values other than the fact that good results are obtained, the explanation perhaps lies in the inappropriateness of the term "joint stops." For the purposes of this study, the joint stop angles were defined to be those angles at which a human subject is unable or unwilling to move his head any further in a given direction. No measurements have been made, however, of the forces it took to achieve this final position. There is little doubt that for motivated subjects the torques required to go beyond their voluntary effort are compatible with the magnitude of the stiffness coefficients used in the MVMA-2D model, and that the assumption that the torque is proportional to the square of the angle beyond the stop is reasonable. But it is also reasonable to expect that the joint torques have been increasing in some manner up to this final position. By reducing the quadratic coefficients and adding the viscous damping constant, it was possible in some suitable but still inexact way, to model the complex characteristics of the physiological joint. In addition, by adding the viscous damping coefficient, the resistive torque is made sensitive to angular velocity which also seems to be a reasonable attempt to model effects of passive tissue such

as ligaments. There is no doubt, however, that further research and study is needed in this area before confidence in this aspect of the model will be achieved. In any case, for the results presented, neck viscous damping coefficients have been set to .01 and .03 N-m-sec/deg. for the upper and lower neck joints respectively. For the joint stop quadratic deflection coefficients which become effective when the joint stop angles are exceeded, the following values have been used:

$K_{C_7-T_1}$ (flexion and extension) = .0087 N-m/deg^2

$K_{condyles}$ (flexion) = .0261 N-m/deg^2

$K_{condyles}$ (extension) = 1.0 N-m/deg^2

In choosing the value for the condyles in extension, consideration was given to the fact that the subject is initially positioned very close to his measured head-neck joint stop angle in extension (see sections 2 and 6) where the resistive torques are significant. Consequently, this constant was maintained reasonably close to the MVMA baseline value.

4. Neck Muscle Model. There are several models in the literature which attempt to simulate muscle based upon experimental observations, all of which have limitations and deficiencies and are simplified approximations of a complex mechanism. The MVMA-2D simulator models the active element by a spring and dashpot in series as shown in Figure 3.3.

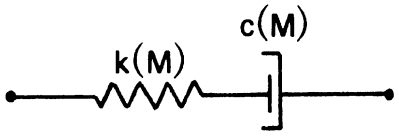

Figure 3.3 Muscle Element

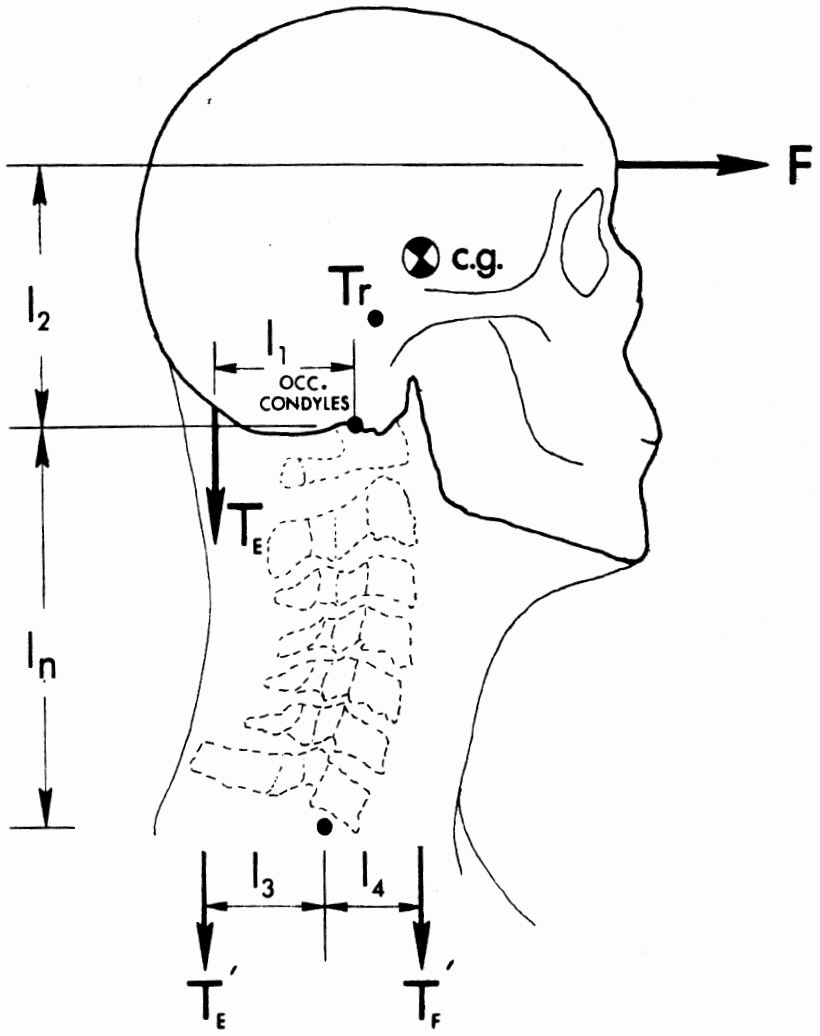

Figure 3.4 Simplified Free-Body Diagram of Head and Neck Showing Major Forces Involved During Isometric Strength Testing.

Here the coefficients K(M) and C(M) are considered simple functions of the voluntary static moment, M (i.e., of the "tightness" of the muscles), as given by the following equations:

$$K = a_1 + a_2 |M|$$

$$C = a_3 |M|$$

From these equations it is seen that when the muscles are relaxed (i.e., M = 0), the muscle has no effect on joint torque since C = 0. The muscle tension is time-dependent and is input to the model in tabular form.

The values of a_1, a_2, and a_3 in the above equations are joint parameters and are dependent on the particular muscle strengths of the occupant and the particular joints involved. Baseline data for these values have been determined by Bowman (1) and are derived from experimental data on the knee joint obtained by Moffatt, Hassis, and Haslam (17). For the lower neck joint and |M| max = 27.73 N-m, Bowman gives:

$$a_1 = .1668 \text{ N-m/deg}$$

$$a_2 = .153 \text{ deg}^{-1}$$

$$a_3 = .0129 \text{ sec/deg}$$

For the NAMRL population, the actual forces in the neck muscles at the upper and lower neck joints were estimated from the measured isometric pull forces by summing moments about the condyles and C_7-T_1 respectively as shown in Figure 3.4. The distance ℓ_2 was estimated from measurements taken from tragion to the head band during strength tests and by x-ray measurements from the condyles to tragion. Average values used for the NAMRL population were 3.32 cm and 2.1 cm respectively giving an ℓ_2 distance of 5.42 cm. The value for ℓ_n was the neck length as computed in Section 1. For the extensor muscles, ℓ_1 and ℓ_3 were estimated at 2" or 5.08 cm. from x-ray and skull measurements.

Using these values and the average muscle pull force for the five subjects in extension (48.28 lbf.), the values of T_E and T_E' were calculated as:

$$T_E = 51.5 \text{ lbf.} = 229.1 \text{ N}$$

$$T_E' = 157.96 \text{ lbf.} = 702.6 \text{ N}$$

While the baseline values for a_1, a_2, and a_3 were computed assuming a maximum joint torque of 27.73 N-m due to muscle, these values were used for the lower neck joint muscle model where the maximum estimated torque in extension is 5.08 cm times 702.6 N or 35.7 N-m and they were scaled to the condyle joint where the maximum estimated torque in extension is 11.6 N-m. Bowman (1) has shown that a_1, a_2, and a_3 may be reasonably scaled as follows from joint to joint in an individual or from individual to individual:

$$(1) \quad a_{1,II} = \left(\frac{L_{II}}{L_I}\right)^2 a_{1,I} \left|\frac{F_{max,II}}{F_{max,I}}\right|$$

$$(2) \quad a_{2,II} = \left(\frac{L_{II}}{L_I}\right) a_{2,I}$$

$$(3) \quad a_{3,II} = \left(\frac{L_{II}}{L_I}\right) a_{3,I}$$

where the subscripts I and II refer to the two joints involved. Since the distances through which the extensors act are assumed the same for both neck joints, the only constant that is altered for the condyles is a_1. This is scaled by the ratio of the maximum muscle tensions which is:

$$\frac{T_E}{T_E'} = \frac{230.0 \text{ N}}{702.6 \text{ N}} = .326$$

Table 3.4 gives the muscle parameter constants used in simulations of this report based upon these assumptions and calculations.

Table 3.4

Muscle Parameter Values Used in NAMRL Simulations

Joint	Parameter			
	a_1(N-m/deg)	a_2(deg^{-1})	a_3(sec/deg)	100% Muscle Torque(N-m)
Occ. Condyles	.053	.153	.0129	11.6
C_7-T_1	.1668	.153	.0129	35.7

For neck stretch, these constants were converted to lineal coefficients (as opposed to angular) and scaled appropriately by considering the total muscle tension due to flexors and extensors. For computing flexor muscle tension a similar technique of taking moments about C_7-T_1 was used considering the primary muscle group (the sternomastoids) to act at an average distance of about 1" (ℓ_4) relative to the lower neck joint. For the average flexion pull strength for the 5 NAMRL subjects of 36 lbf. and the same values of ℓ_2 and ℓ_n as for extension (see Figure 3.4), a maximum flexor tension of 235.5 lbf. or 1047.5 N is calculated. When added to the maximum extensor muscle tension of 702.6 N, the total neck muscle tension is estimated to be 1750.1 N or 393 lbf. Bowman (1) has shown that the muscle parameter constants in neck stretch, a_1^{ℓ}, a_2^{ℓ}, and a_3^{ℓ}, are related approximately to the angular coefficients used above — a_1, a_2, a_3 — by:

$$(4) \qquad a_1^{\ell} = 2a_1/\ell^2 \; ; \quad a_2^{\ell} = 2a_2/\ell$$

$$a_3^{\ell} = a_3/\ell$$

where ℓ is the moment arm distance for the angular constants, taken in this study to be the average for extension and flexion or 1.5". Using a_1, a_2, and a_3 from the baseline data gives:

$$a_1^{\ell} = 131.7 \quad N/cm$$

$$a_2^{\ell} = 2.3 \quad cm^{-1}$$

$$a_3^{\ell} = .193 \; sec/cm$$

In addition to these parameter values which the model uses to compute K(m) and C(m), values for the maximum muscle tension and torque are required. In previous studies (22,23) it has been assumed that for the situation where there is prior warning of impact, an individual will be able to pretense his neck muscles to 100% or more of the tension measured in an isometric laboratory exertion. On further examination of this question in this study, it appears that this may be an inaccurate assumption. Based upon subjective feelings and a brief study of EMG signals, it appears that an individual is only able to develop about 1/4 to 1/2 of his maximum isometric pull strength when tensing without an external reacting surface. Thus, even for the NAMRL subjects who are fully prepared for the impact and are aware of the exact time it will occur, it is questionable whether they can be "fully" tensed at time t = 0. As a result of these considerations, muscle tensions and torques were set at 33% of maximum and maintained constant throughout the simulations. Whether the constant tension assumption is reasonable is unknown at this time. It may be that the muscles build quickly (in 50 msec or less) to their maximum tension once the head

begins to angulate, and this time may be even shorter than the reflex times measured in this study since the muscles are already in an active state. It may also be, however, that the muscle is somehow "cut out" by the violent stretching produced by the impact. The problem requires further study and experimental testing.

In any case, rather than attempting to guess some time-dependent muscle input function, a constant muscle tension or torque of 33% of maximum was used. This resulted in the following values for the five NAMRL subjects:

Maximum muscle torque about condyles =	3.87	N-m
Maximum muscle torque about C_7-T_1 =	11.9	N-m
Maximum muscle force in neck stretch =	583.4	N

5. Neck Stretch and Compression Parameters. The MVMA-2D model simulates the stretch and compression characteristics of the neck due to passive tissue by a spring-damper combination. von Gierke (24) has reported that the undamped natural frequency of the head caused by z-excitation of the upper torso is about 30 Hertz. A first-order spring rate for the neck can be approximated by:

$$K_s = 4\pi^2 f_o^2 (M_h + 1/3\ M_n);$$

where M_h = head mass and M_n = neck mass.

For NAMRL subjects M_h = 4.093 Kg and M_n = 1.533 Kg. Using f_o = 30 Hz gives K_s = 1636 N/cm.

For a mass-spring-damper model of the human body with spinal column, von Gierke (24) gives a range of .221 to .266 for the damping ratio for the composite spinal column. For lack of better data, an estimate of one fourth of this has been assumed reasonable for the cervical spine alone.

Using a value of .243 from von Gierke's data, and with the critical damping value given by $2\sqrt{K(M_h + 1/3\ M_n)}$ the damping coefficient is given by:

$$1/4(.243) = \frac{C_s}{2\sqrt{K(M_h + 1/3\ M_n)}}$$

$$C_s = .0608 \times 2\sqrt{1636(4.093 + .511)}$$

$$C_s = 10.55 \text{ N-sec/cm}$$

6. Neck and Head Initial Angles. Initial neck angle was based upon the results of Ewing, et al., 1975 (10) in which the neck angle was calculated from the coordinates of the head anatomical and T_1 anatomical origin locations at first sled motion. By this procedure, the neck angle is estimated by a line drawn from the anterior-superior corner of T_1 through tragion. For the five NAMRL subjects the average neck angle is approximately 20° to the vertical.

Head angle is determined by the pitch orientation of the Frankfort plane relative to the vertical. Initial head angle was determined from the sled test experimental curves for head pitch angle at time t = 0. For the 6 G runs the average head angle for the five subjects was calculated to be 95.54 degrees (head back) while for the 15 G runs the average head angle was calculated as 93.64 degrees (head back).

7. Restraint System. One of the most difficult aspects of the sled test simulation was in modeling the restraint system. While complete satisfaction in this area has still not been achieved, some reasonable progress has been made as reported in the results in Section C of this chapter. As an initial step, two pieces of the webbing material used in the restraint system were tested for stress-strain characteristics under static loading

conditions. From these tests a value of K = 112,000 N per unit strain was determined and used in the model.

Because of the manner in which the belts are placed during the sled tests and because actual belt loading curves are not measured, it is difficult to determine exactly how the belt forces interact with the torso (i.e., where the belts grab or push on the torso). Figure 3.5 shows the actual belt configuration while Figure 3.6 shows the final belt configuration used in the simulations presented in this report and described below.

a. Lap belt. The lap belt was attached to the anterior-superior part of the hip segment and anchored to the sled behind and below the point of attachment to the occupant. The force strain characteristics were doubled from that determined above since there are effectively two lengths of webbing restraining the subject (i.e., the belt wraps around the subject and is anchored at two points on the sled).

b. Upper and Middle Torso belts. From repeated observations of high speed films, the impression was gained that the primary restraining of the torso is a result of belt forces applied to the chest in the region of or just below the sternum, and that the forces restraining at T_1 and the shoulders are not sufficient to prevent some flexion of the torso above this point. Initially it was thought that these forces at the chest were due to the chest belt which wraps around from behind and passes just beneath the arms. Later in the study, Dr. Thomas indicated that this belt is only a backup safety belt and has too much initial slack to be of major importance. This point is academic to the simulation, however, since it only means that the shoulder belts have their primary restraining action on the chest rather than the shoulders. With these points in mind, the torso restraint system was modeled as shown in Figure 3.6.

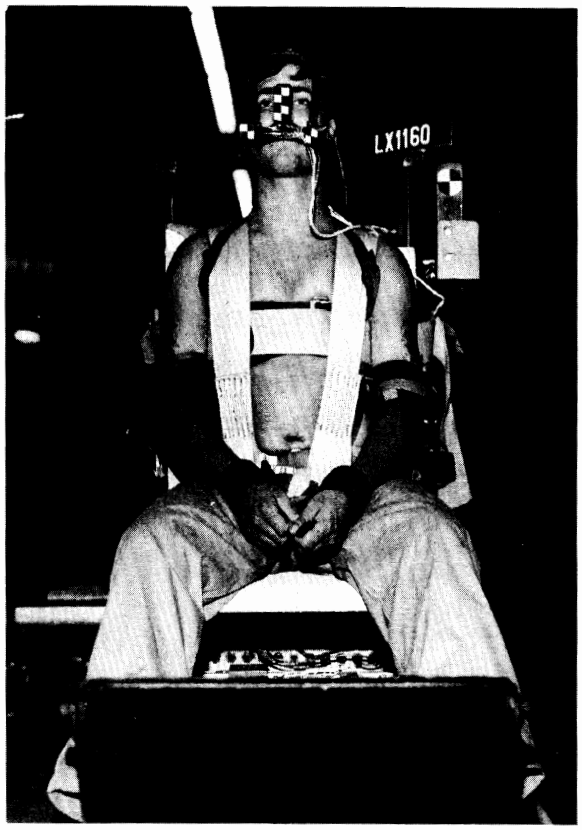

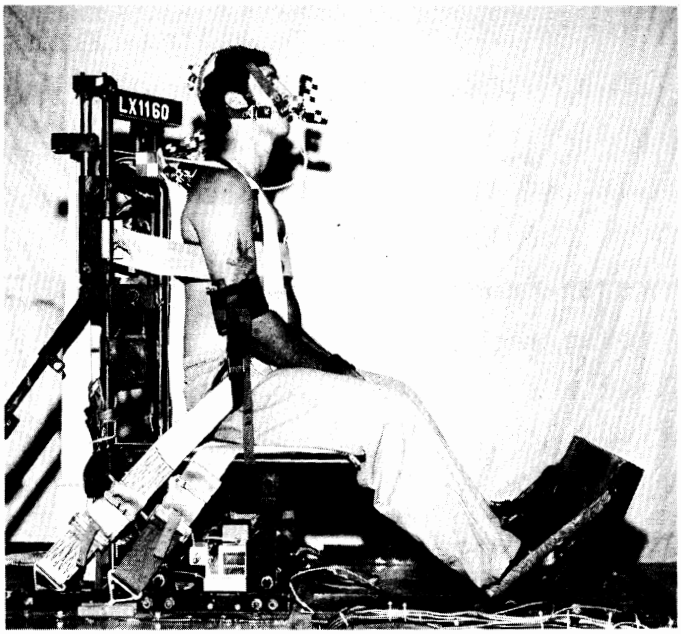

Figure 3.5 Front and Side Photographs of NAMRL Subject in Sled Chair Showing Restraint System.

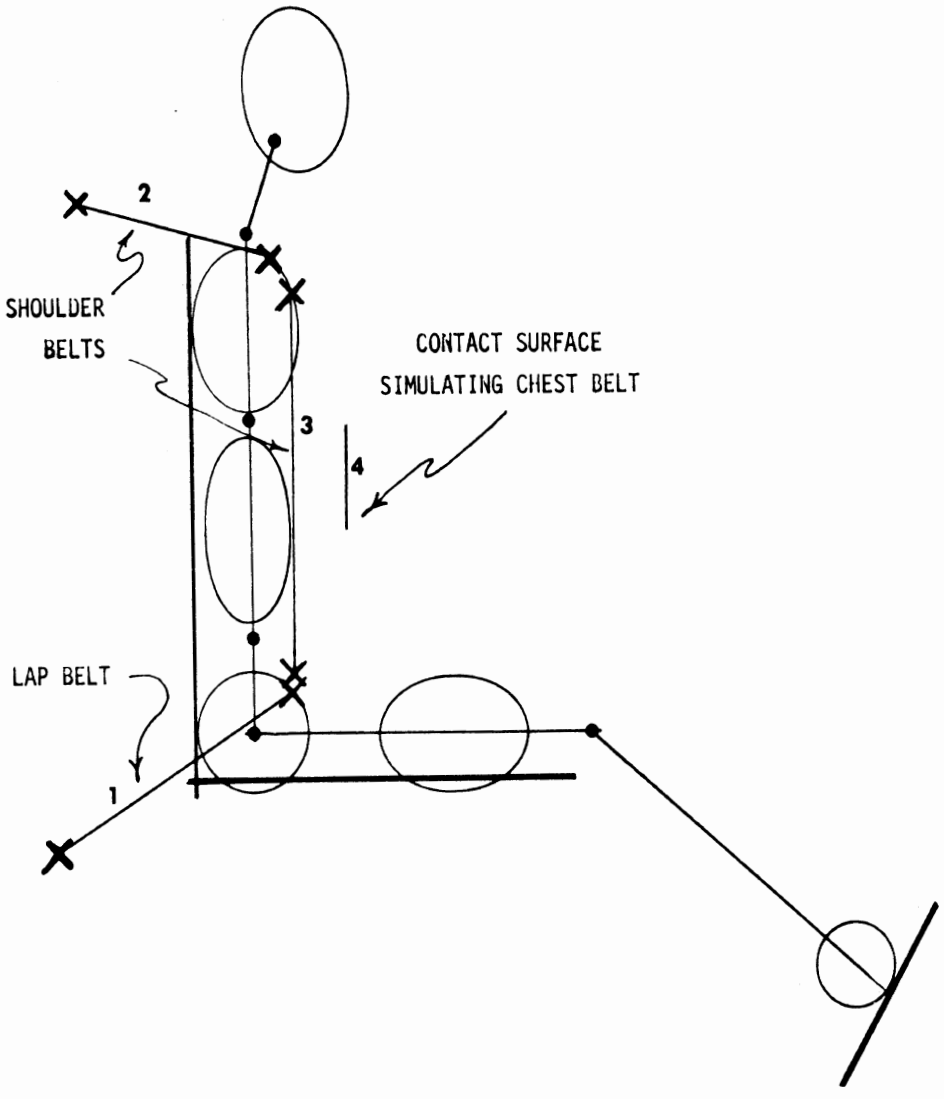

Figure 3.6 MVMA-2D Simulated Occupant Showing Restraint System Configuration.

The shoulder belts are simulated by one belt (belt 2) which anchors slightly above and behind the shoulders and attaches to the superior-anterior region of the upper torso segment, and a second belt (belt 3) which attaches just below this belt on the upper torso and anchors vertically below near the hip. The chest restraining forces are simulated by a rigid contact surface[1] (line 4) which is specified such that it is initially in contact with a contact ellipse on the superior-anterior part of the middle torso segment, just below joint 3.

In order to simulate slipping of the shoulders relative to the shoulder belts, two techniques were used. First, a model option was implemented for belts 2 and 3 which limits the tension in belt three to 50% of the tension in belt 2. Second, in order to simulate slipping, the belt material properties of belt two were altered from the measured webbing properties for the first 5 centimeters of T_1 movement as shown in Figure 3.7. As illustrated,

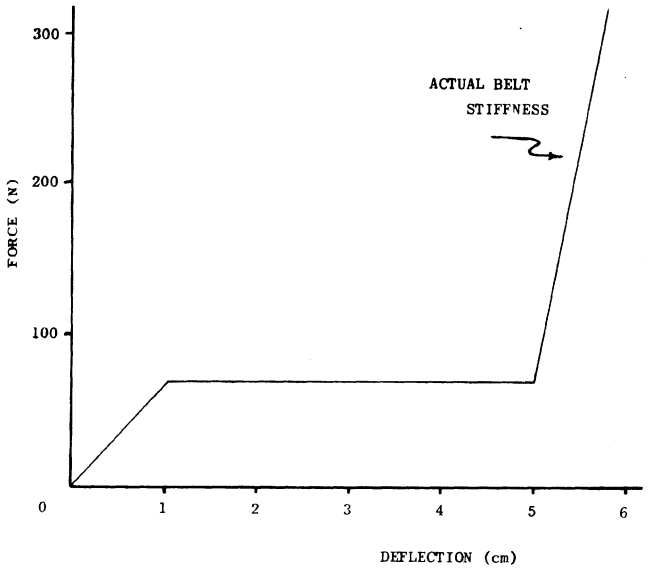

Figure 3.7 Force-Deflection Specifications for Upper Torso Belts.

[1]Since the belt system in the MVMA-2D model is not sufficiently general to represent the complex restraint system used in the NAMRL testing, a fake-belt was needed to simulate the chest restraint.

the slipping force is set equal to 70 N for the belts on the two shoulders. At 5 centimeters of slip, the measured belt properties (considering lengths and numbers of webbings) take effect.

As discussed in Section B.1, the option to include torso flexion resulting from belt slip at the shoulders is provided for by placing joint 3 just above the chest restraining belt. For most runs in this report, however, the stiffness coefficient of joint 3 is set to a value which makes the torso essentially rigid from joint 2 to joint 5.

c. Chest Compliance. In comparison to the chest compliance, the belt material may be considered essentially rigid and so, for simplicity, the contacting surface used to simulate the belt acting on the chest was made rigid. Values of chest compliance in the literature cover a wide range depending on the condition of the cadaver, the rate of force application, and the size and mass of the deforming disk. Most experiments use a disk of about 6" diameter applied to the sternal area of the chest, and it is doubtful that the compliance factor arrived at in this manner would agree with that obtained by using a belt of low mass which contacts a substantial surface of the chest. As a result of these considerations, a value for the chest compliance of 1000 lb./in. or 1751 N/cm was arbitrarily specified for the middle torso contacting ellipse. Effects of this varying compliance factor will be illustrated.

C. NAMRL Simulations

1. General. This section contains the graphical comparisons of the MVMA-2D simulations and experimental results for 6 and 15 G sled runs. Unless otherwise noted, the simulations use the data set described in Section B of this chapter developed from physical measurements on the 5 NAMRL subjects (described in Chapter 2) and other available data and assumptions. For each run the time dependent

variables of head angular acceleration, head angular velocity, head angular position, head resultant acceleration, and where appropriate, T_1 resultant acceleration are plotted and compared with experimental results. In all cases, a dashed line is used for simulations while a solid line is used for the average experimental curves. These average curves are shown by the dashed lines in each plot of Appendix C which illustrate the individual response curves from which these averages were obtained. Except for the T_1 resultant accelerations at 15 G's, it is seen that all 5 subjects show very consistent and similar responses.

2. Results using T_1 acceleration input.

a. General. Initial attempts to simulate the NAMRL sled tests at 6 and 15 G's were less than satisfactory. Because of the uncertainty in modeling the restraint system, it was difficult to know whether adjustments were needed in occupant parameters or in the restraint system. In order to separate these two factors and allow "tuning" of head and neck parameters for optimal matching to sled test results, it was decided to fix T_1 rigidly to the sled and use the experimentally determined linear T_1 accelerations in the x and z directions as sled acceleration input curves. Use of T_1 angular acceleration was also considered but a review of the NAMRL results for this signal and for T_1 angular position suggested that this was not always a reliable measurement. Figures 3.8 and 3.9 illustrate these T_1 acceleration curves obtained by averaging the data for the five NAMRL subjects.

Figures 3.10 and 3.11 illustrate the simulation results for head angular acceleration, velocity, and position, and head resultant linear acceleration in comparison to the averaged sled test results at 6 and 15 G's respectively. These results were obtained after some

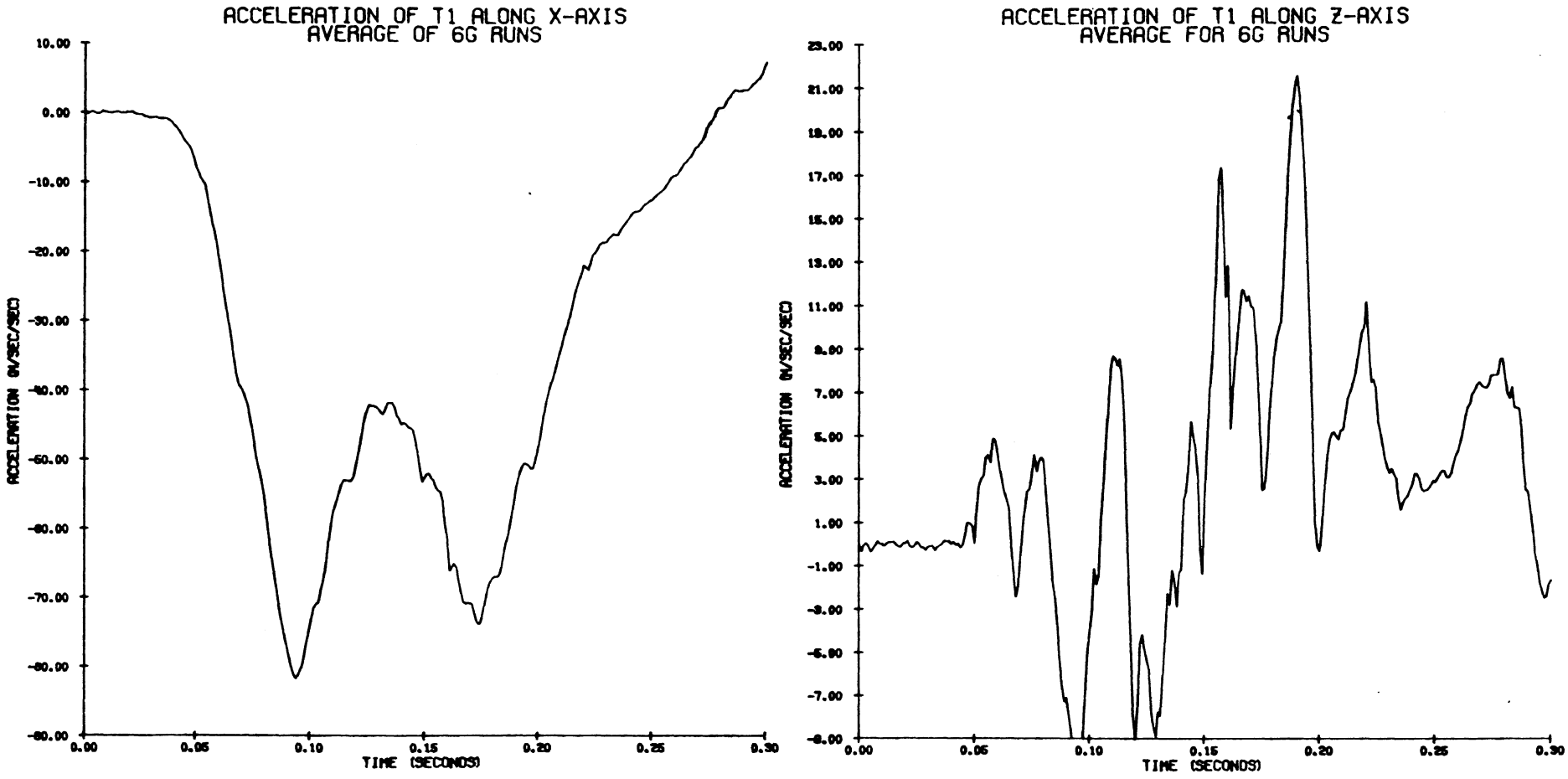

Figure 3.8 Averaged Experimental T_1 Accelerations from Five NAMRL Subjects at 6 G's.

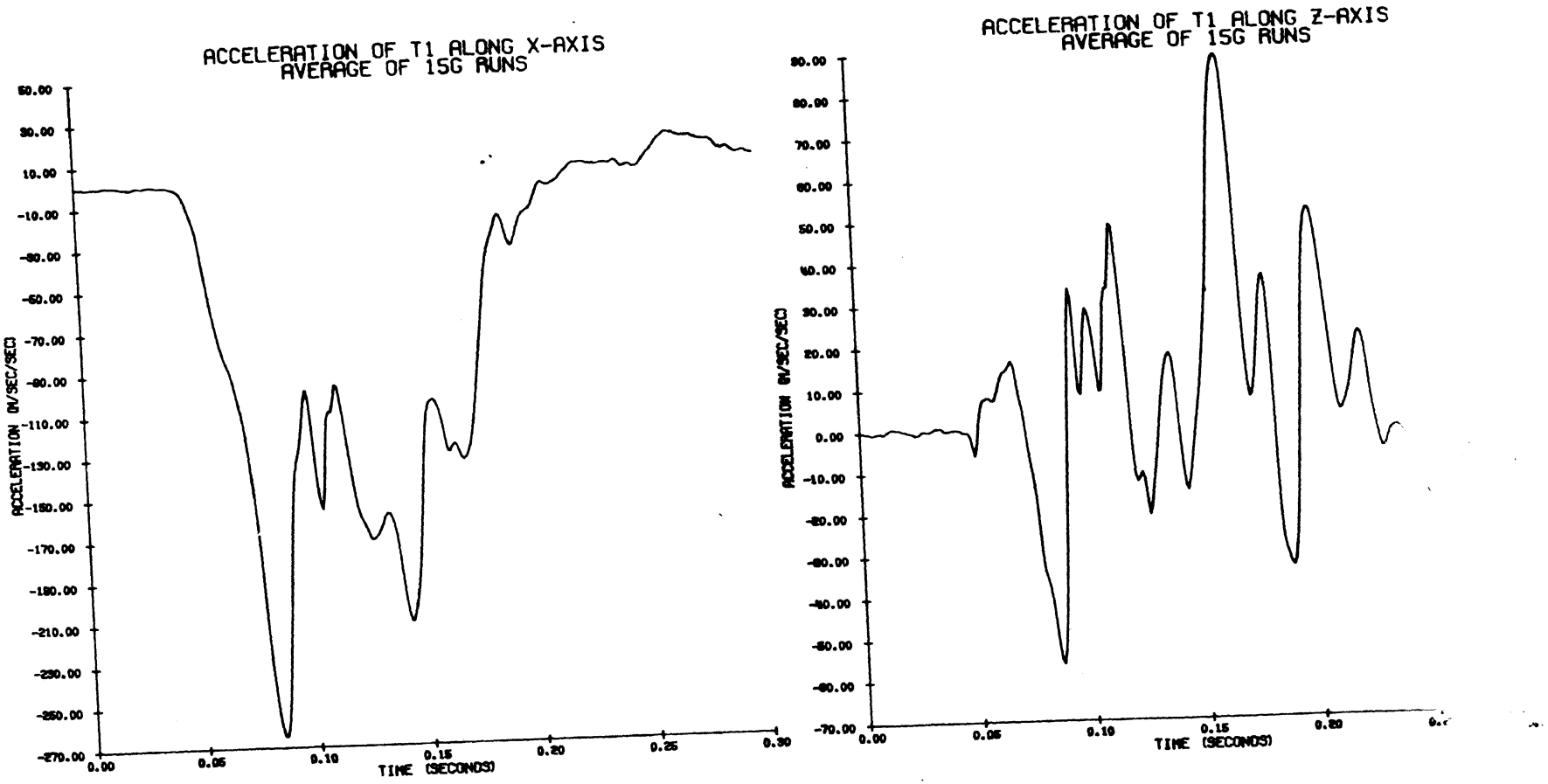

Figure 3.9 Averaged Experimental T_1 Accelerations from Five NAMRL Subjects at 15 G's.

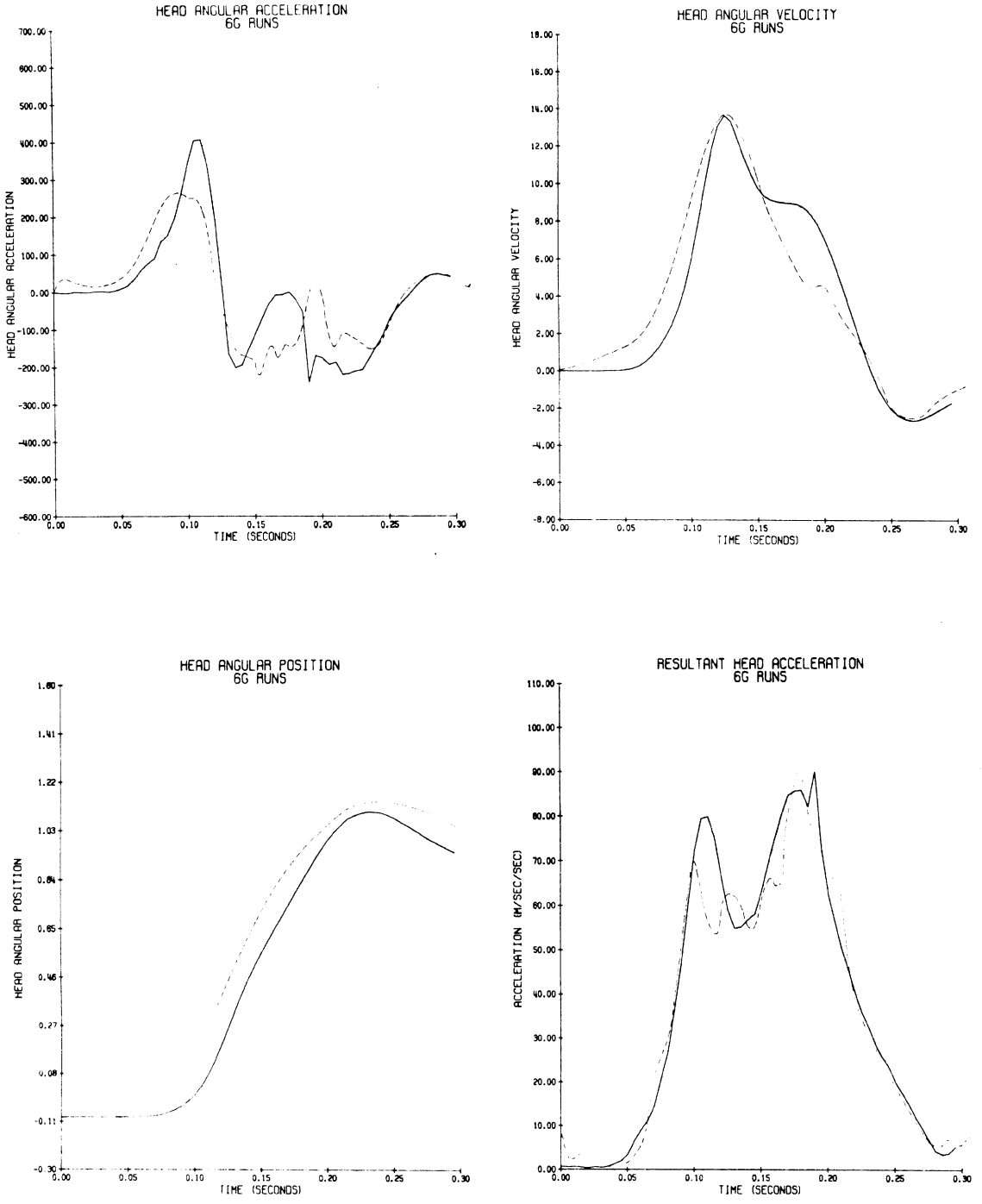

Figure 3.10 Simulation Results Using 6 G T_1 Accelerations-
Muscle Tension = 33% Maximum.

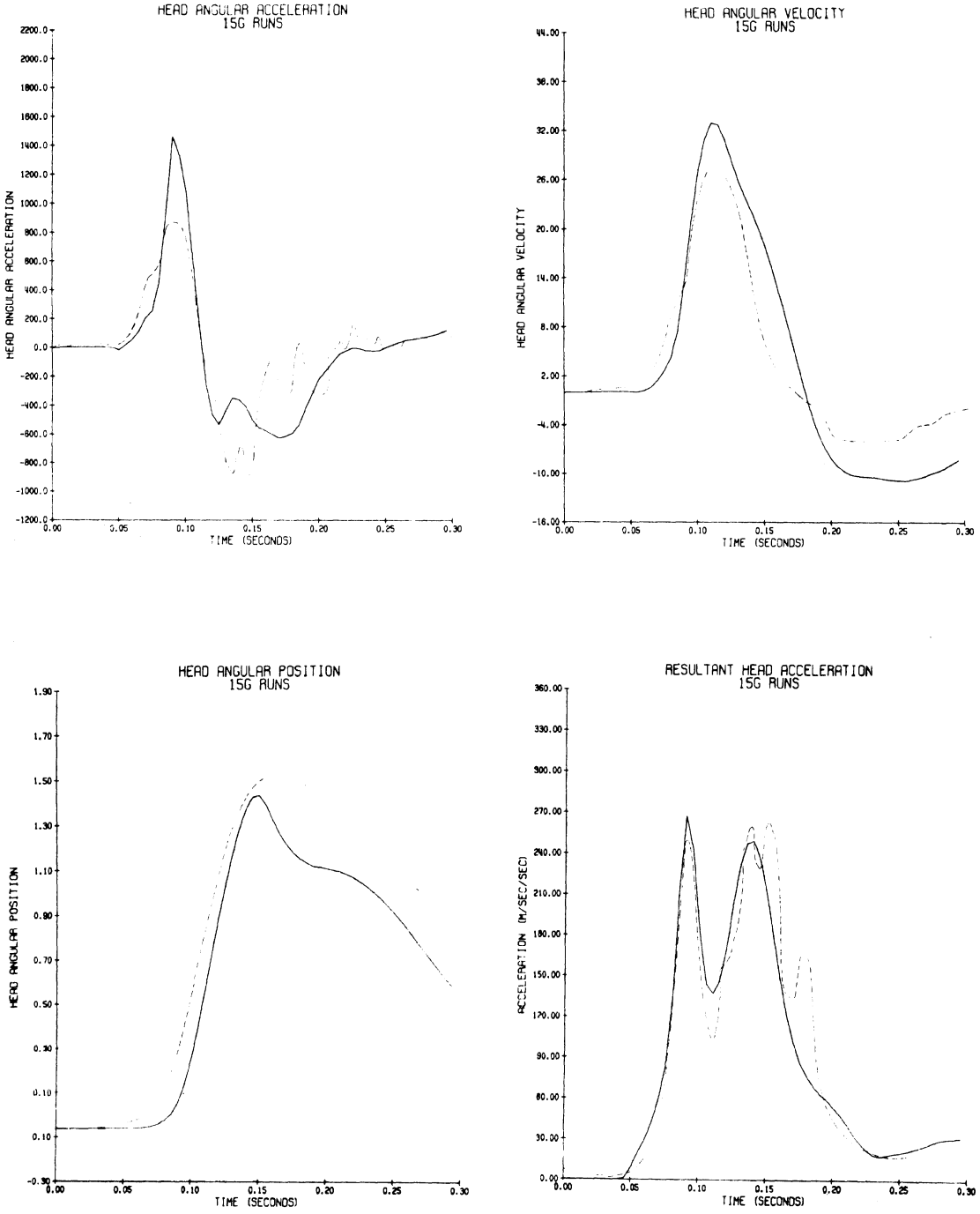

Figure 3.11 Simulation Results Using 15 G T_1 Accelerations-Muscle Tension = 33% Maximum.

adjustments in parameters such as joint viscous friction, joint stop stiffness, and muscle tension as discussed in Section B of this Chapter. The initial neck angle is 70 degrees from the horizontal in both cases and the initial head angles are 95.4 and 93.6 degrees from the horizontal (head slightly back) for the 6 and 15 G runs respectively. From these curves, it is seen that the simulations match the experimental curves quite well. In both simulations, however, the initial spike in head angular acceleration is smaller and more rounded than in the experimental results and the head angular position curves rise earlier but at similar slopes. At 6 G's the angular velocity shows a plateau on the downward slope but this occurs later than in the experimental curve. While these results could perhaps be improved by further adjustments in the parameters, this was not considered justified due to the uncertainty of the T_1 signals themselves (i.e., review of the high-speed films indicate that the T_1 accelerometers have considerable movement relative to T_1, especially in 15 G tests).

b. Effects of Muscle Tension. The question of the importance of muscle mechanics on the dynamic response of the head and neck has been of interest in recent years. While this study has not completely resolved the question, some preliminary insight has been gained and also the validity of the assumption of 33% maximum muscle tension has been tested by running the model while changing only the level of muscle tension. Figures 3.12 through 3.15 illustrate the results obtained if muscle tension is set and maintained at 0% and 100% of maximum. The general characteristics of the curves are not changed appreciably, except for head angular position.

At 0% of muscle tension (i.e., no muscle input) the angular positions are uncontrolled and become unrealistic, while at 100% muscle tension the angular position is

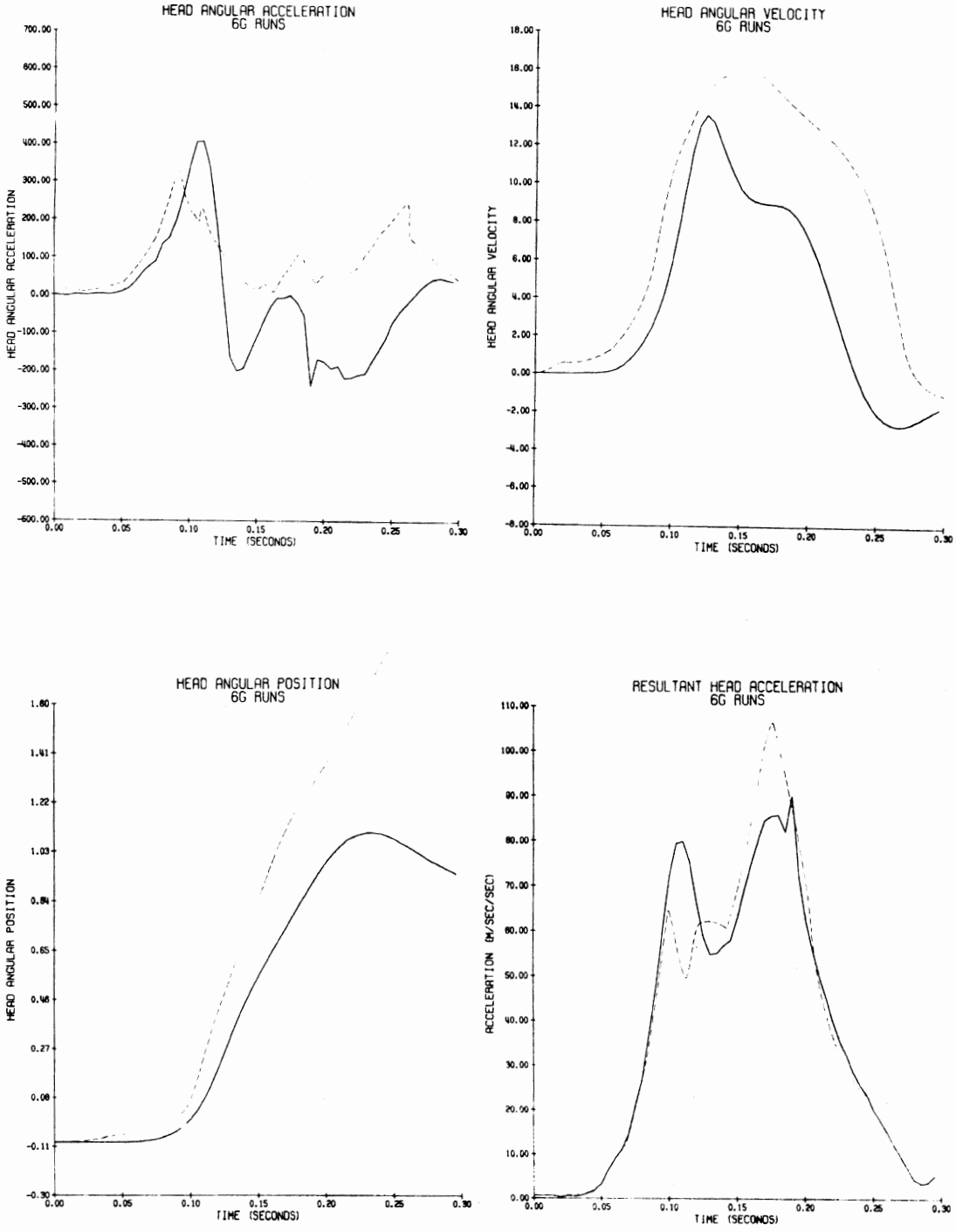

Figure 3.12 Simulation Results Using 6 G T_1 Acceleration-Muscle Tension = 0% Maximum

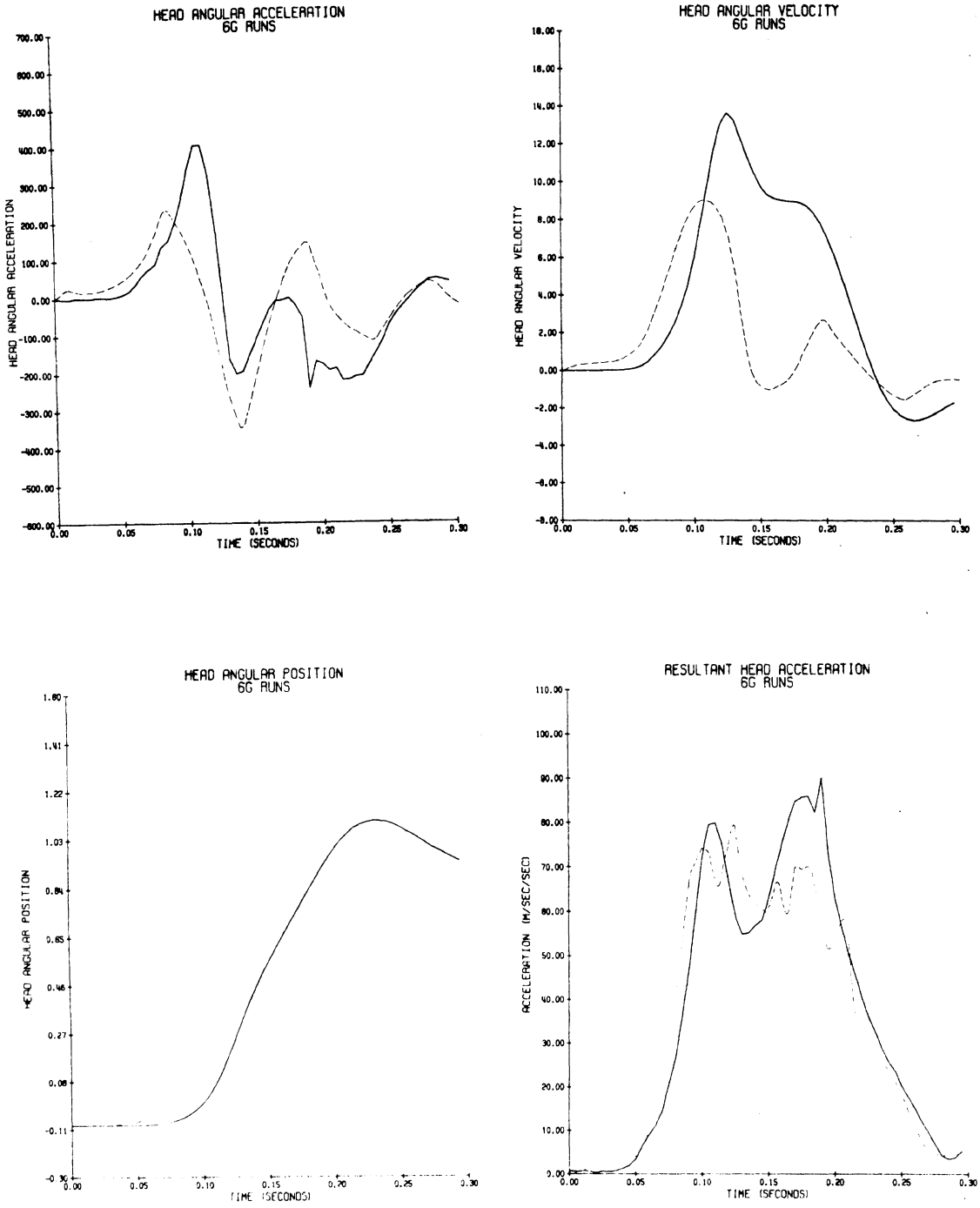

Figure 3.13 Simulation Results Using 6 G T_1 Acceleration-Muscle Tension = 100% Maximum.

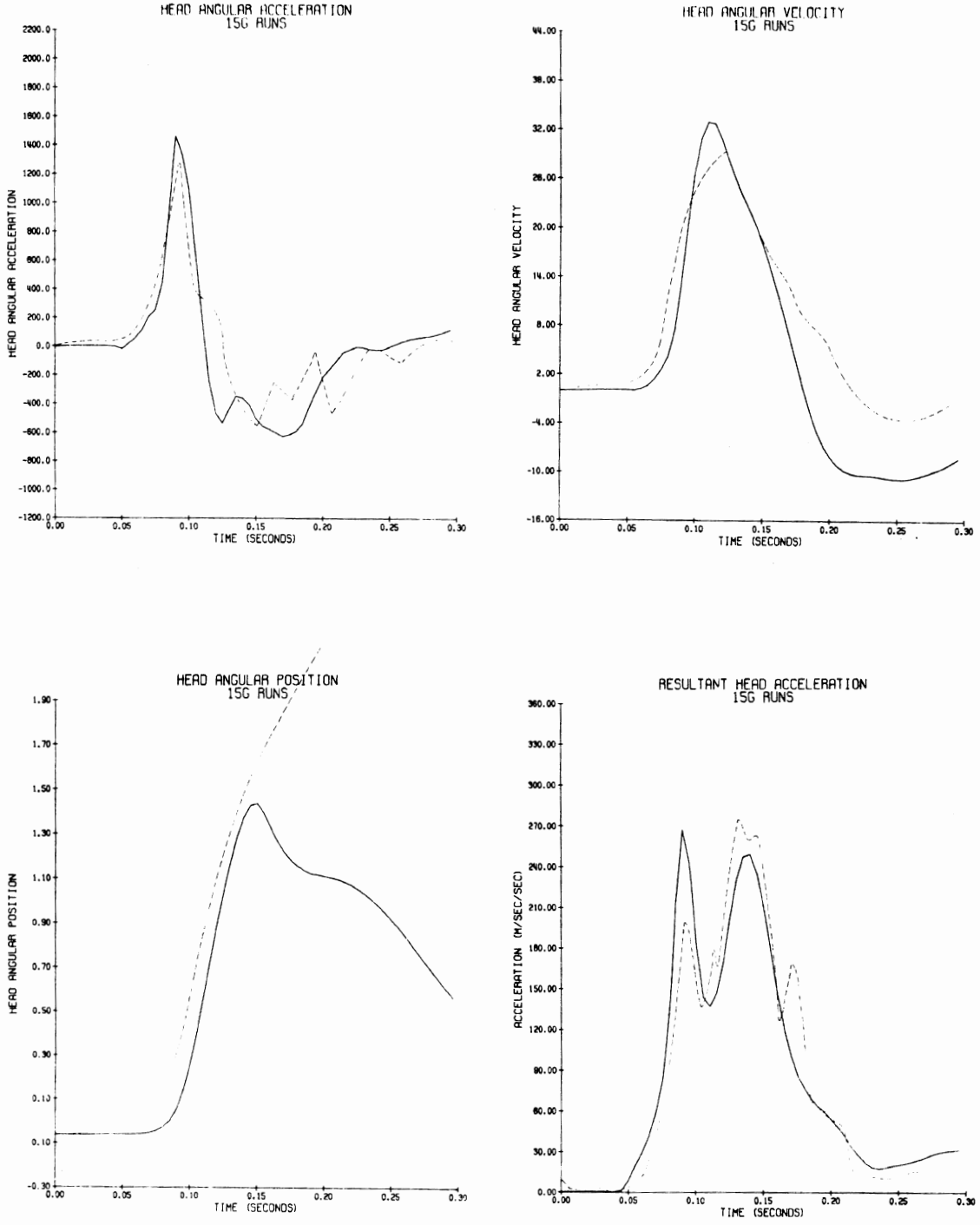

Figure 3.14 Simulation Results Using 15 G T_1 Acceleration - Muscle Tension = 0% Maximum.

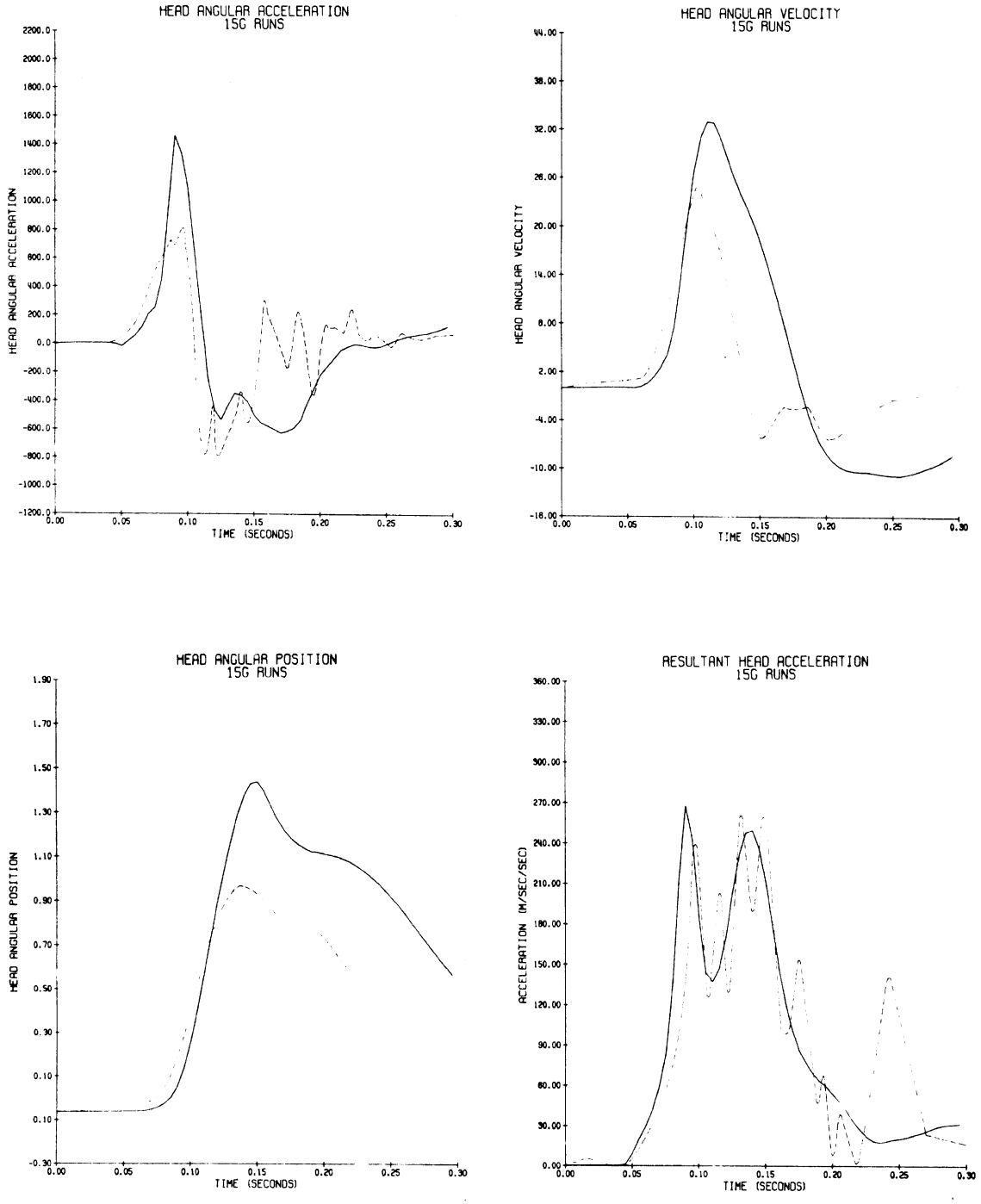

Figure 3.15 Simulation Results Using 15 G T_1 Acceleration - Muscle Tension - 100% Maximum.

greatly reduced. It is interesting that at 15 G's the effects of changing the muscle tension are considerably less than at 6 G's. At 15 G's, the angular acceleration, angular velocity, and head resultant acceleration curves are changed little at 100% muscle tension and fit the experimental data extremely well at 0% muscle tension. At 6 G's the effects of muscle tension are more dramatic in head angular acceleration and particularly head angular velocity.

These results suggest that for the 6 G runs, the muscles play a major role and that the assumption of 33% muscle tension is reasonable. At 15 G's, the muscular effects are less important and they may in fact be eliminated by some protective reflex. The fact that the angular head position increases greatly at 0% muscle tension should not be a major consideration at this time since the joint stop resistance coefficients used probably do not represent the true physiological situation. Further, the condition of 0% muscle tension is also unrealistic and has been used only to dramatize the effects.

3. Results with Sled Acceleration Input and Restraint System.

a. General. Since satisfactory results were obtained from the model simulations with T_1 fixed, it was assumed that established parameter values for the occupant head and neck were at least "in the ball park". Therefore, attempts at simulating the complete occupant with appropriate torso and restraint system modeling were undertaken. The final configuration of the restraint system used in the model is discussed in section B.7 of this chapter while Figure 3.16 shows the sled acceleration profiles used for 6 and 15 G runs.[1]

[1]These profiles are for NAMRL's high rate of onset, long duration acceleration pulses.

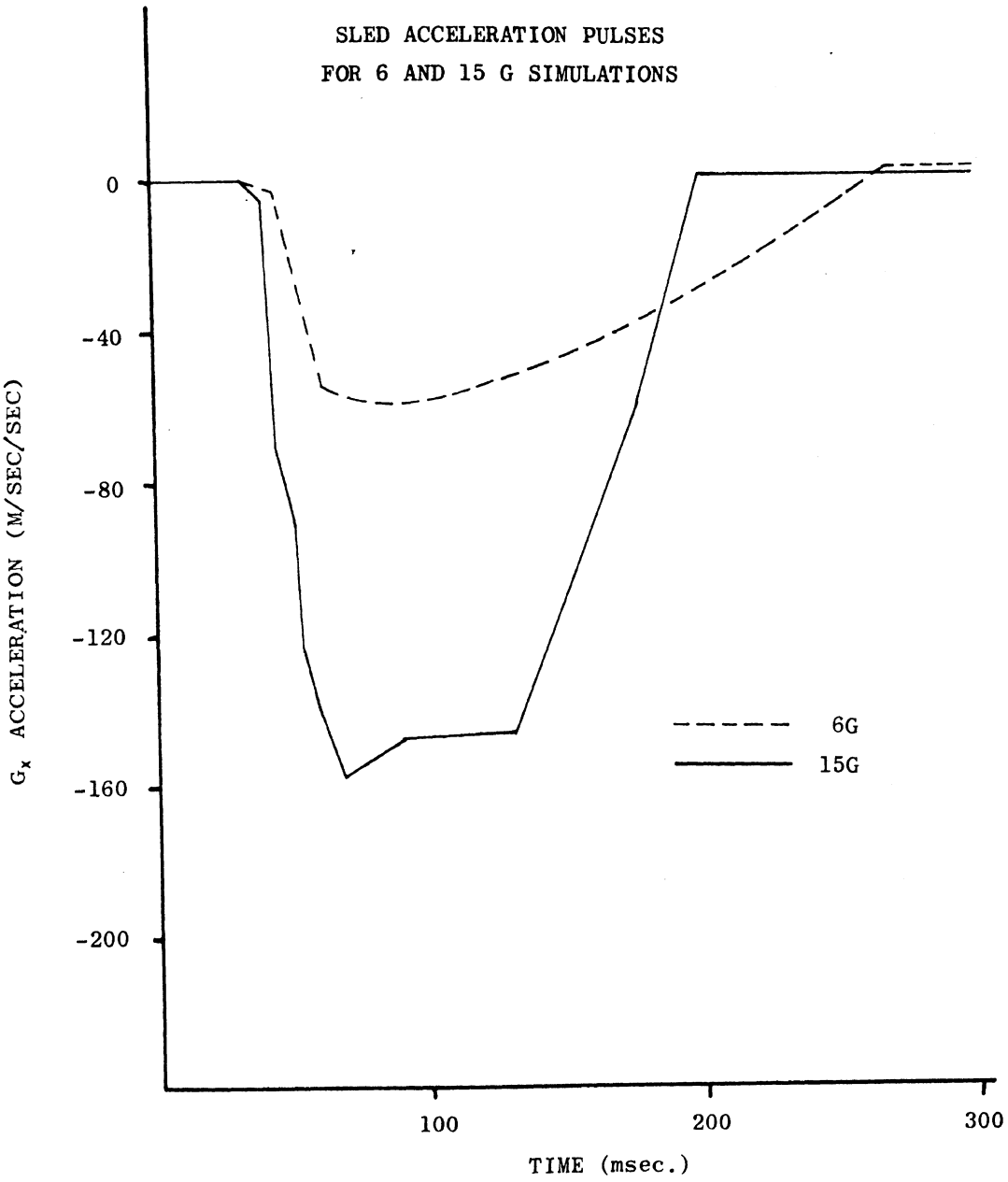

Figure 3.16 6 and 15 G Sled Acceleration Profiles Obtained from NAMRL Maximum Rate of Onset-Maximum Duration Sled Runs.

Figures 3.17 and 3.18 show the simulation results and averaged experimental results at 15 and 6 G's respectively using a constant 33% maximum muscle tension, a nearly rigid torso (i.e., no bending at joint 3) and a chest compliance factor of 1750 N/cm (1000 lb/in). In addition to the four variables shown previously, T_1 resultant accelerations are also compared.

At 15 G's, there is good agreement between experimental and simulated results. For angular acceleration, the initial positive spikes match extremely well in magnitude although in the simulation this spike occurs about 10 msec too soon. The initial negative spike is of considerably larger magnitude in the simulation. For angular velocity, the magnitudes of the peak velocities match well although the simulation curve reaches a peak about 5 msec earlier than the experimental curve and decreases to zero with a greater slope, reaching zero about 25 msec earlier. The angular position curves peak at the same time with the simulation peak being about .15 radians or 8.5 degrees greater. The two curves rise to their peaks with approximately the same slopes although the simulation curve precedes the experimental curve by about 10 msec. The T_1 resultant curves match extremely well considering the fact that there is probably some error in the experimental curve (due to the inability to attach the accelerometers rigidly to T_1) and the fact that these curves are a result of the complex interactions of the restraint system with the torso and dynamic feedback from the head. Both curves show the bimodal nature with peaks of similar magnitude at similar times. The head resultant accelerations do not match quite as well but both curves are of a similar bimodal nature matching well in magnitudes but not as well in times.

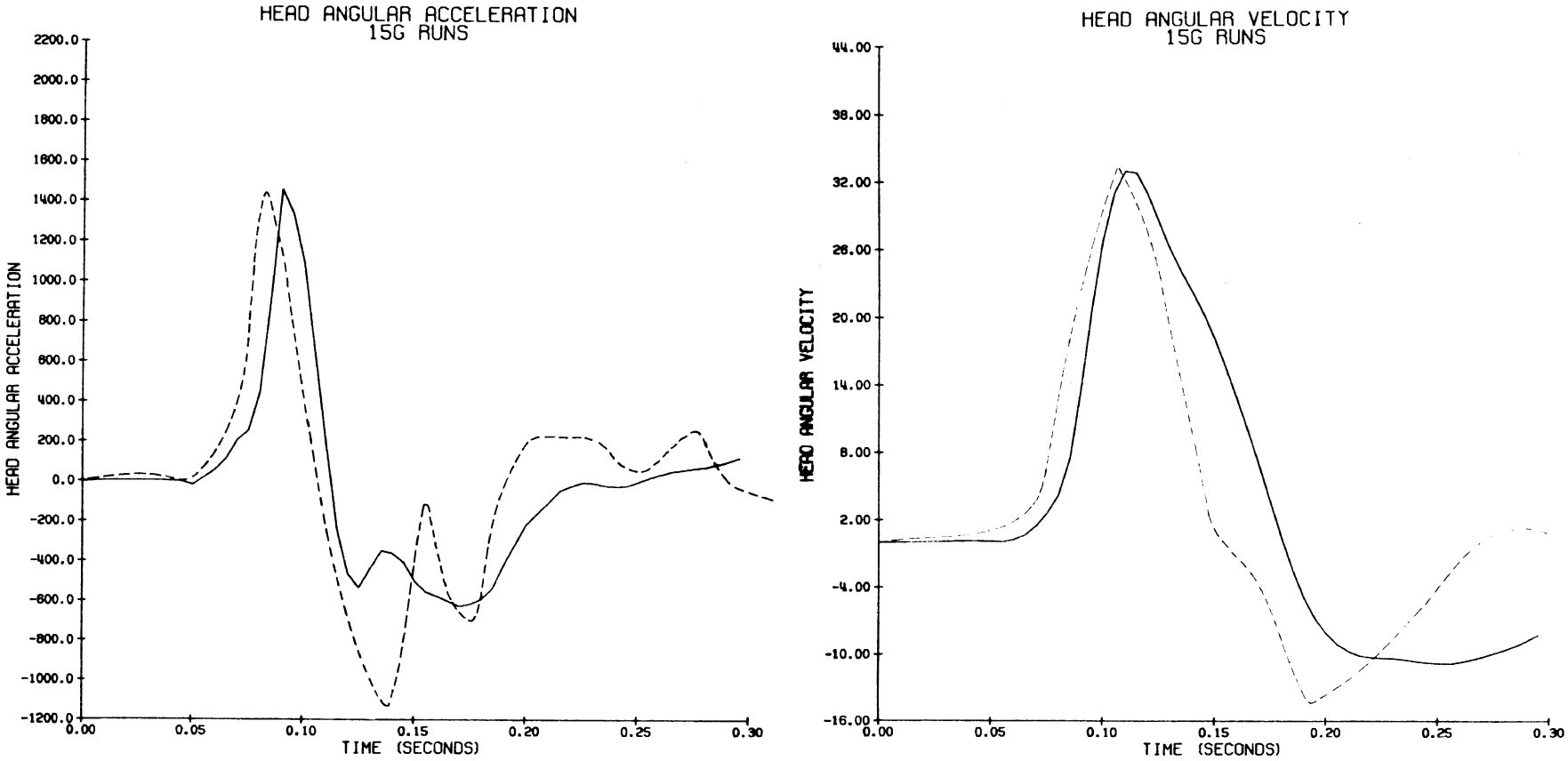

Figure 3.17 Simulation Results for 15 G Sled Acceleration - Muscle Tension = 33% Maximum, Chest Compliance = 1750 N/cm.

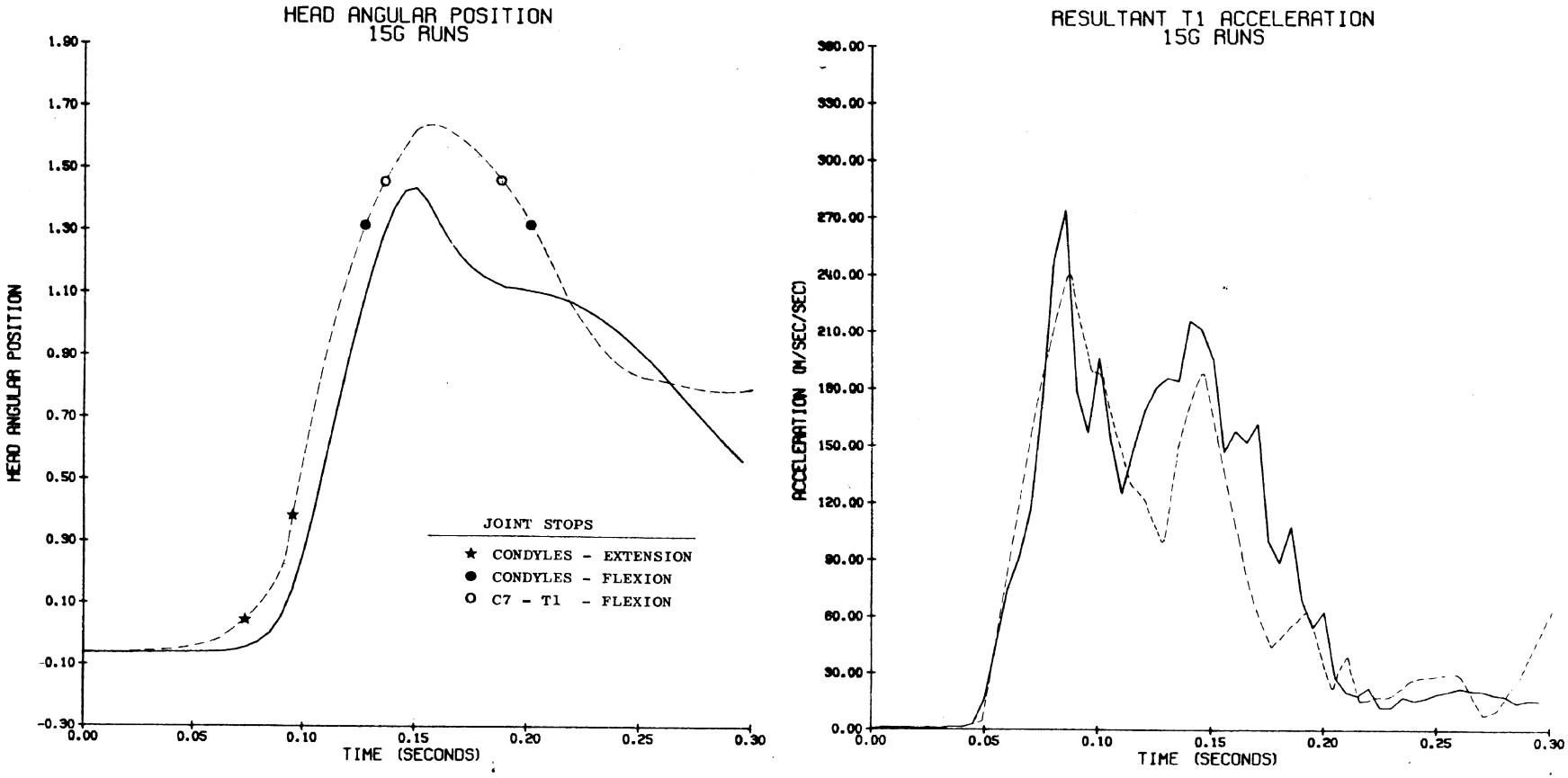

Figure 3.17 (continued)

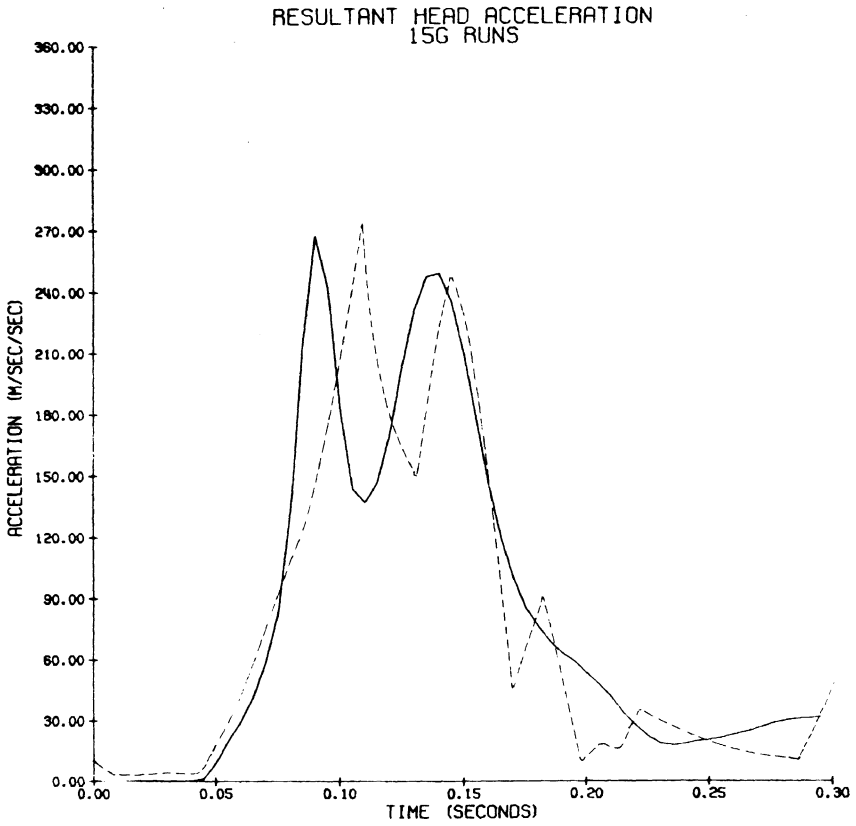

Figure 3.17 (continued)

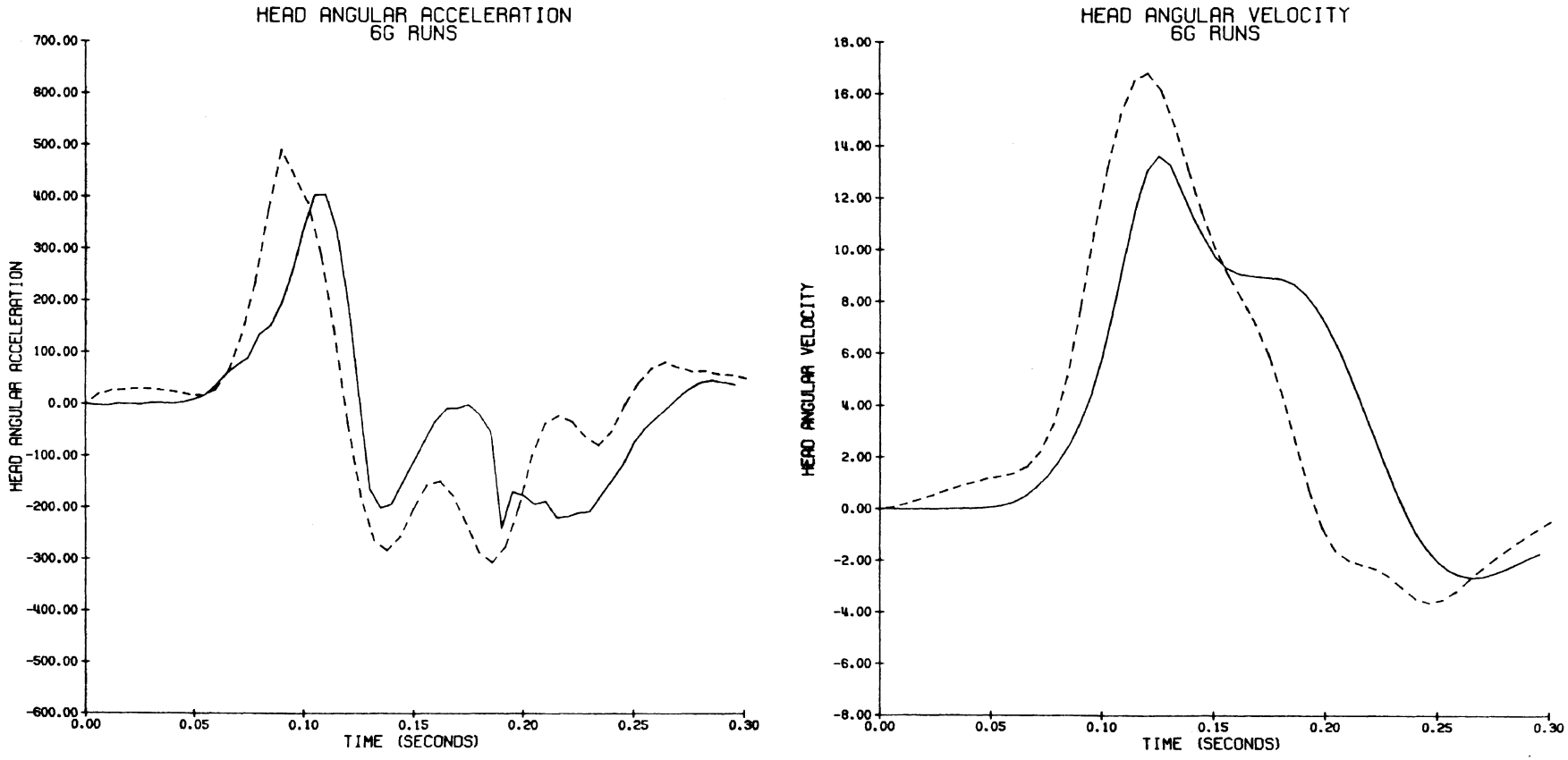

Figure 3.18 Simulation Results for 6 G Sled Acceleration - Muscle Tension = 33% Maximum, Chest Compliance = 1750 N/cm.

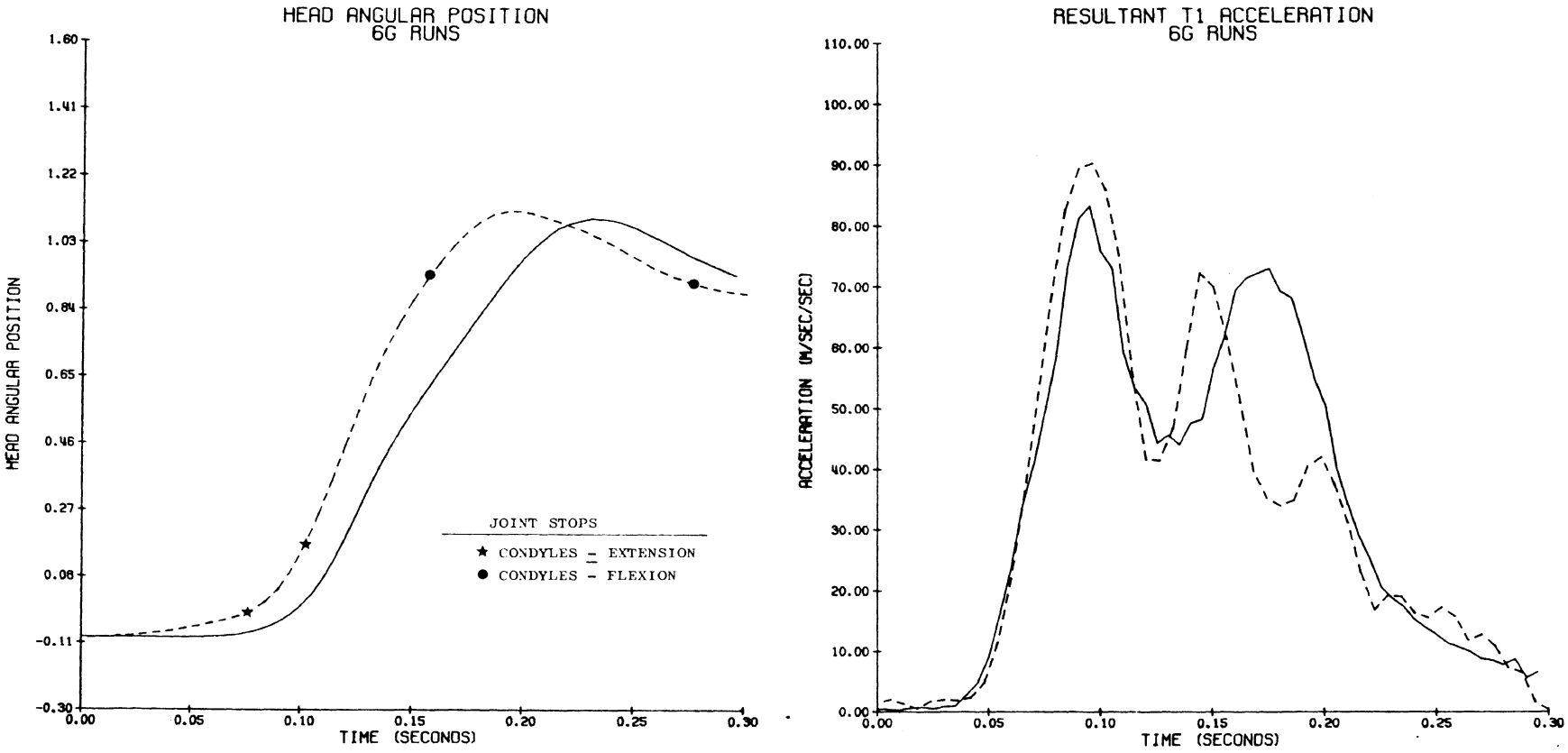

Figure 3.18 (continued)

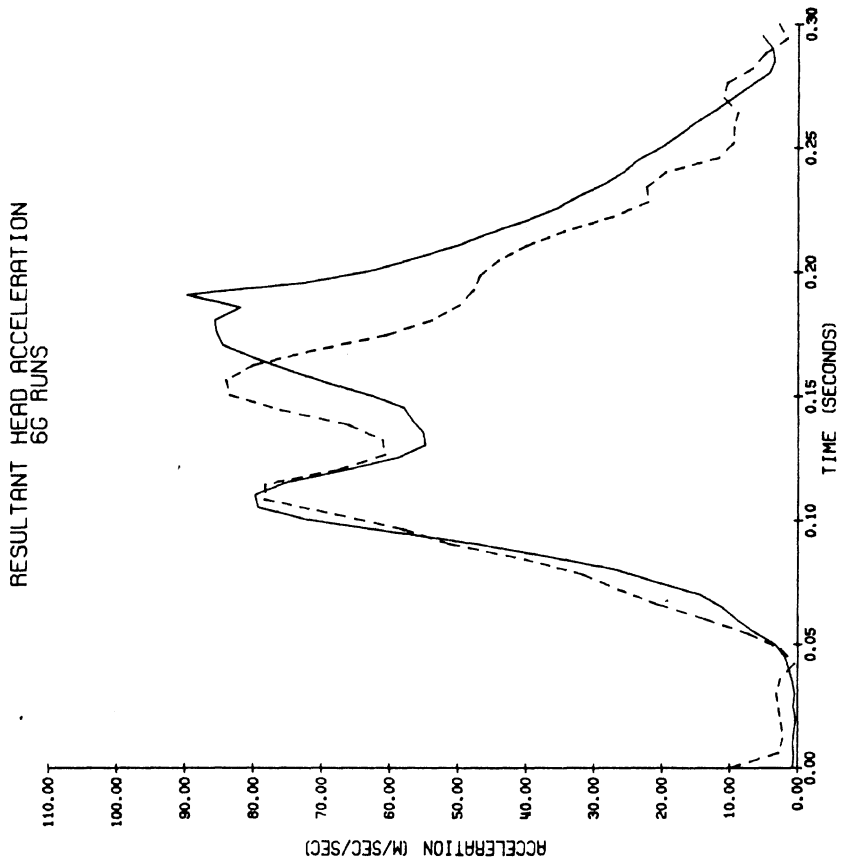

Figure 3.18 (continued)

At 6 G's, the matching is a reasonable fit, though not as close as the 15 G results. The simulation curve for angular acceleration shows a positive peak slightly larger and about 20 msec earlier than the experimental curve, but there is excellent agreement on the negative acceleration portion of the curve. The angular velocity curves match less well with the simulation having a larger peak and, as with the 15 G test, decreasing to zero at a greater rate. The simulation curve also does not show the plateau at about 150 msec although there is a slight change in the slope at this point. The angular position curves match well in magnitudes, but again the simulation curve peaks about 40 msec sooner than the experimental curve. Head resultant and T_1 resultant acceleration simulation curves show the bimodal characteristics and are of similar magnitude to the experimental curves but the second spikes occur earlier (i.e., the frequency is higher) for the simulation curves.

On the angular position curves, the symbols indicate the times at which the subject has reached the joint stops as determined by the procedures in Section B.2. In both cases the subject initially contacts the joint stop at the condyles with the head/neck joint in extension (i.e., angle β in Figure 3.2 initially increases). At 15 G's the subject reaches the condyle joint stop in flexion at about 123 msec and then reaches the lower neck joint stop in flexion at about 132 msec. At 6 G's the subject reaches the condyle joint stop in flexion at about 156 msec and does not reach the lower neck joint stop.

b. Neck Forces and Torques. Figures 3.19 and 3.20 show the magnitudes of the neck joint torques contributed by viscous, muscular, and joint stop mechanisms in the simulations at 6 and 15 G's respectively. It will be noted that the contributions due to joint stops are relative-

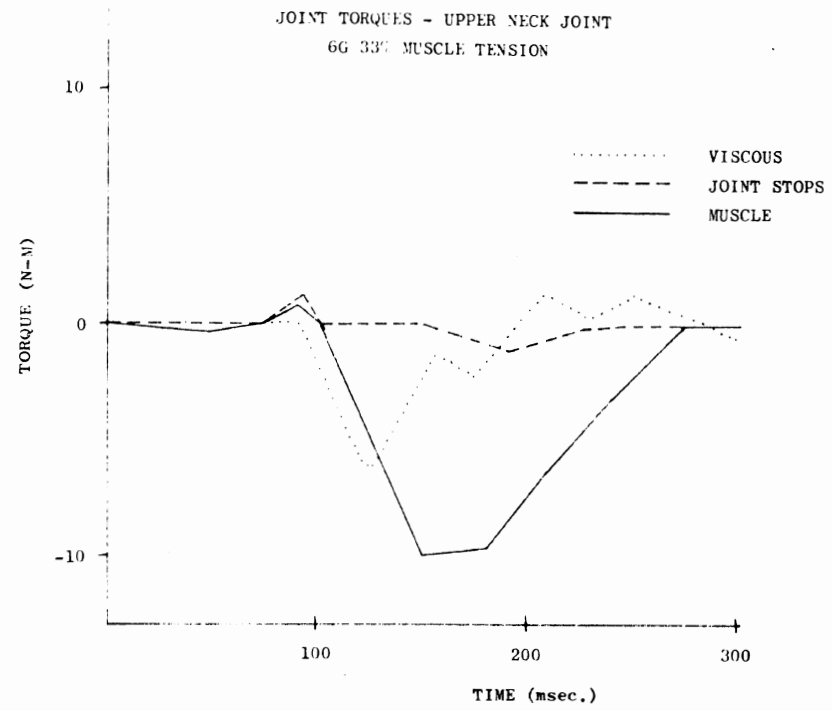

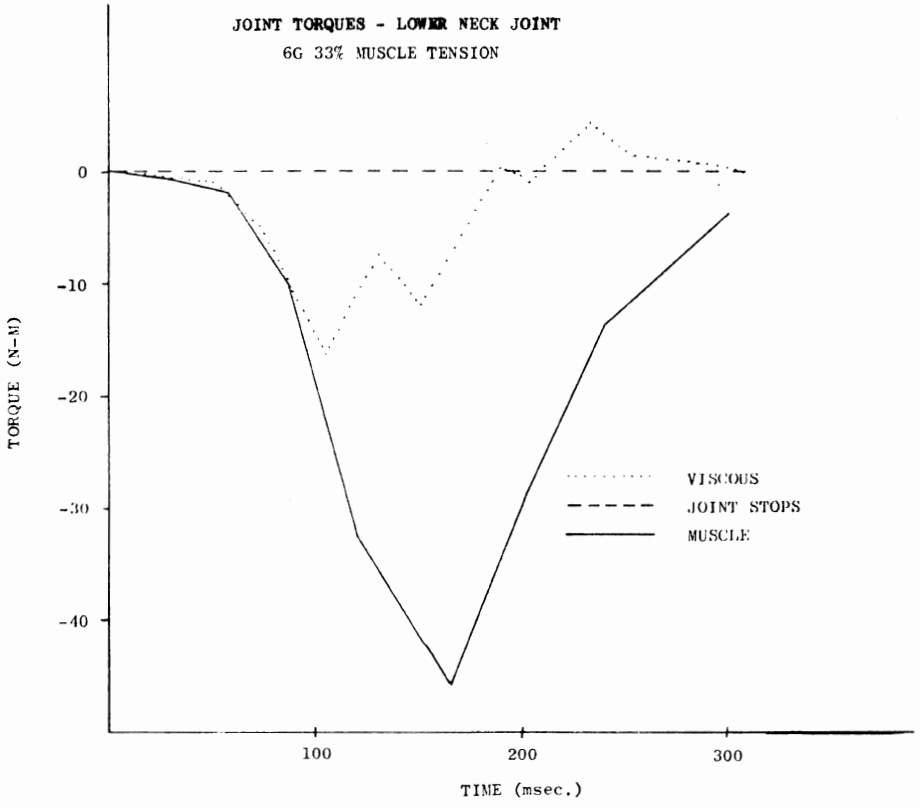

Figure 3.19 Neck Joint Torques in 6 G Simulation. Muscle Tension = 33% Maximum, Viscous Coefficients = .01 N-m-sec/deg for Upper Neck and .03 N-m-sec/deg for Lower Neck. Joint Stop Coefficients = .0261 N-m/deg for Upper Neck in Flexion, 1.0 N-m/deg for Upper Neck in Extension, and .0087 N-m/deg for Lower Neck in Flexion and Extension.

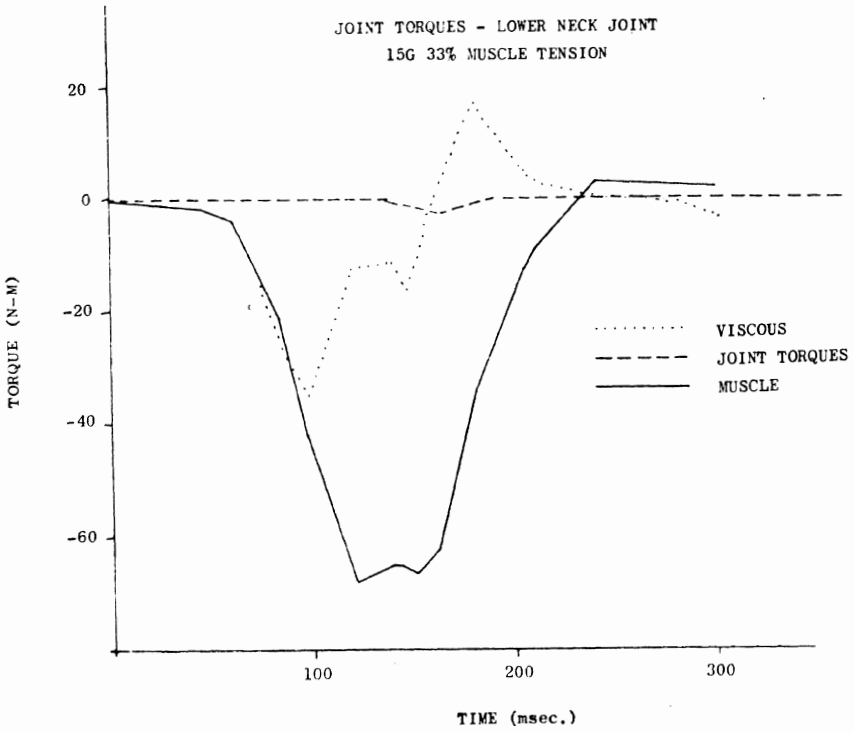

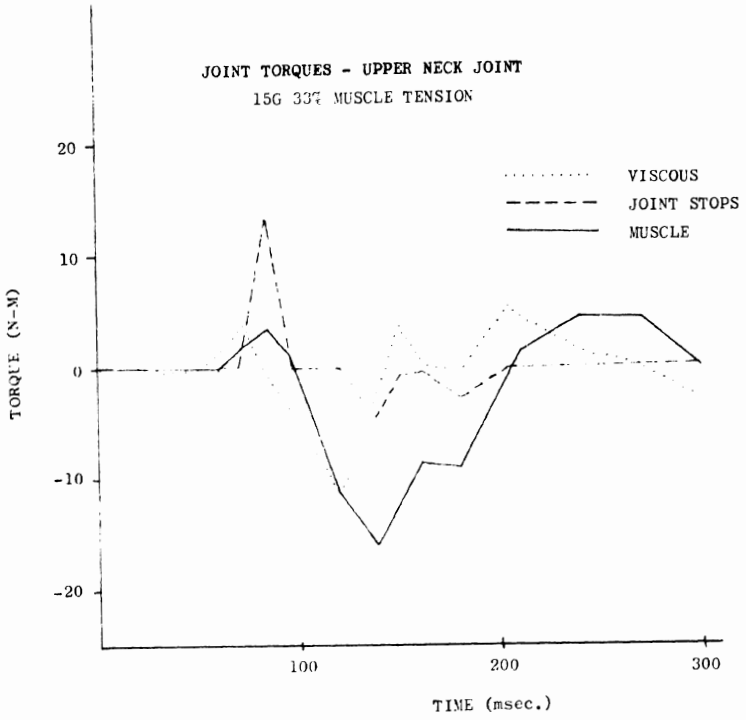

Figure 3.20 Neck Joint Torques in 15 G Simulation. Muscle Tension = 33% Maximum, Viscous Coefficients = .01 N-m-sec/deg for Upper Neck and .03 N-m-sec/deg for Lower Neck. Joint Stop Coefficients - .0261 N-m/deg for Upper Neck in Flexion, 1.0 N-m/deg for Upper Neck in Extension, and .0087 N-m/deg for Lower Neck in Flexion and Extension.

ly small (except for the condyles in extension) due to the small values of quadratic deflection coefficients used. It is also seen that the muscle provides the major restraining torque at both joints and at both G levels, the proportion to viscous torques being greater for the 6 G simulation.

Figure 3.21 illustrates the neck forces in tension (negative) and the compression (positive) contributed by muscle, viscous, and elastic components at 6 and 15 G's. It is seen that the proportional contribution of the force due to muscle is greater at 6 G's than at 15 G's.

c. Belt Forces. Figure 3.22 illustrates the belt forces developed versus time for each run. Since the deflection of the upper torso belt does not exceed 5 cm (it reaches about 3.5 cm at 15 G's) the forces in this belt (belt 2) and belt 3 (see Figure 3.6) do not exceed 70 N. As one might expect, the force time-curve for the fake chest belt shows the same multi-peak characteristics as the T_1 resultant acceleration curves.

d. Effect of Increasing Neck Joint Stop Stiffness. Figure 3.23 illustrates the effect on the 15 G results of increasing the joint stop quadratic deflection coefficients to what would seem to be more realistic values of 2.0 N-m/deg^2 at the condyles and 1.0 N-m/deg^2 at C_7-T_1. The primary effect (compare with Figure 3.18) is the large negative spikes on the head angular acceleration curve which result from the head suddenly contacting the more rigid stops. It will be noticed, however, that the peak head angle position is not reduced significantly from that which resulted from the softened stops used in all other simulations.

e. Effect of Chest Compliance. Figures 3.24 and 3.25 illustrate the effects of changing the chest compliance factor to 3500 N/cm and 875 N/cm respectively. As expected, the primary change is in the frequency or

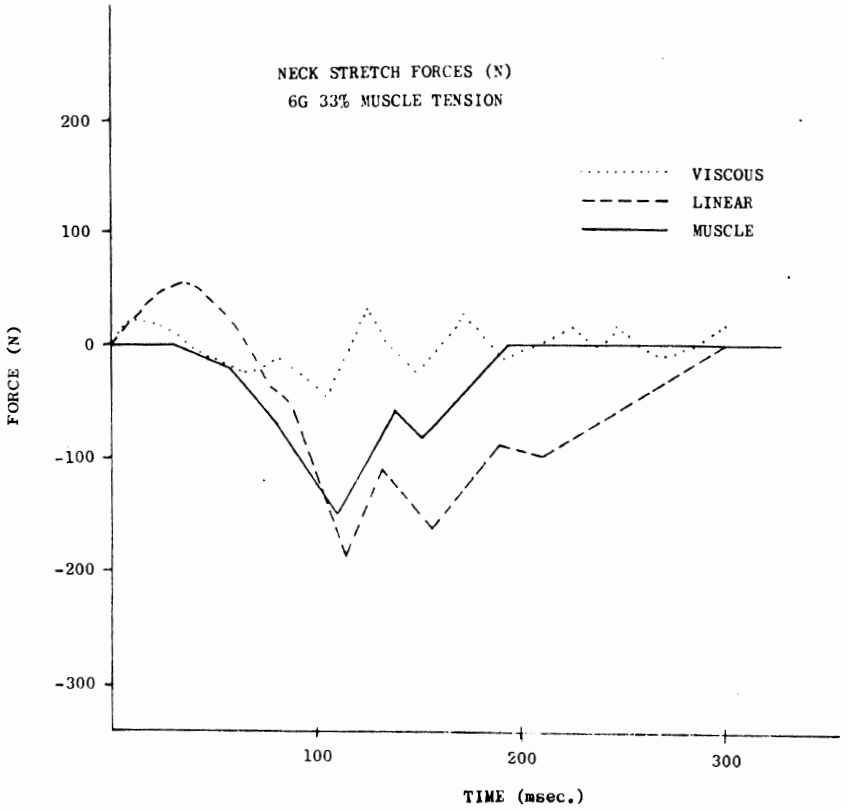

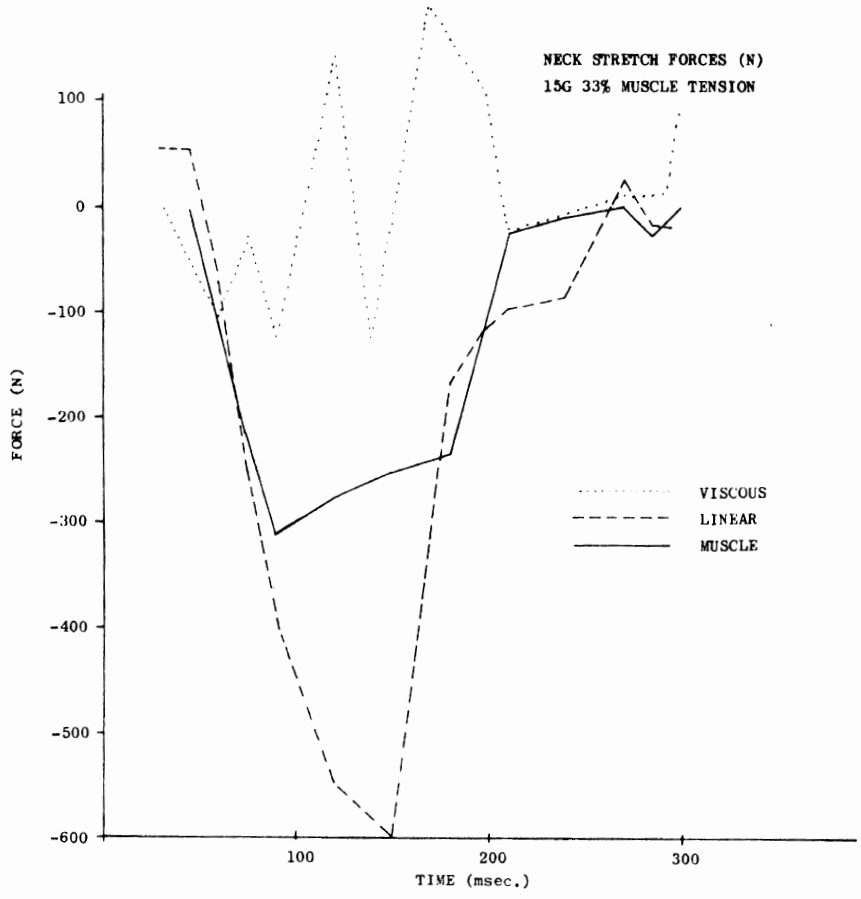

Figure 3.21 Longitudinal Neck Forces in 6 G (upper) and 15 G (lower) Simulations.

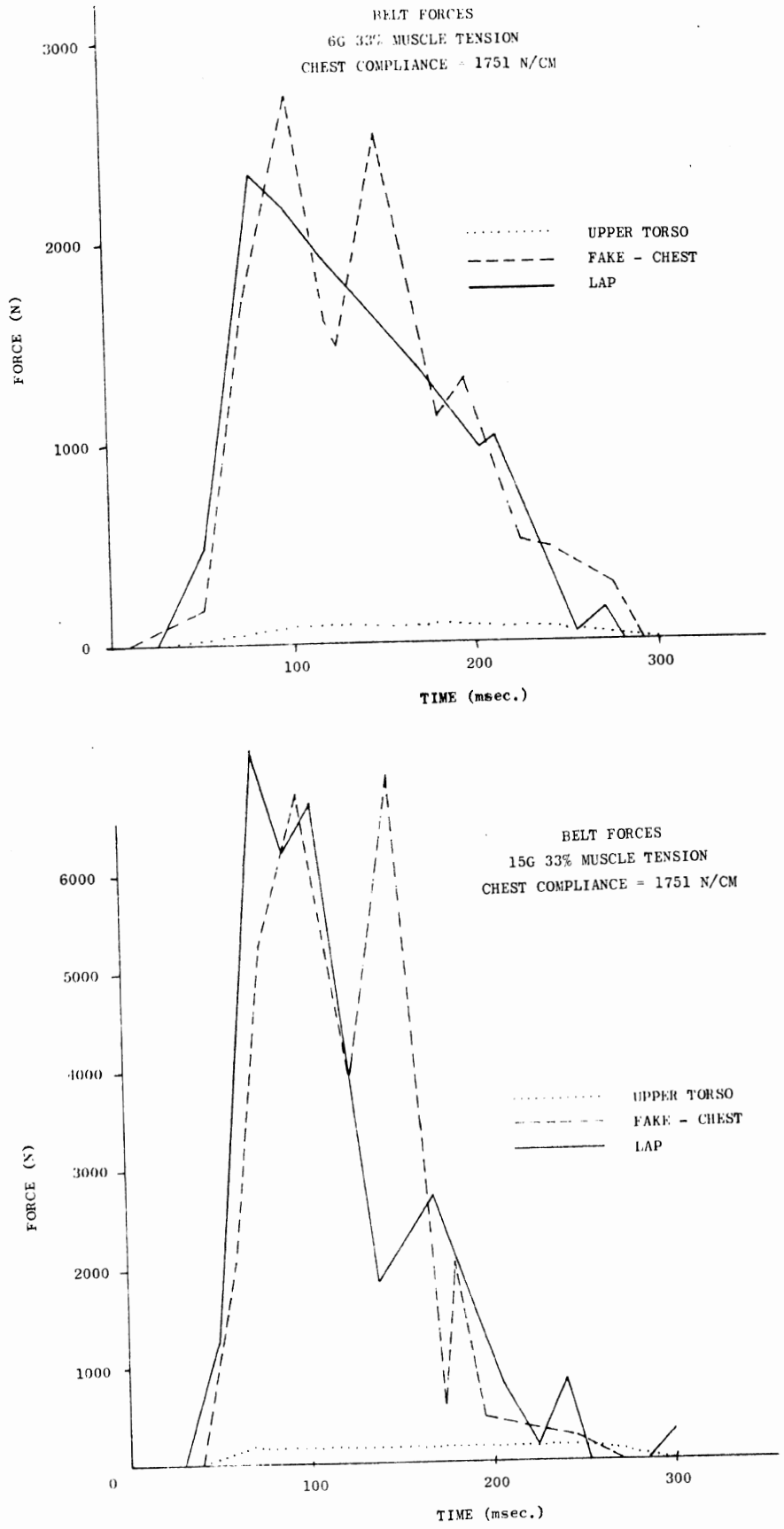

Figure 3.22 Belt Forces from 6 G (upper) and 15 G (lower) Simulations.

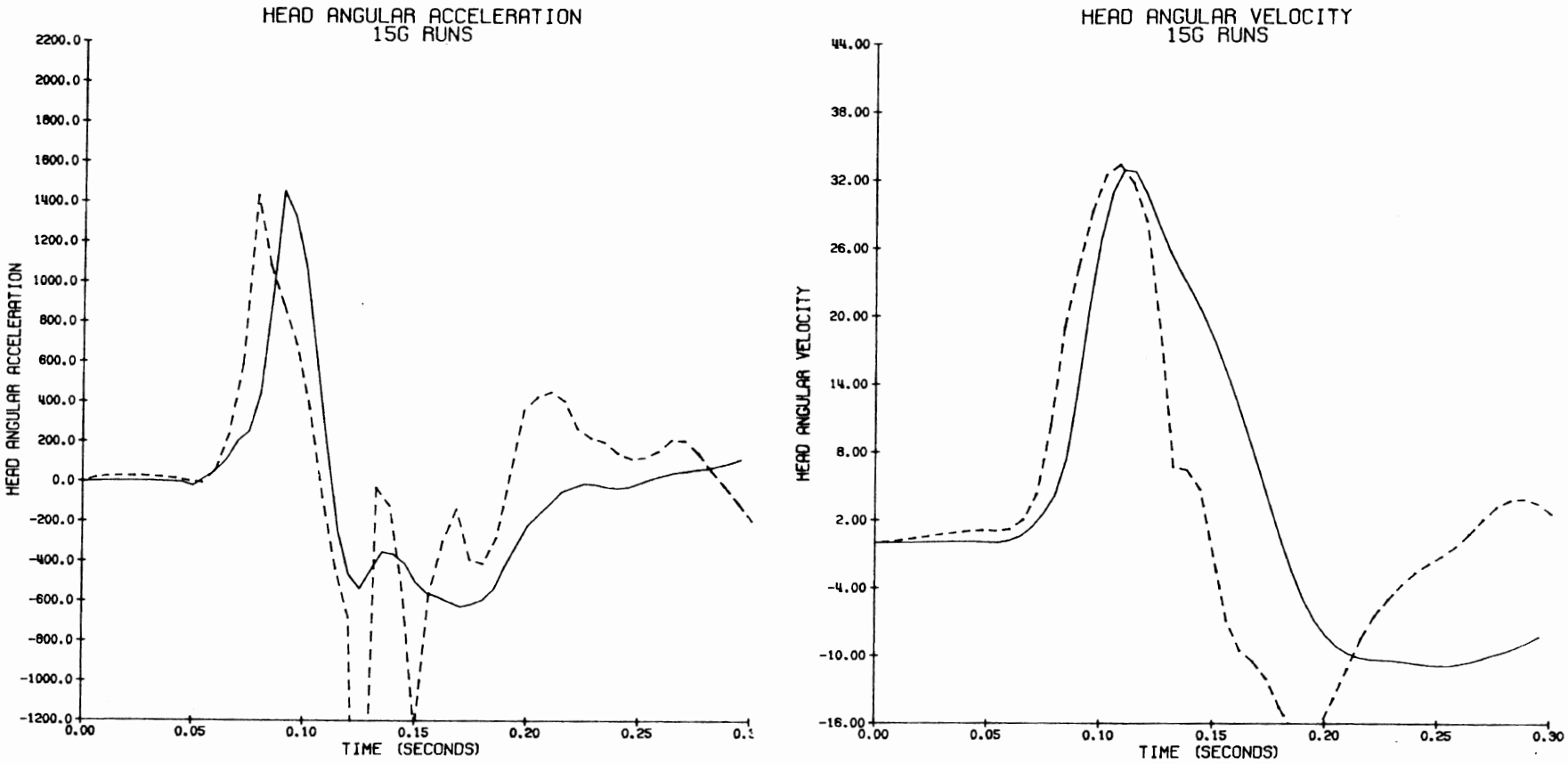

Figure 3.23 Simulation Results for 15 G Sled Acceleration. Muscle Tension = 33% Maximum, Chest Compliance = 1750 N/cm, Joint Stop Quadradic Deflection Coefficient Increased to 2.0 N-m/deg^2 for the condyles and 1.0 N-m/deg^2 for C_7-T_1.

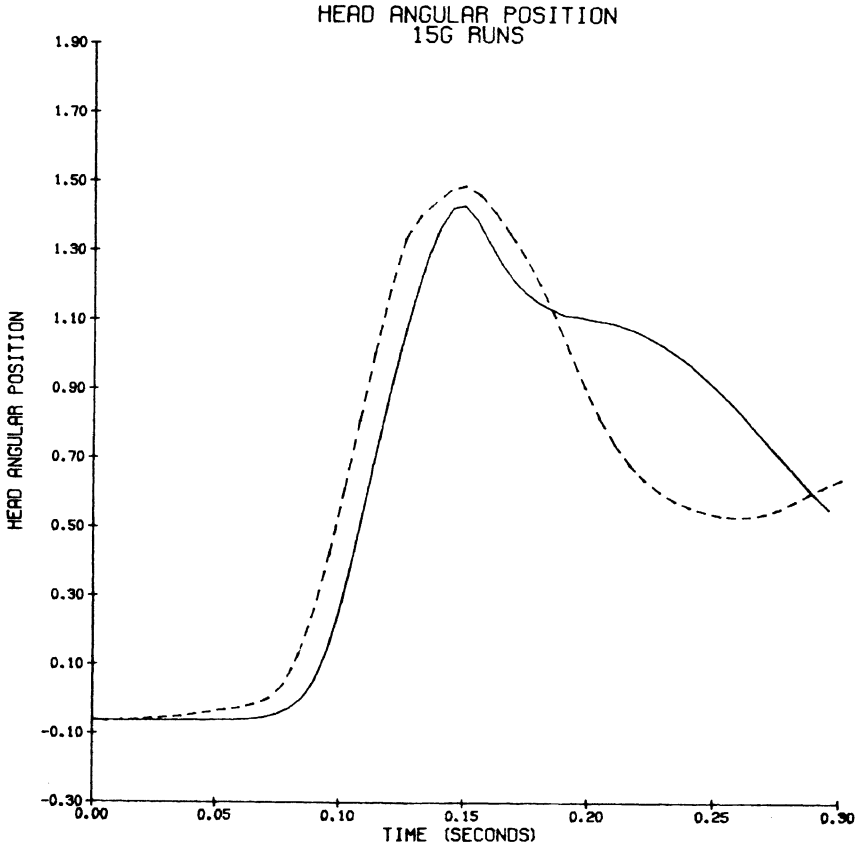

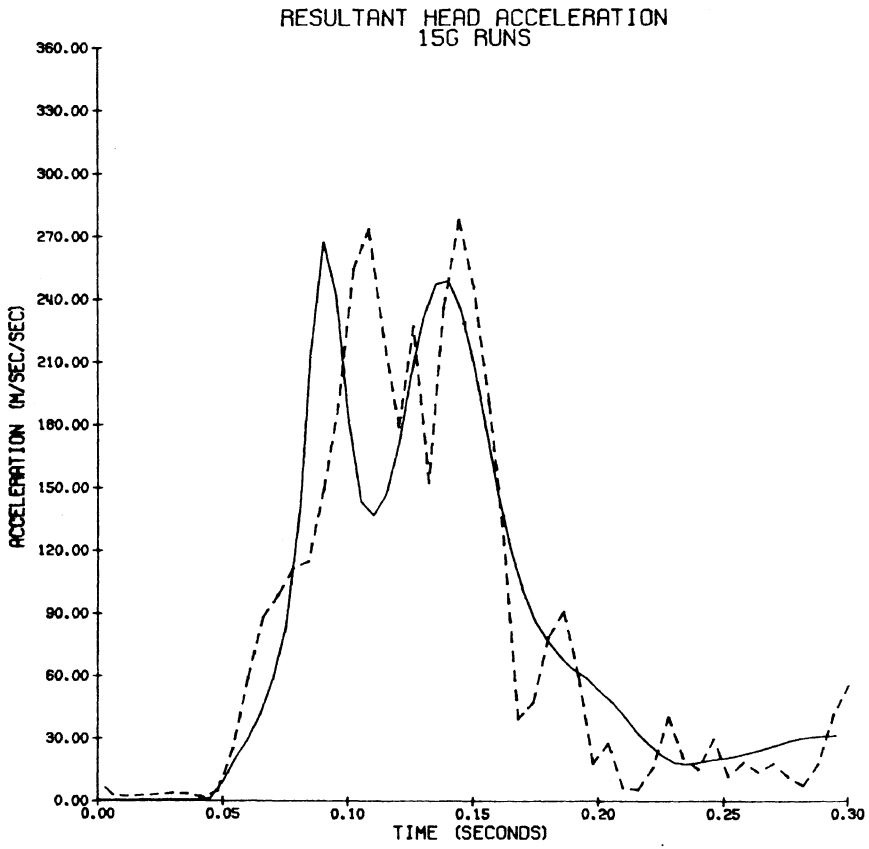

Figure 3.23 (continued)

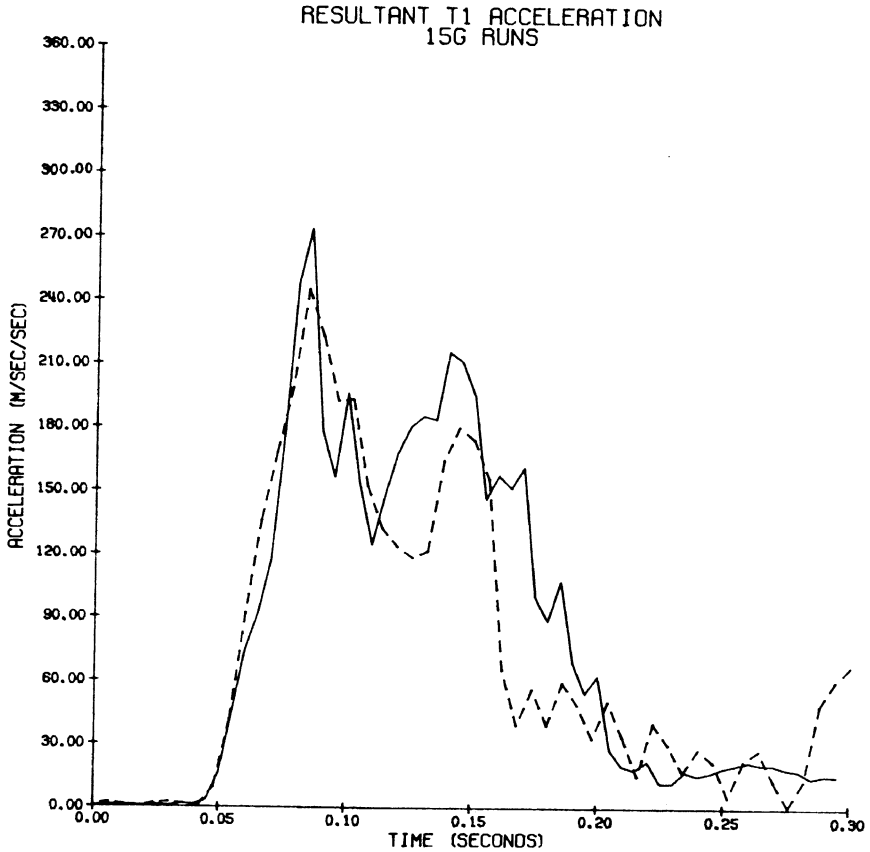

Figure 3.23 (continued)

times of occurrence of the peaks and valleys. With a stiffer chest the curves are sharper and peaks occur earlier. If one considers the T_1 resultant acceleration to be the best measure of chest compliance, then it would appear that 1751 N/cm (Figure 3.17) is the best value. The results for 875 N/cm (Figure 3.25) are complicated, however, by the fact that this lower chest compliance allowed greater than 5 cm deflection of the upper torso belt and the real belt properties came into play at about 96 msec. (see Figure 3.7) This resulted in a sudden additional acceleration to the chest and head causing the curves to change shape more than would have been produced by changing chest compliance alone. It is clear that further work is needed to improve this part of the restraint system modeling.

f. Effect of Reducing Condyle Joint Stop Stiffness in Extension. As indicated in Section B.3, the condyle joint stop stiffness coefficient in extension was maintained reasonably close to the MVMA-2D baseline values at 1.0 N-m/deg^2 while other joint stop coefficients were reduced substantially. The reasoning behind this was that in the initial position the subject's head/neck angle is very close to the maximum head/neck angle in extension determined by the procedures outlined in Section B.2. Since considerable effort is exerted by the subjects to achieve this position during range-of-motion testing, the MVMA-2D coefficients seemed a more reasonable approximation to model the initial joint torque situation. In an effort to determine the appropriateness of this assumption, a simulation run was made with this joint stop coefficient reduced to .0261 N-m/deg as is used for the condyles in flexion. Figure 3.26 shows the results of this run. In comparing these curves with those of Figure 3.18, it is seen that the only significant change is that the initial peak of the angular acceleration curve is reduced slightly but more important, it is delayed in time so that it is

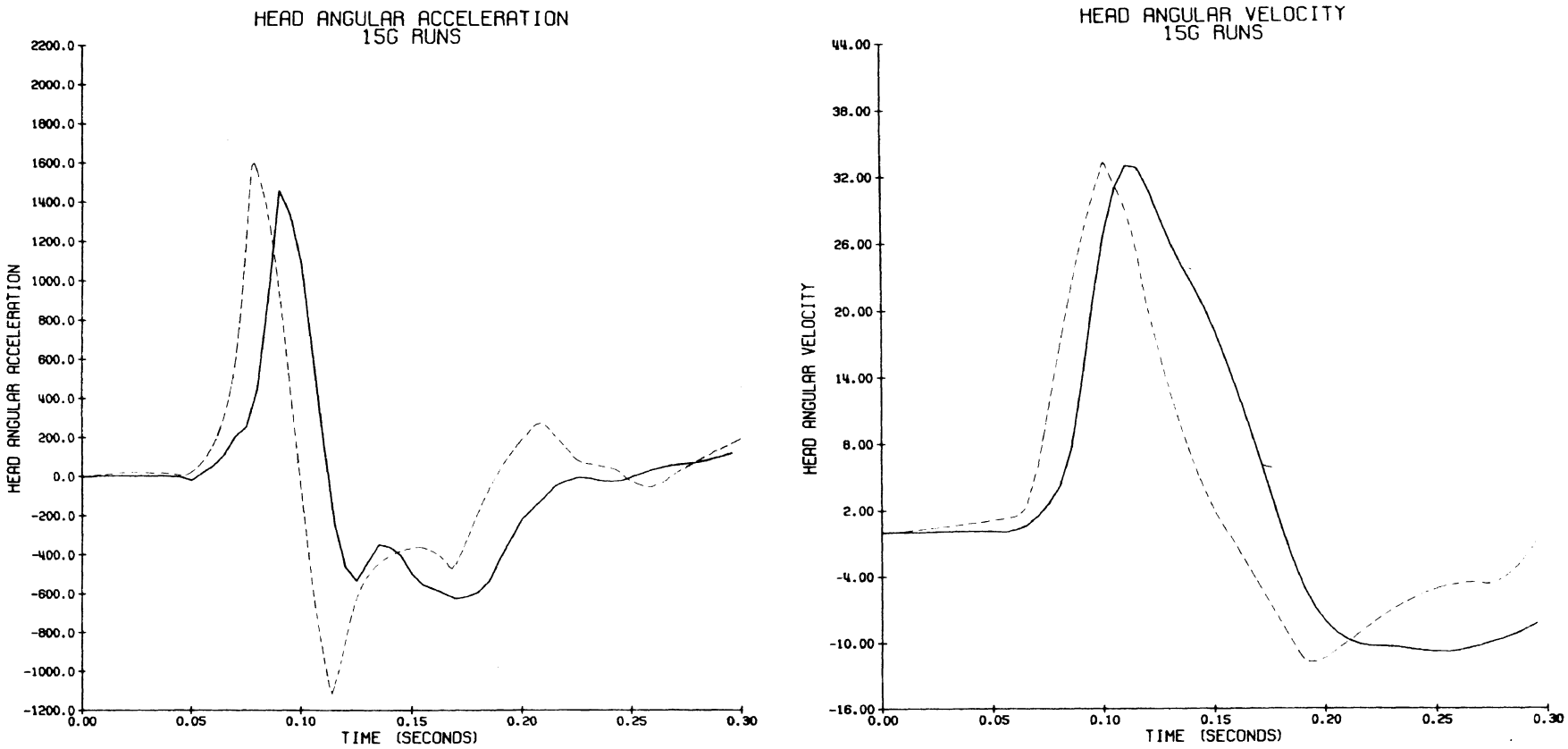

Figure 3.24 Simulation Results for 15 G Sled Acceleration-
Muscle Tension = 33% Maximum, Chest Compliance = 3500 N/cm.

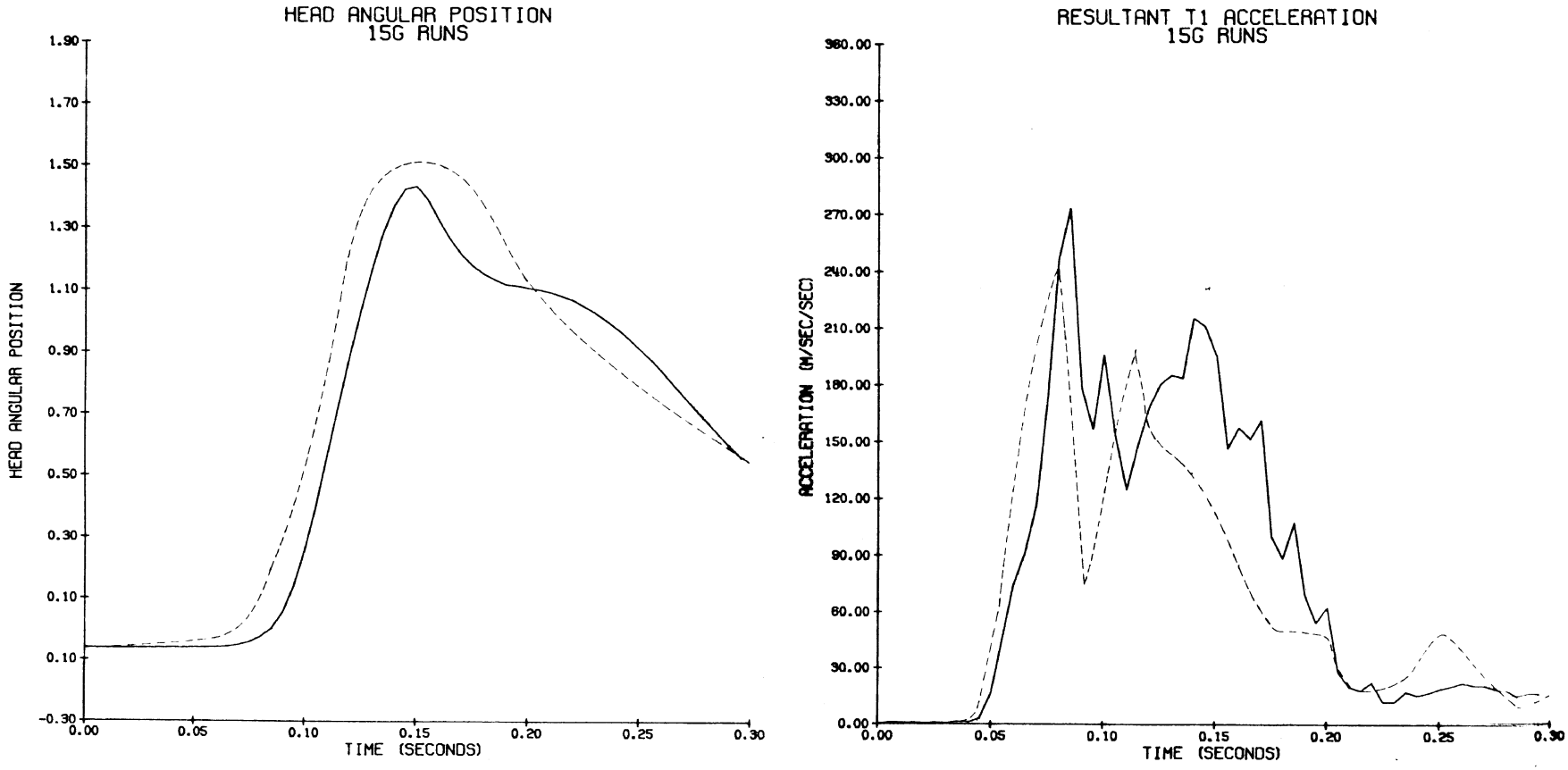

Figure 3.24 (continued)

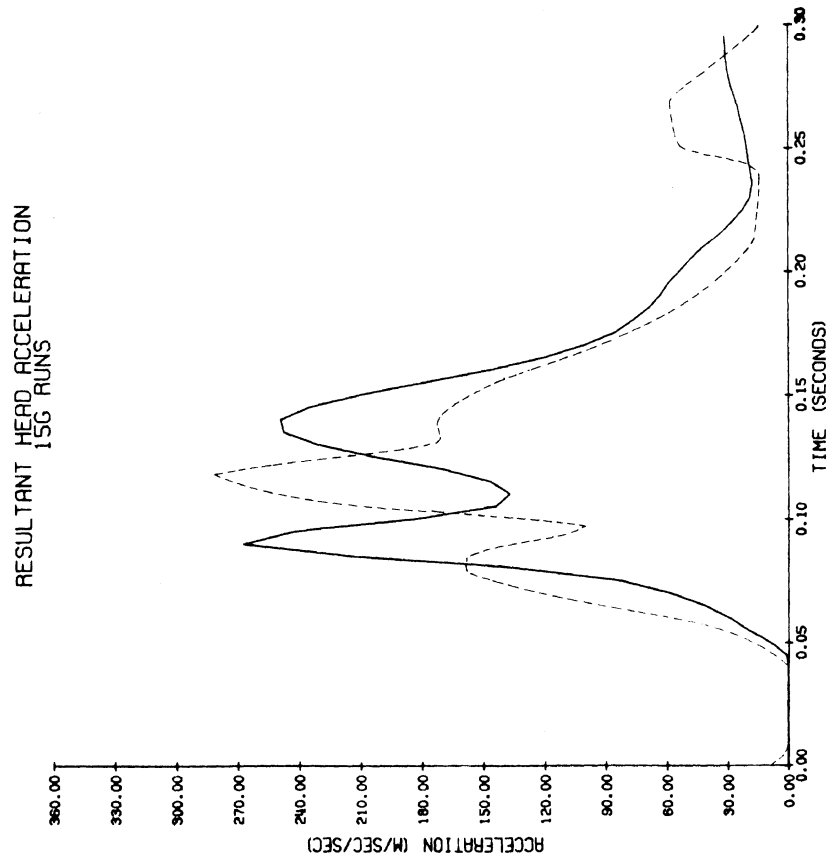

Figure 3.24 (continued)

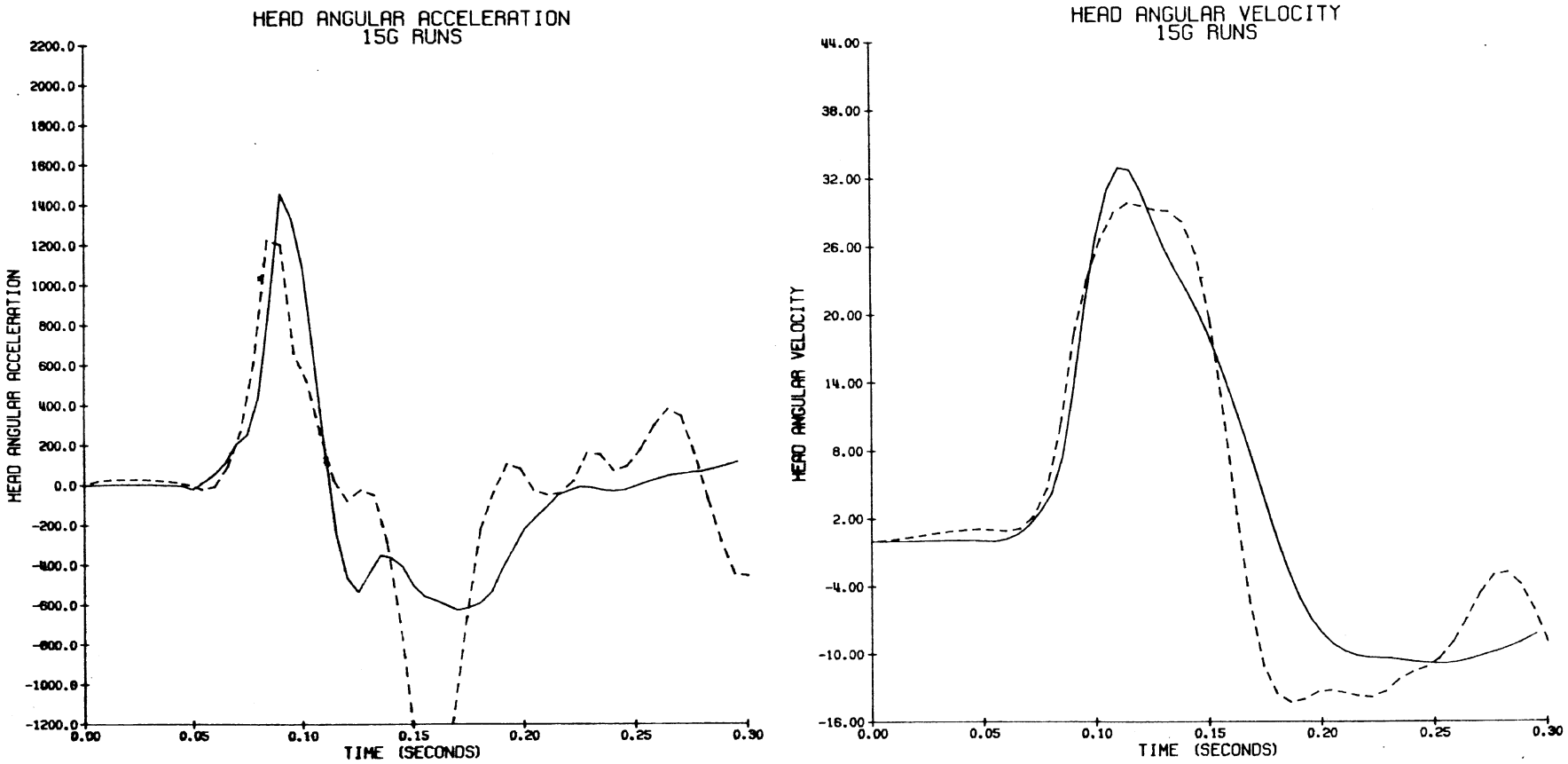

Figure 3.25 Simulation Results for 15 G Sled Acceleration-
Muscle Tension = 33% Maximum, Chest Compliance = 875 N/cm.

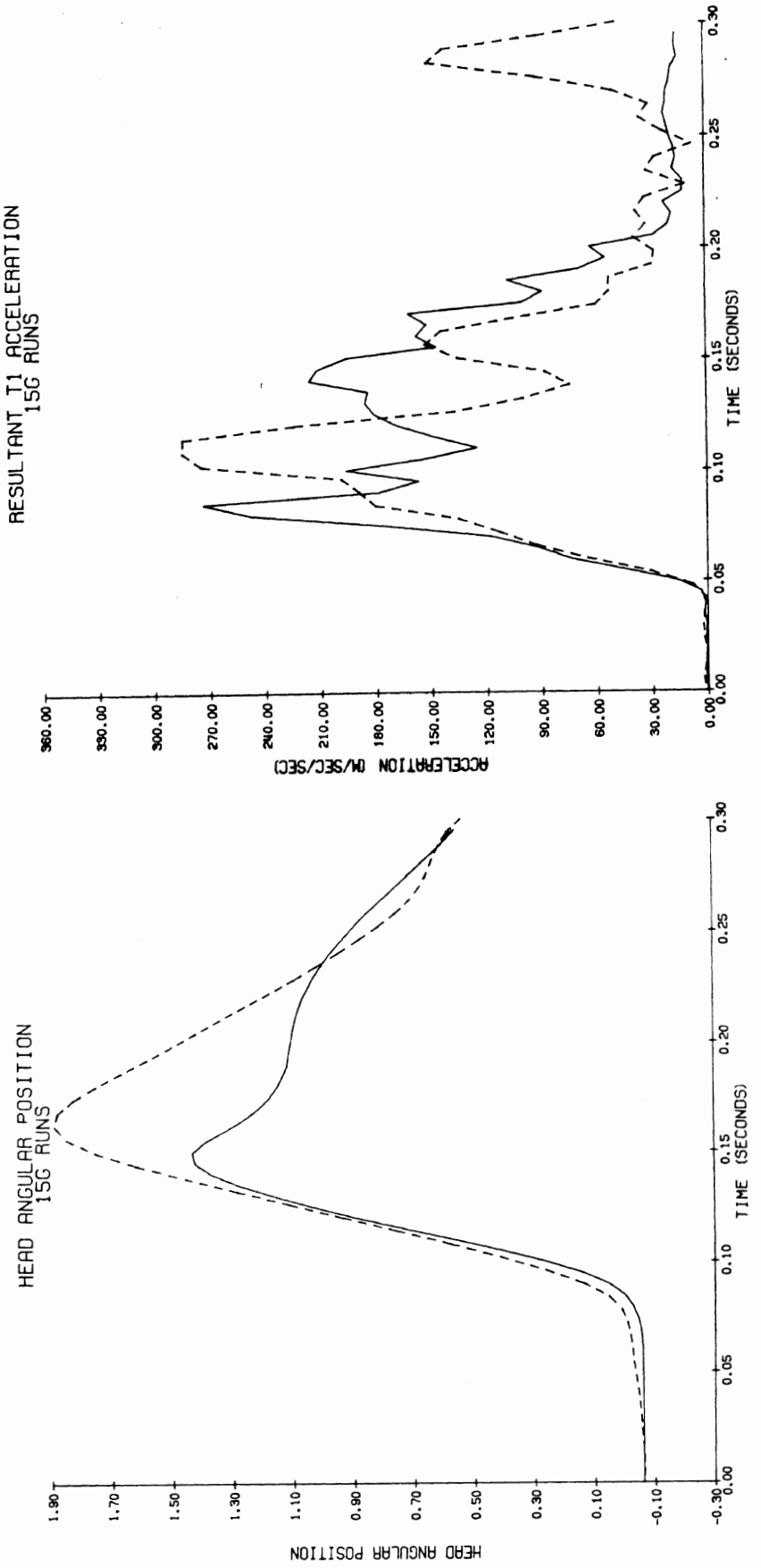

Figure 3.25 (continued)

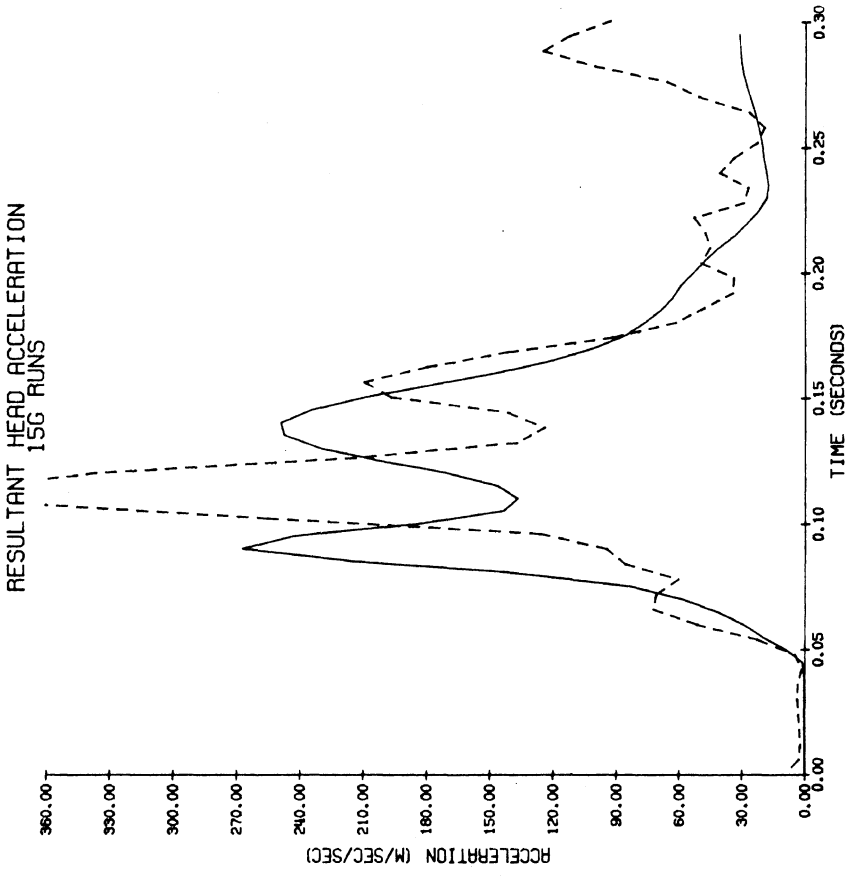

Figure 3.25 (continued)

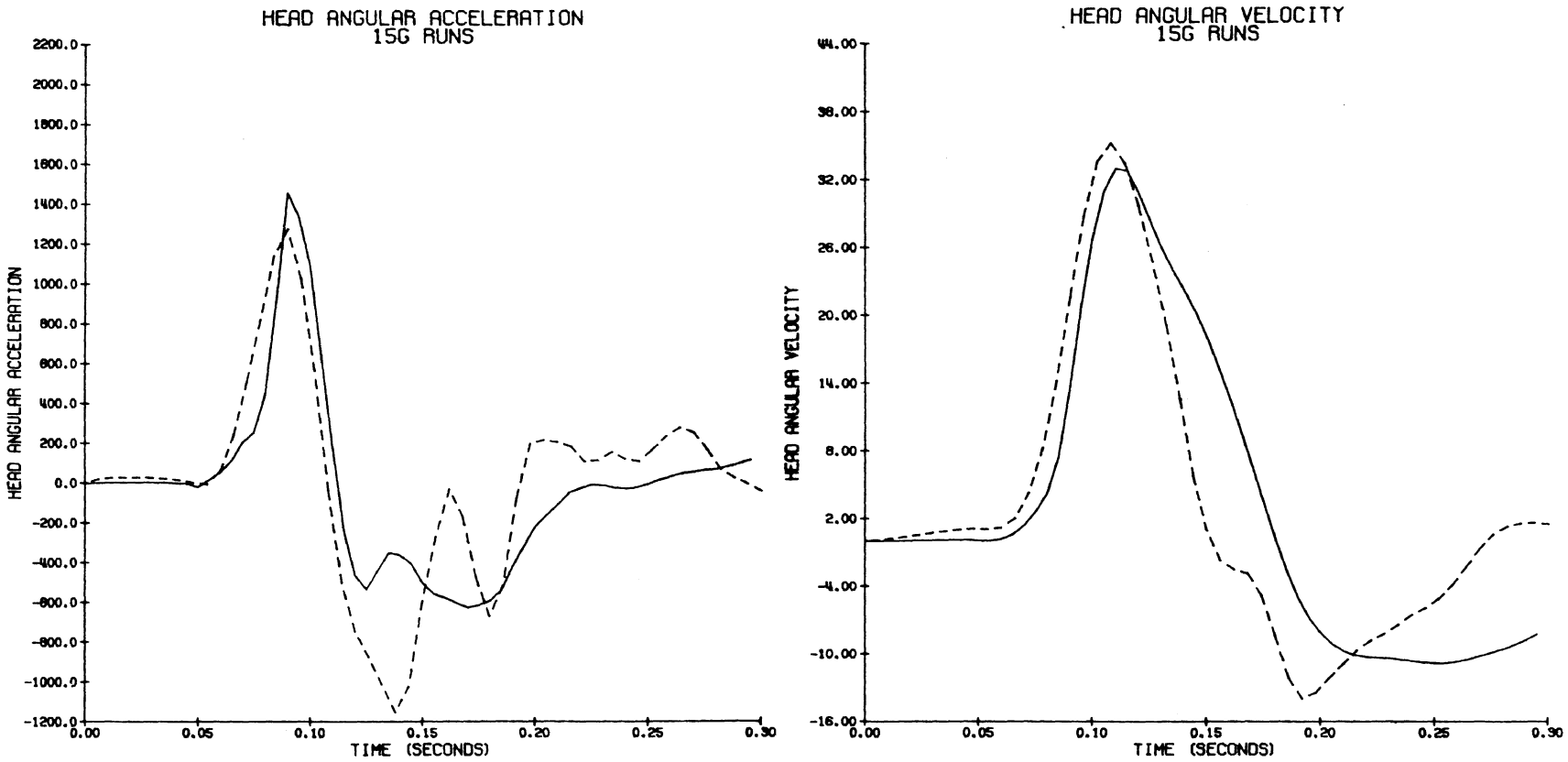

Figure 3.26 Simulation Results for 15 G Sled Acceleration - Muscle Tension = 33% Maximum, Chest Compliance = 1750 N/cm, Condyle Joint Stop Stiffness in Extension decreased to .0261 N-m/deg^2.

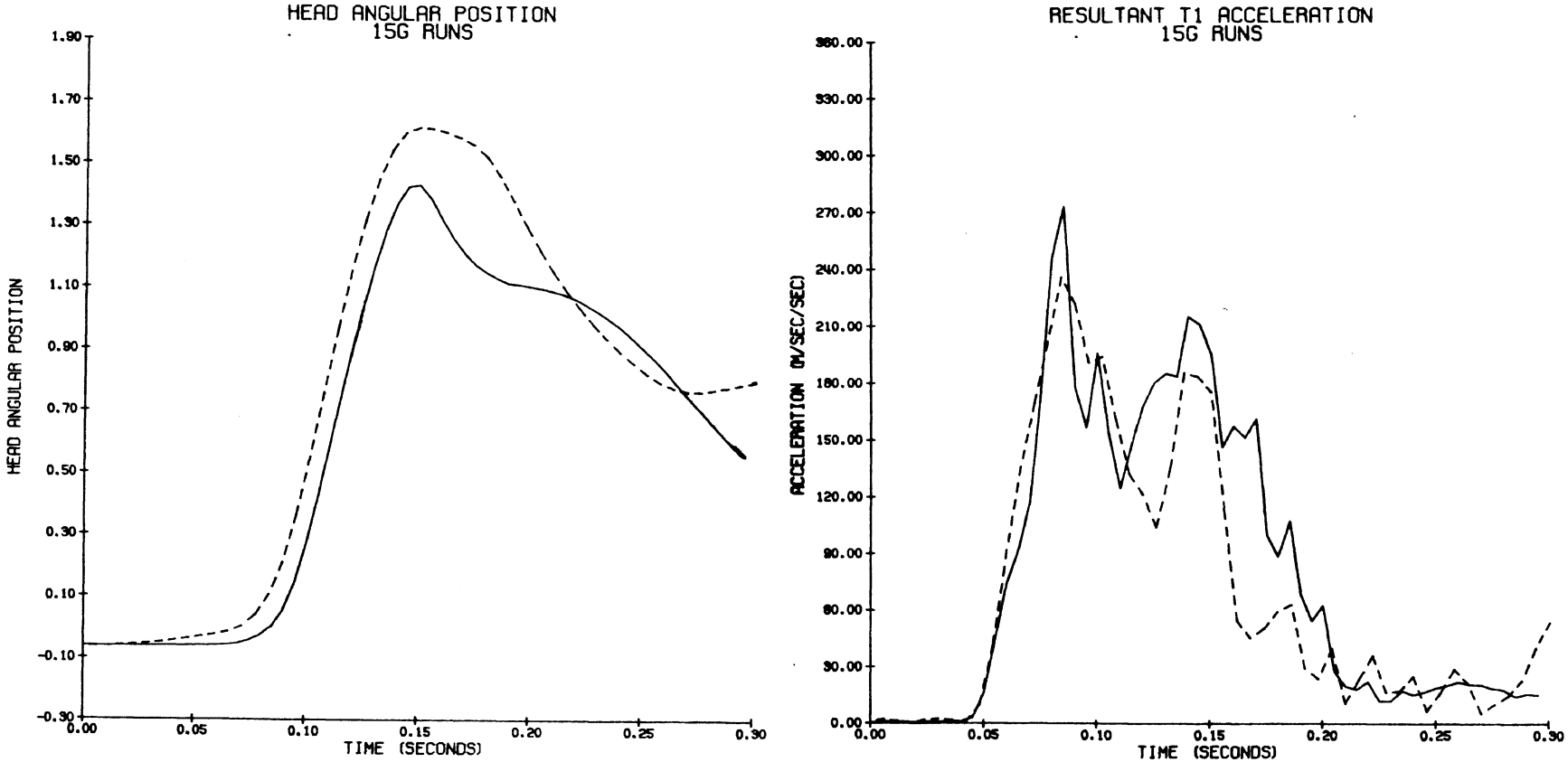

Figure 3.26 (continued)

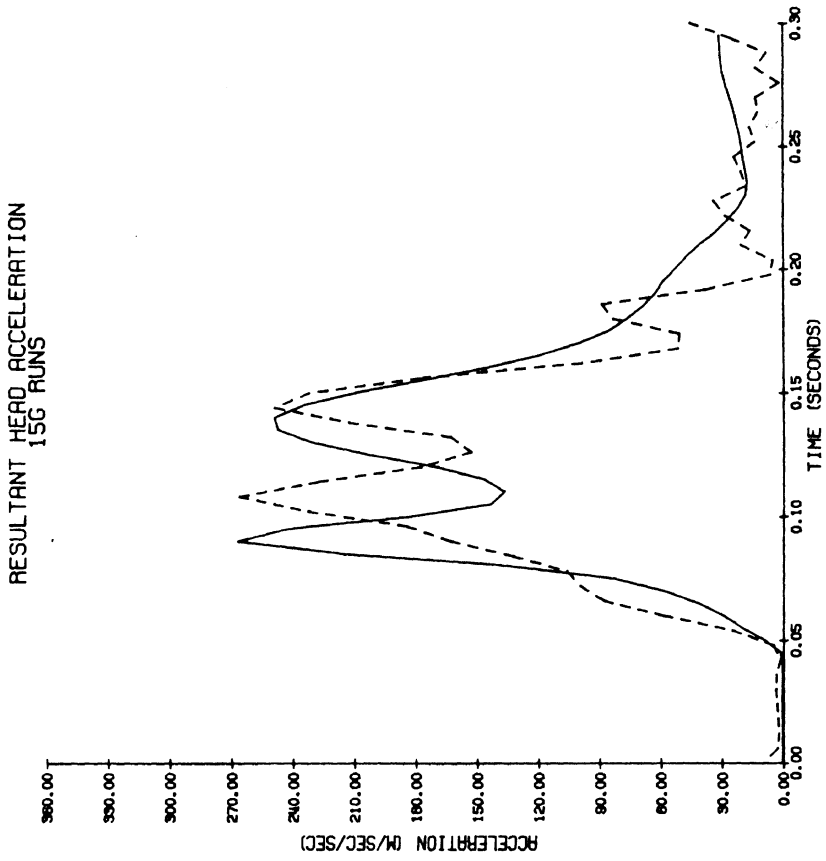

Figure 3.26 (continued)

more in phase with the experimental curve. Figure 3.27 illustrates the head/neck angle curves for the two cases. The difference is small but significant in terms of the time shift in the peak of the angular acceleration curve. For the smaller joint stop stiffness coefficient, the head is allowed to extend backward relative to the neck an additional 2-3 degrees, resulting in a time delay of about 8 msec before the head begins to rotate forward. The effect that this change would have on improving the 6 G simulations has not yet been determined, but it is evident that further work is needed in modeling the joint stop characteristics.

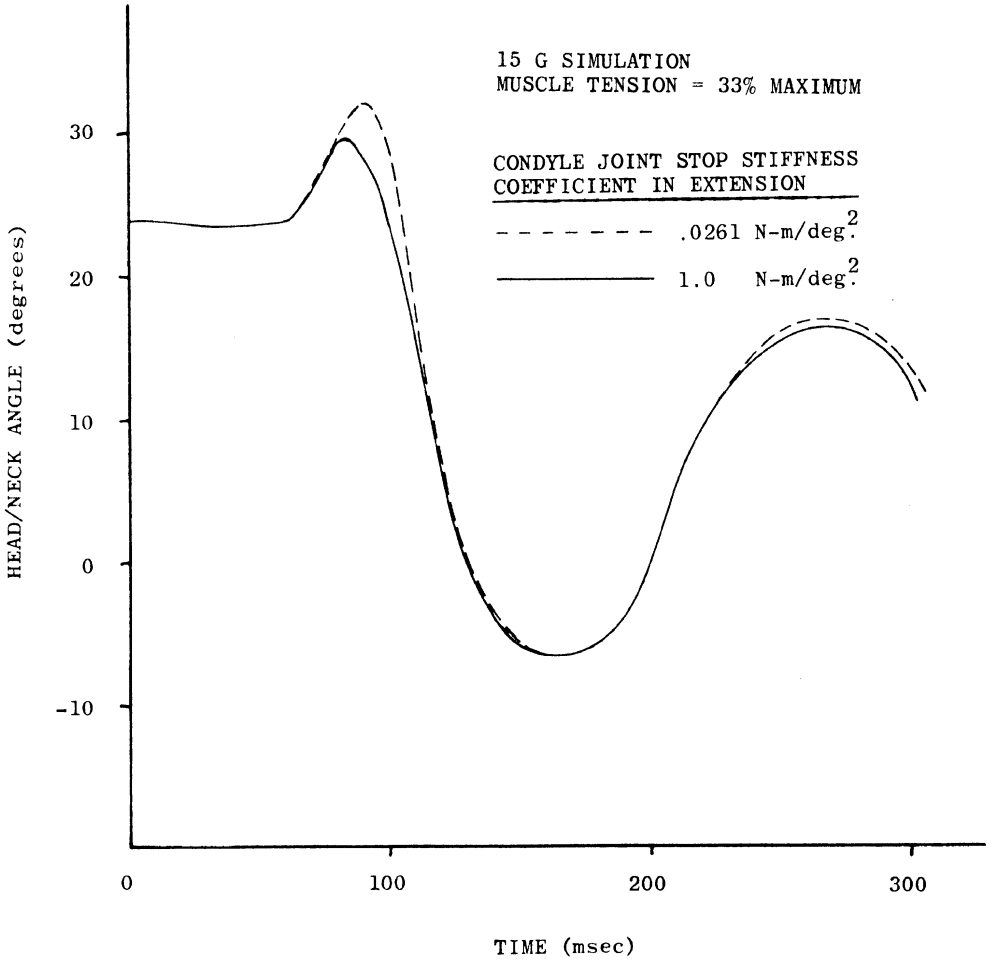

Figure 3.27 Head/Neck Angle versus Time for Condyle Joint Stop Stiffnesses of .0261 N-m/deg.^{2} (dashed line) and 1.0 N-m/deg.^{2} (solid line).

g. Effect of Adding Upper Torso Flexion. As described in section B.1, the torso segment lengths were changed from the proportions of the MVMA-2D baseline data set so that the upper torso joint (joint 3 of Figure 3.1) is above the chest restraint belt. In this way, some amount of torso flexion which is observed in the high speed movies may be added by adjusting the stiffness of this joint. In the runs presented so far, this stiffness was maintained sufficiently high (500 N-m/deg) so that almost no torso flexion occurred. This was done primarily because the maximum head angle of the simulations was already greater than the experimental results and adding torso flexion would increase this angle further. In addition, the parameters established by using T_1 accelerations as the input were based upon no rotation of T_1. It is considered important, however, that this feature be eventually included in the model. Figure 3.28 shows the results obtained at 15 G's by reducing the linear stiffness coefficient of joint 3 from 500 to 75 N-m/deg while maintaining the reduced joint stop coefficient of the condyles in extension (Figure 3.26). Again, the changes are not dramatic but are informative. The angular acceleration curve is seen to be further improved in that the initial peak is increased in magnitude slightly and is a better fit to the experimental curve in the time following this peak. The angular velocity curve no longer has the plateau at 150 msec and crosses zero slightly later in time. While the angular position curve reaches a greater maximum angle by about 6 degrees (the upper torso angle now flexes by about 6 degrees) it does not show the tendency to curve up again at 275 msec. While these changes represent improvement in the simulations, it is curious that the T_1 and head resultant acceleration curves match less well to the experimental results when this torso flexion is allowed.

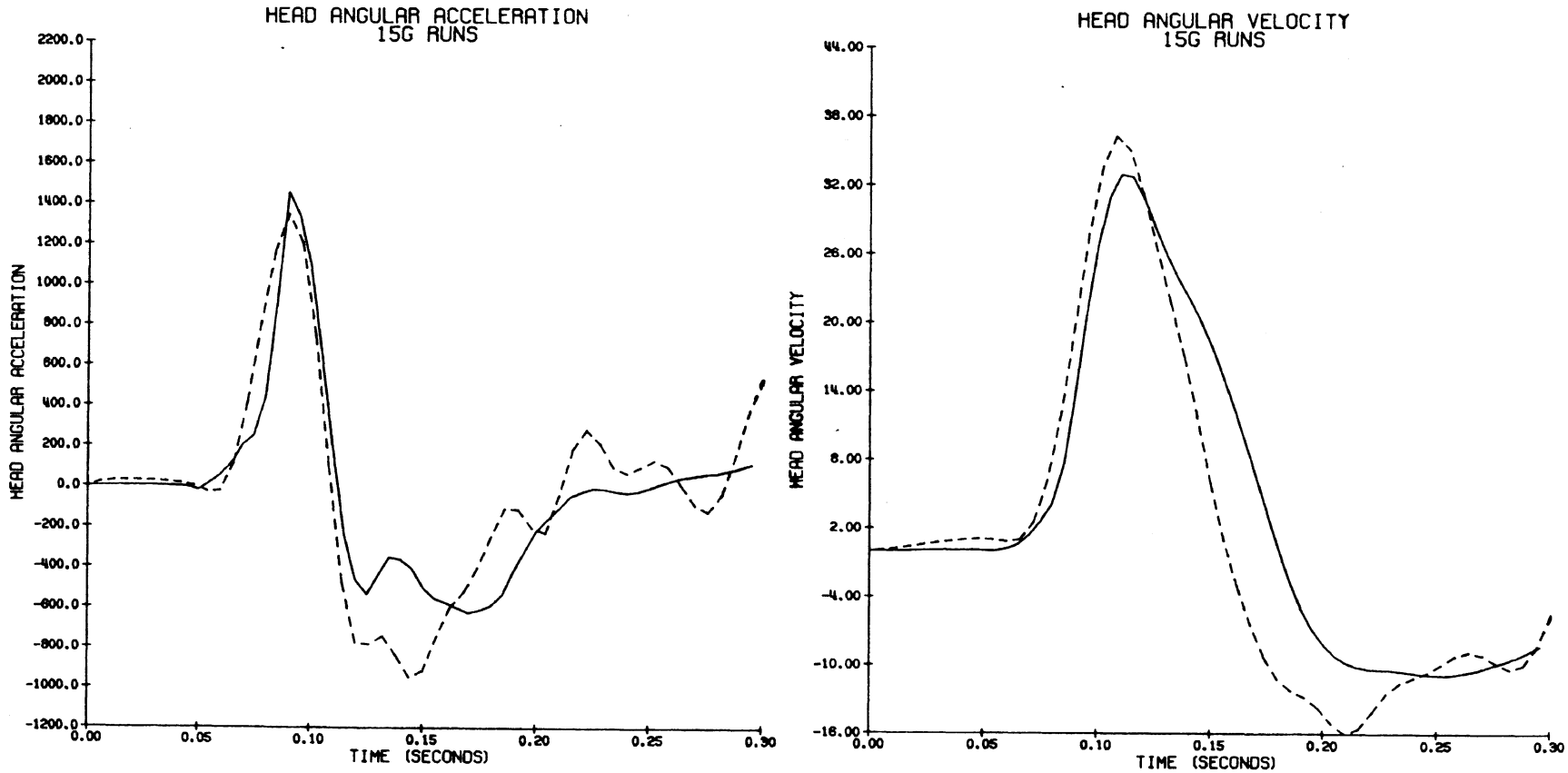

Figure 3.28 Simulation Results for 15 G Sled Acceleration - Muscle Tension = 33% Maximum, Chest Compliance = 1750 N/cm, Condyle Joint Stop Stiffness in Extension decreased to .0261 N-m/deg^2, Joint 3 Linear Stiffness Coefficient Reduced to 75 N-m/deg.

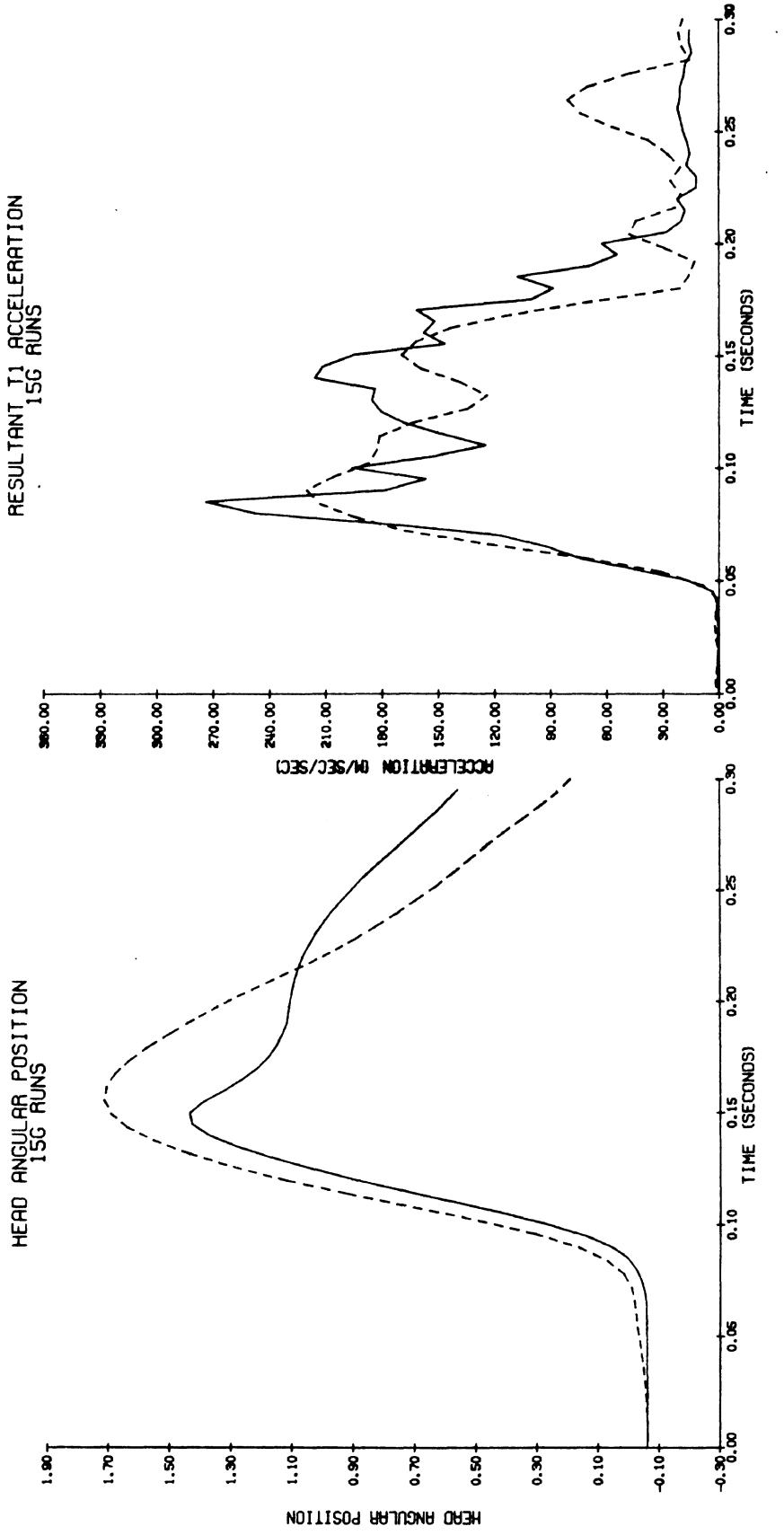

Figure 3.28 (continued)

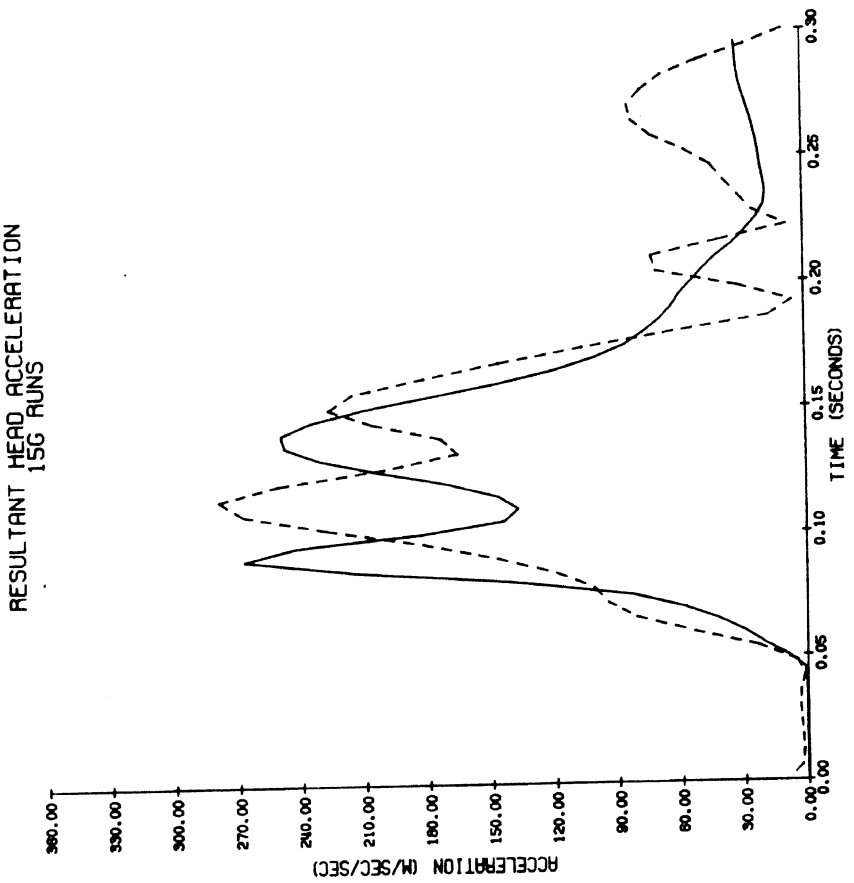

Figure 3.28 (continued)

Chapter 4

SIMULATIONS FOR 18-24 YEAR FEMALES

A. 18-24 Year Female Data Set.

While there are several aspects of the NAMRL data set and simulation which can be improved by further work and investigations, an attempt was made at this time to predict the sled test results that might be expected if young females were tested at 6 and 15 G's. The data set for these subjects was obtained by scaling the NAMRL data set parameter values using similar procedures to those discussed in Chapter 3, Section B and the measurement data obtained for these subjects and presented in references 22 and 23.

1. Segment Specifications

a. Torso and Extremities. Torso length was computed in the same manner as for the NAMRL subjects and the segment lengths taken in the same percentages of total torso length. Extremity lengths were taken from the same anthropometric measurements and again the arms were removed and one half of the upper arm mass was added to the upper torso mass. Values of mass, moment of inertia, and distances to centers of mass from joints were computed by scaling to the NAMRL data set values in a manner similar to that used for scaling NAMRL data to the MVMA baseline data. The result of the calculations gave the parameter values shown in Table 4.1.

Table 4.1

Torso and Extremity Segment Specifications
For 18-24 Year Female Data Set

Segment	Length(cm)	End of Link to Center of Mass (cm)	Mass(kg)	IYY(Kg-m^2)
Upper Torso	17.78	8.89	11.4	.087
Middle Torso	22.95	8.5	7.9	.095
Hip	9.95	3.84	6.55	.133
Upper Leg	41.88	19.03	13.7	.222
Lower Leg	40.5	25.47	7.4	.208

b. Head and Neck Mass and Moment of Inertia. Head mass for the females was estimated by assuming that head mass is proportional to [Head Length x Head Breadth] and scaling to the Navy data based on the ratio of these values for both data sets. By these calculations, the female head mass is .885 times the NAMRL head mass giving an instrumented head mass of 4.164 kg for the females. As with the NAMRL subjects, female head moment of inertia was calculated from the male cadaver data of Chandler, et al. (3) using the relationship that head moment of inertia is proportional to [(Menton to vertex)^2 + (head length)^2] x [Head circumference]. This gives an instrumented head moment of inertia for young females of .0211 Kg-m^2.

Female neck mass was scaled to the NAMRL neck mass by assuming that mass is proportional to volume and that the neck is a cylinder whose circumference is equal to the average of superior and inferior neck circumference and whose length is proportional to erect sitting height. This gives a female neck mass of 1.194 Kg. of which 33% was placed at the condyles and 67% at C_7-T_1.

c. Neck Length and Location of Head Center of Gravity. The location of the head center of gravity relative to the condyles was determined by measuring distances

from tragion to the condyles on x-rays from young females in the IIHS sagittal study. This gave average distances for tragion of .987 cm forward and 1.966 cm above the condyles. The distances given by Ewing, et al. (8) for the location of the c.g. relative to tragion and the shift in the c.g. due to the instrument package (9) on young males were assumed for the females also, and were added to the distances of tragion to condyles to give the location of the head center of gravity relative to the condyles. This gave:

x distance condyles to head c.g. = 2.3 cm.

y distance condyles to head c.g. = -4.07 cm.

Neck lengths for young females were obtained by direct measurement on x-rays of the linear distance from the condyle to C_7-T_1 disk. After appropriate scaling this give an average neck length of 10.6 cm. This is in good agreement with the value of 10.4 cm which would be obtained if neck length were scaled to the NAMRL neck length by the proportions of erect sitting height [i.e., (female sit. ht./NAMRL sit. ht.) x NAMRL neck length = (86.24/92.88) x 11.2 = 10.4 cm].

2. Head and Neck Range of Motion. Values of α, β, γ, δ, were determined for the NAMRL data set from x-rays of young males in the IIHS sagittal study (see Section B.2). The mean ranges of motion in flexion and extension for this group were 62.5 and 79.6 degrees respectively. For the young females the mean values for flexion and extension were 60.9 and 77.1 degrees respectively. Since these values do not differ significantly from the values for the males, the same values for α, β, γ, and δ were used for the female data set.

3. Passive Joint Torques and Joint Stops. Since the joint stop quadratic deflection coefficients used for the

NAMRL subjects have little physiological basis, the same values were used for the young females. Viscous coefficients, however, were scaled to the NAMRL data set values of .01 N-m-sec/deg and .03 N-m-sec/deg for the upper and lower neck joints respectively by the proportion of neck cross-sectional areas. The average of superior and inferior neck circumferences was used to determine neck radius which was computed to be 5.99 cm for the NAMRL subjects and 5.49 cm for the females. This gave a scaling factor of .84 which gives values of .0084 and .0252 N-m-sec/deg for the female upper and lower neck viscous coefficients.

4. Neck Muscle Parameters. Neck muscle parameters a_1, a_2, a_3, and a_1^{ℓ}, a_2^{ℓ}, a_3^{ℓ} were scaled to the NAMRL parameters using the relations given in equations 1 through 4 of section B.4 of Chapter 3. Distances ℓ_1, ℓ_2, ℓ_3, and ℓ_4 (see Figure 3.4) were assumed to be the same for the young females as were estimated for the NAMRL subjects. The neck length of 10.6 cm was used for ℓ_n. In extension, the average pull force for young females was 27.04 lbf compared to 48.3 lbf for the NAMRL subjects. In flexion the average pull force for young females was 19.4 lbf compared to 36 lbf for NAMRL subjects. Using these values and the procedures outlined in section B.4. of Chapter 3 and in greater detail in reference 1, the muscle parameter values shown in Table 4.2 for the young female data set were calculated.

Table 4.2

Muscle Parameter Values Used in 18-24 Year Female Data Set

	Parameter			
Location	a_1(N-m/deg)	a_2(deg^{-1})	a_3(sec/deg)	100% Muscle Torque (N-m)
Occ. Condyles	.03	.086	.007	6.51
C_7-T_1	.093	.086	.007	19.99
	a_1^{ℓ}(N/cm)	a_2^{ℓ}(cm^{-1})	a_3^{ℓ}(sec/cm)	100% Muscle Tension (N)
Neck Stretch	73.7	1.29	.15	938.5

As with the NAMRL subjects the muscle torques and tensions were maintained constant at 33% of maximum throughout the simulation.

5. Neck Stretch and Compression Parameters. The elastic and viscous coefficients which describe the viscoelastic properties of the neck in stretch and compression were maintained at C_s = 10.55 N-sec/cm and K_s = 1636 N/cm for the young female subjects. Variations of these values in simulations of NAMRL subjects showed the model to be relatively insensitive to changes in these parameters.

6. Head and Neck Initial Angles. The initial position of the head and neck were maintained the same as for the NAMRL subjects.

7. Restraint System and Chest Compliance. The restraint system configuration was maintained the same as for NAMRL subjects except for repositioning the anchor points and attachment points due to the change in body segment sizes. Chest compliance was maintained at 1751 N/cm or 1000 lb/in.

B. Simulations for 18-24 Year Females.

Figures 4.1 and 4.2 show the simulation results (dashed lines) in comparison to the NAMRL experimental results (solid line) and NAMRL simulation results (dotted line) for 6 and 15 G sled tests. In general, the results are not markedly different from the NAMRL results. The primary difference is in the angular position curves where the maximum head rotation is approximately 40 and 25 percent greater in the 6 and 15 G runs respectively. This increase in peak head angle is probably largely due to the weaker neck muscles and consequent changes in neck muscle model parameters. A second probable consequence of the weaker muscles is seen in the angular velocity curve at 6 G's where the curve is seen to return to zero more slowly (and interestingly in closer approximation with the NAMRL experimental curve). At 15 G's this portion of the angular velocity curve is not changed as much and this is perhaps another indication that the role of neck muscles is less important at higher G levels.

At 6 G's the initial peak in the angular acceleration curve is nearly identical in magnitude and time to the NAMRL simulation, but both occur sooner in time than the experimental results. At 15 G's the initial peak for the females is slightly larger and occurs slightly earlier than the NAMRL simulation. This earlier peaking may be a consequence of the smaller head mass and moment of inertia for the females. At both 6 and 15 G's the initial negative peak is reduced from the NAMRL simulations and this may also be a consequence of the reduced muscle strength. The reduction in these negative peaks is seen to be greater at 6 G's than at 15 G's.

Concerning the resultant acceleration, it is seen that at 6 G's the frequency of the bimodal portion of the curves is increased from the NAMRL simulations although the

initial spike occurs at about the same time. At 15 G's the initial spike occurs sooner but the frequency is not significantly different.

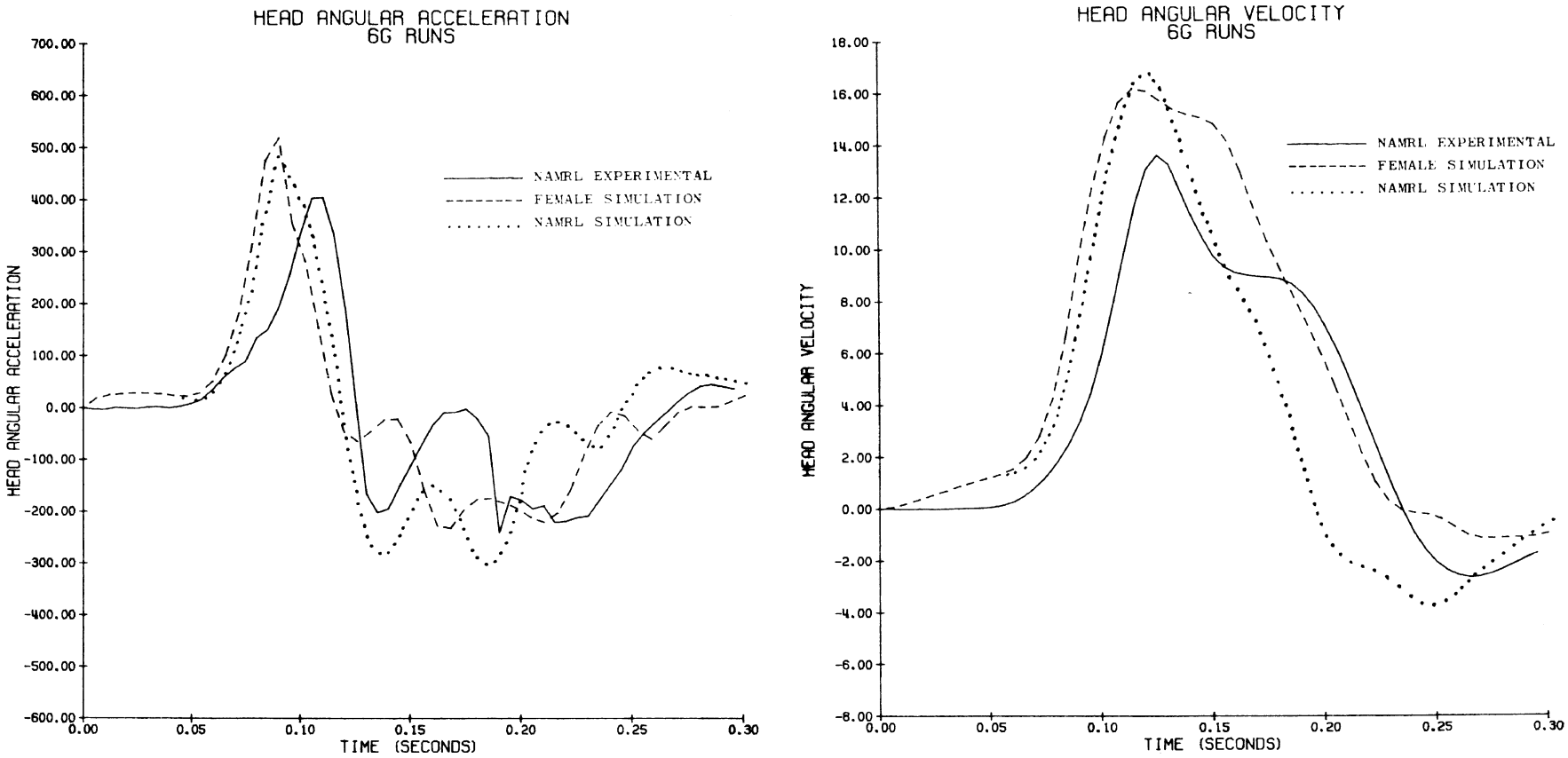

Figure 4.1 6 G Simulation Results for 18-24 Year Females (dashed lines) in Comparison with NAMRL Experimental (solid lines) and NAMRL Simulations (solid lines).

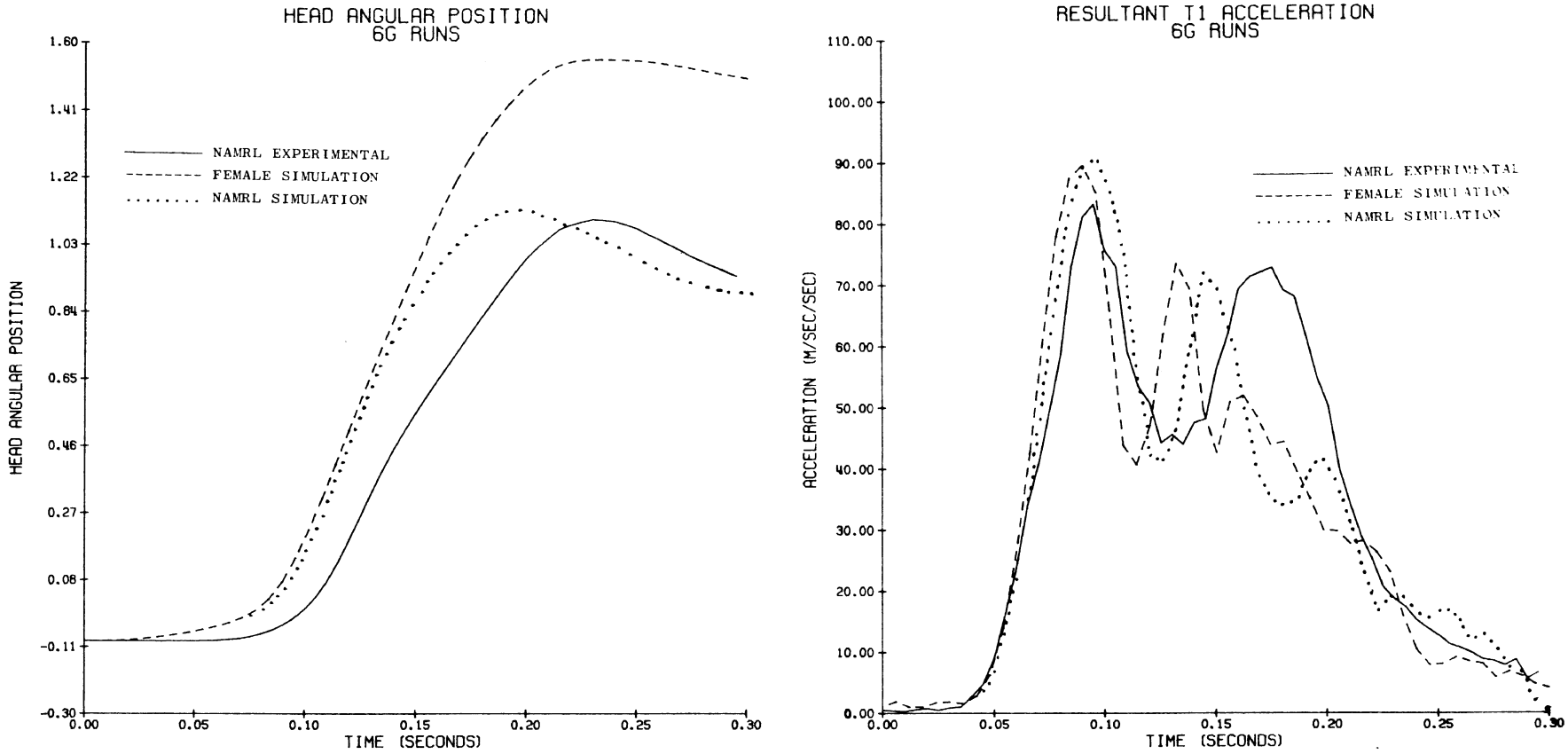

Figure 4.1 (continued)

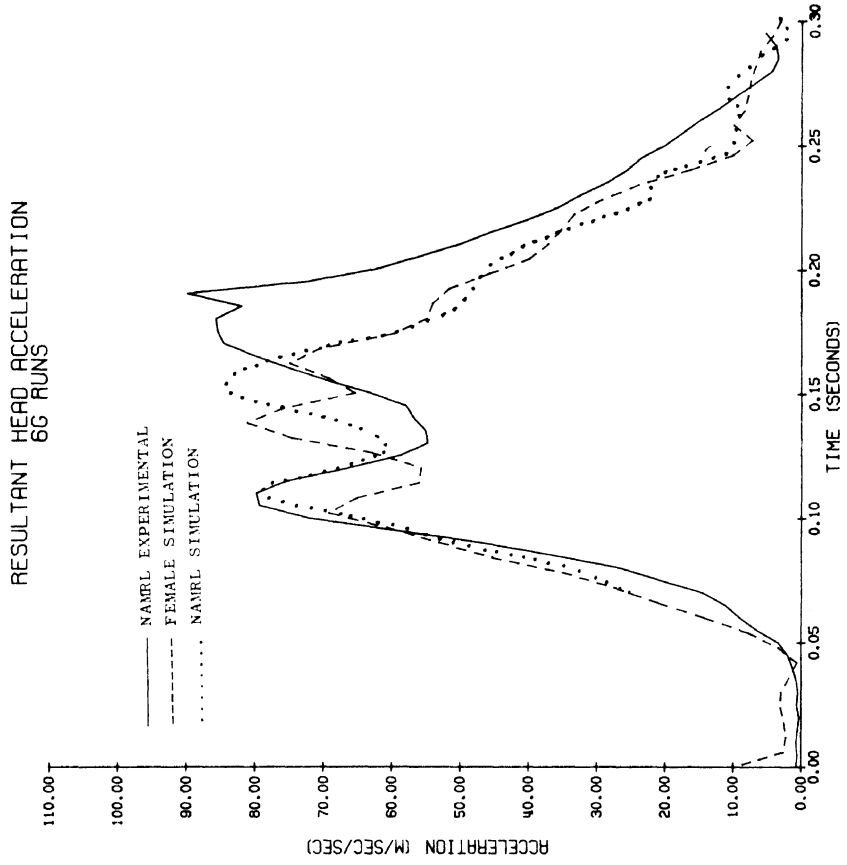

Figure 4.1 (continued)

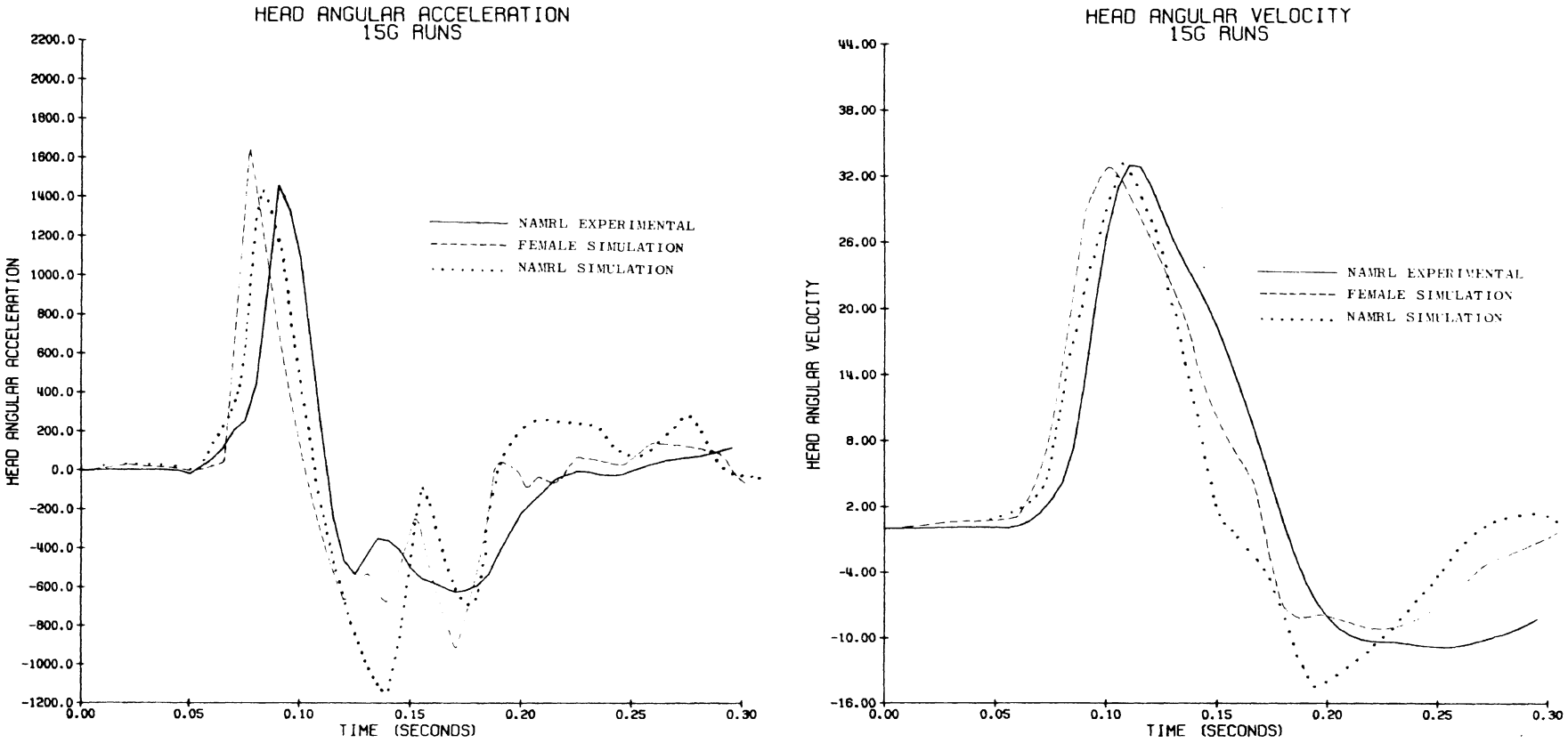

Figure 4.2 15 G Simulation Results for 18-24 Year Females (dashed lines) in Comparison with NAMRL Experimental (solid lines) and NAMRL Simulation (dotted lines).

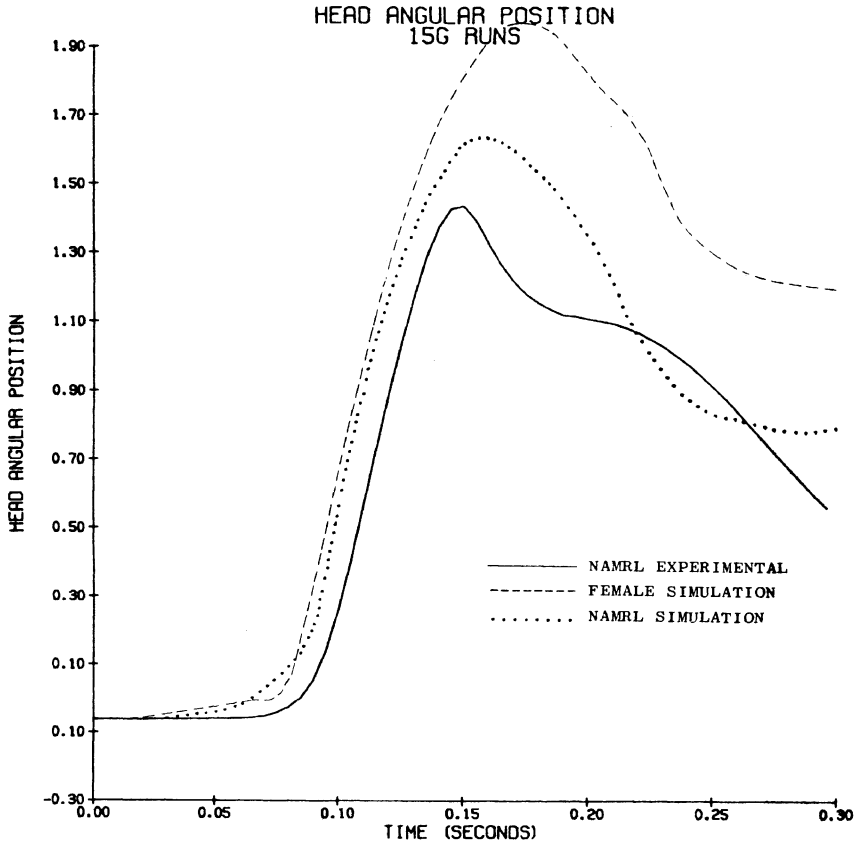

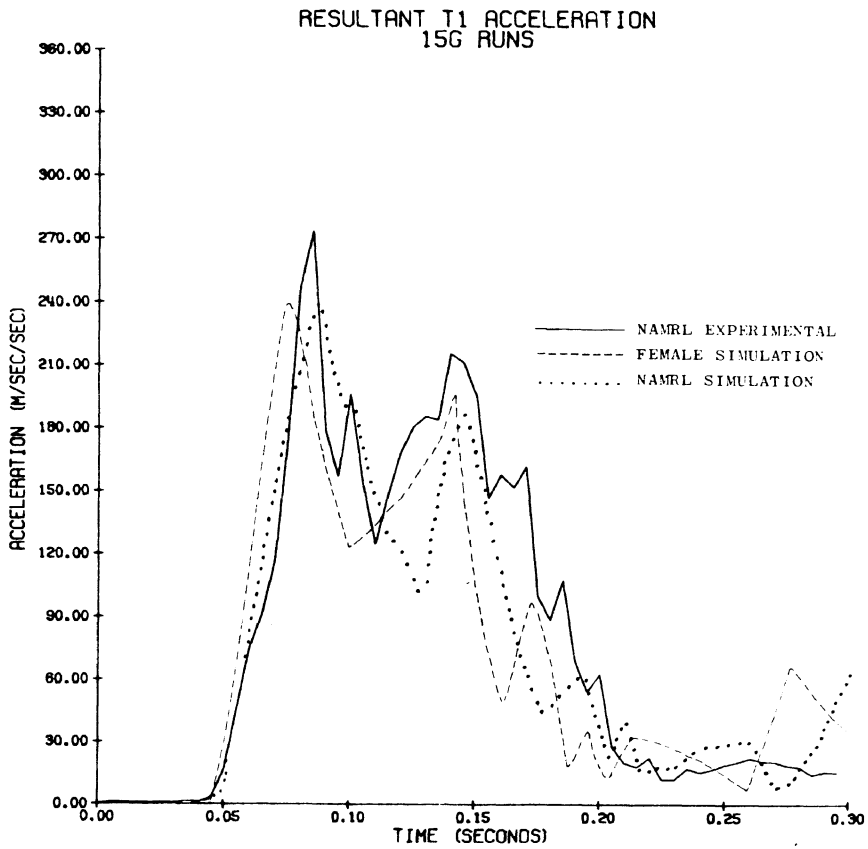

Figure 4.2 (continued)

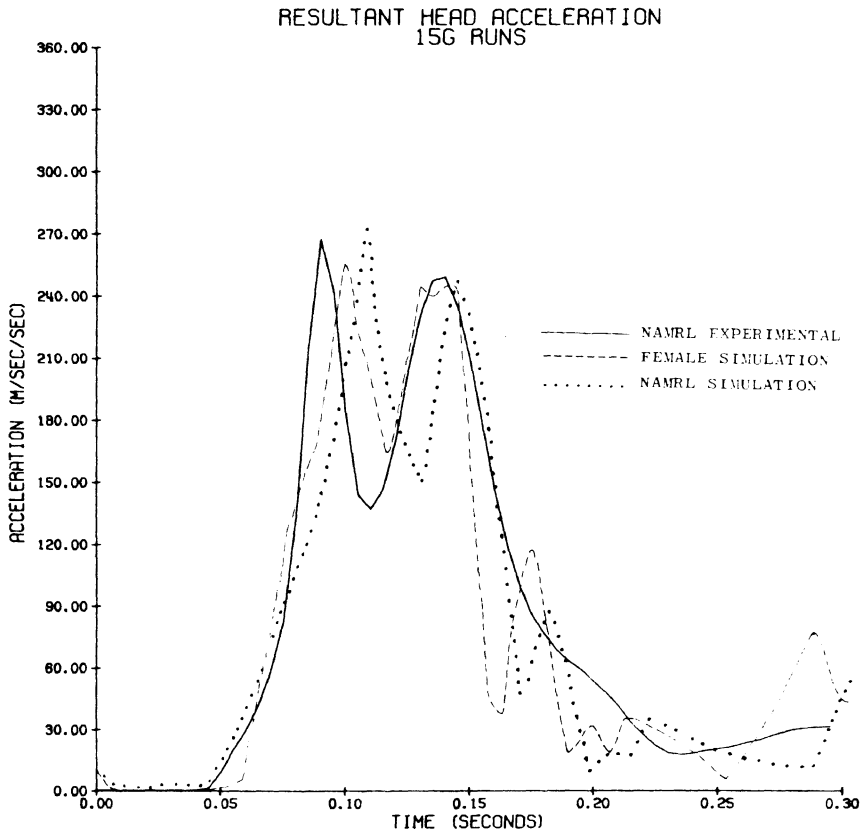

Figure 4.2 (continued)

Chapter 5

DISCUSSION AND RECOMMENDATIONS

Ideally, the fulfillment of the objectives of this research effort will ultimately result in 1) a better understanding of the relationships and importance of various physical characteristics to the dynamic response (and therefore injury susceptibility) of the head and neck, and 2) a mathematical model which utilizes these parameters and which will enable accurate and reliable predictions of head and neck responses over a large range of conditions and variations in subject physical characteristics. The results and accomplishments of the initial 12 months of this study have been satisfying and encouraging toward achieving these goals.

The simulation results of Chapter 3 illustrate excellent reproductions of NAMRL sled test results for head angular acceleration, head angular velocity, head angular position, and head and T_1 resultant acceleration curves. Indeed, it might be concluded that these results are sufficient and that the model can now be used to obtain reasonable predictions for tasks 6 through 8 (see section C, Chapter 1). It is believed, however, that there are significant improvements which can still be made in the model validation which will both add to our understanding of the mechanisms involved in a dynamic situation and improve the capability and credibility of the model.

One area of particular concern in the simulations presented to date is in the modeling of joint stops and passive tissue resistance, and the manner in which measured voluntary range-of-motion limits relate to these phenomena. While the simulations presented in Chapter 3 are reasonable fits to experimental results, there is considerable question as to the values of joint stop parameters used.

This question must be resolved if the model is to be a reliable predictor for persons with smaller ranges of motion (e.g., elderly persons) or for higher G levels where the stop plays a more significant role in restraining the head. A more complete resolution of the problem will require experimental measurements on humans and animals, but it is also likely that further attempts at simulating these characteristics will lead to more suitable and realistic simulation results and a better understanding of this area.

The importance of muscle forces in the dynamic response of the human neck has been investigated to some degree in this study, but there is more to be done. Results so far suggest that muscle effects are more significant at 6 G's than at 15 G's on the NAMRL sled tests but that subjects may not be using their muscles to the maximum extent possible even during the 15 G sled runs. While an increase in muscle tension above the 33% of maximum used would improve the simulation head angular position curve by reducing the peak, it would also result in a more rapid decline of head angular velocity which is already too steep. Further work with this aspect of the model should prove useful in understanding the role of muscle and improving the model performance. The use of EMG signals during dynamic testing and experiments with animals would provide useful information for understanding the action of muscle under dynamic conditions.

For the NAMRL sled test simulations and predictions, further work with the restraint system is needed, especially with regard to the apparent slipping of the shoulders relative to the shoulder belts and the consequent torso bending. Measurements of belt forces during sled tests would be extremely useful to improving this aspect of the model which is essential if sled test results are to be accurately extended to the general adult population.

In Chapter 1, section C, eight tasks were listed which would lead to achievement of the project goals. Of these, the first three have been completed and a substantial and promising start has been made on task four. In view of these achievements and the results to date, it is recommended that efforts toward completing task four (as outlined in the above discussion) be continued, and where appropriate and feasible that experiments be conducted to assist with the model validation. As an additional part of this validation, it is also recommended that efforts be included to:

1) extend simulations to include 3, 10, and greater than 15 G (if available) sled tests.

2) include simulations of sled tests with acceleration profiles of different rates of onset and different durations.

3) include simulations of sled tests with different head/neck initial positions.

At the same time work on task five can be started. This will involve:

1) studying experimental results of NAMRL subjects whose physical characteristics differ from the group used for simulations of this report.

2) extending simulations to these other NAMRL subjects.

3) performing statistical correlations of physical measurement results with peak parameter values of sled tests for the 18 NAMRL subjects measured.

Upon completion of these tasks, work on tasks six through eight can be undertaken with the expectation that the predictions will be reliable extrapolations. The results will therefore be useful toward defining the envelopes of impact acceleration which result in injury. In addition,

by these procedures which combine physical measurements, experimental data, and mathematical modeling, an increased understanding of the factors influencing dynamic responses during impact can be achieved. This will provide important information for design of improved dummies for impact investigations.

References

1. Bowman, B. M. Analytical Model of a Vehicle Occupant For Use in Crash Simulations. Ph.D. Thesis. The University of Michigan 1971.

2. Bowman, B. M., Bennett, R. O. and Robbins, D. H. MVMA Two-Dimensional Crash Victim Simulation, Version 3 Volume 1 and Volume 2. Final Report No. UM-HSRI-BI-74-1, June 1974.

3. Chandler, R. F., Clauser, C. E., McConville, J. T., Reynolds, H. M. and Young, J. W. Investigation of Inertia Properties of the Human Body. Final Report DOT-HS-801 430, March 1975.

4. Clarke, T. D., et al., "Human Head Linear and Angular Accelerations During Impact," 15th Stapp Car Crash and Field Demonstration Conference Proceedings, SAE #710857, November 1971.

5. Ewing, C. L, Thomas, D. J., Beeler, G. W., Patrick, L. M., and Gillis, D. B. "Dynamic Response of the Head and Neck of the Living Human to Gx Impact Acceleration." Proceedings, Twelfth Stapp Car Crash Conference. Society of Automotive Engineers, Inc. New York. SAE #680792, October 1968.

6. Ewing, C. L., Thomas, D. J., Patrick, L. M., Beeler, G. W., and Smith, M. J. "Living Human Dynamic Response to -Gx Impact Acceleration. II. Accelerations Measured on the Head and Neck." Proceedings, Thirteenth Stapp Car Crash Conference. Society of Automotive Engineers, Inc. New York. SAE #690817, December 1969.

7. Ewing, C. L., and Thomas, D. J. "Human Dynamic Response to -Gx Impact Acceleration." AGARD Conference Proceedings, AGARD-Cp-88-71, June 1972.

8. Ewing, C. L. and Thomas, D. J. Human Head and Neck Response to Impact Acceleration. NAMRL Monograph 21 USAMRL 73-1, August 1972.

9. Ewing, C. L. and Thomas, D. J. "Torque Versus Angular Displacement Response of Human Head to -G Impact Acceleration." Proceedings, Seventeenth Stapp Car Crash Conference, SAE #730976, November 1973.

10. Ewing, C. L., Thomas, D. J., Lustick, L., Becker, F. Williams, G. and Muzzy, W. H. III, "The Effect of the Initial Position of the Head and Neck on the Dynamic Response of the Human Head and Neck to $-G_x$ Impact Acceleration." Proceedings of Ninteenth Stapp Car Crash Conference, SAE #751157, November 1975.

11. Foust, D.R., Chaffin, D.B., Snyder, R.G. and Baum, J.K., "Cervical Range of Motion and Dynamic Response and Strength of Cervical Muscles." Proceedings, 17th Stapp Car Crash Conference, SAE #730975, November 1973.

12. Gurdjian, E.S., "Discussion of Tolerance of Sub-human Brain to Cerebral Concussion," in Impact Injury and Crash Protection, pp. 370-371, 1970.

13. Hodgson, V.R., "Physical Factors Related to Experimental Concussion," in Impact Injury and Crash Protection, pp. 275-302, 1970.

14. Holbourn, A.H.S., "The Mechanics of Brain Injuries," British Medical Bulletin, 3:147-149, 1945.

15. Mahone, R., Carrao, P., Ommaya, A., Hendler, E., and Schulman, M., "A Theory on the Mechanics of Whiplash produced Concussion in Primates," Preprint, 40th Scientific Meeting, Aerospace Medical Association, pp. 44-45, May 1969.

16. Martinez, J.L., and Garcia, D., "A Model for Whiplash," Journal of Biomechanics, 1:23, 1968.

17. Moffatt, C.A., Harris, E.H., and Haslam, E.T., "An Experimental and Analytic Study of the Dynamic Properties of the Human Leg." Journal of Biomechanics, Volume 2, No. 4, 373-387, October 1969.

18. Ommaya, A.K. and Hirsch, A.E. "Tolerances for Cerebral Concussion from Head Impact and Whiplash in Primates," Journal of Biomechanics, 4:13-21, 1971.

19. Pudenz, R.H. and Sheldon, C.H. "The Lucite Calvarium -- A Method for Direct Observation of the Brain. II Cranial Trauma and Brain Movement," Journal of Neurosurgery, 3:487-505, 1946.

20. Robbins, D.H., Bowman, B.M. and Bennett, R.O.: "The MVMA Two-Dimensional Crash Victim Simulation." Proceedings of 18th Stapp Car Crash Conference. SAE #741195, 1974.

21. Schneider, L. W., Foust, D. R., Bowman, B. M., Snyder, R. g., Chaffin, D. B., Abdelnour, T. A., and Baum, J. K. "Biomechanical Properties of the Human Neck in Lateral Flexion." Proceedings of Nineteenth Stapp Car Crash Conference, SAE #751156, November 1975.

22. Snyder, R. G., Chaffin, E. B., Schneider, L. W., Foust, D. R., Abdelnour, T. A., Bowman, B. M. and Baum, J. K., Basic Biomechanical Properties of the Human Neck Related to Lateral Hyperflexion Injury. Prepared for Insurance Institute for Highway Safety, Washington, D.C., Final Technical Report (UM-HSRI-BI-75-4) NTIS PB 241246, March 31, 1975.

23. Snyder, R. G., Chaffin, D. B., and Foust, D. R. Bioengineering Study of Basic Physical Measurement Related to Susceptibility to Cervical Hyper-extension - Hyperflexion Injury. Prepared for Insurance Institute for Highway Safety, Washington, D.C., Final Technical Report, (UM-HSRI-BI-75-4) NTIS PB 241246, September 1975.

24. Von Gierke, H. E., "Biodynamic Response of the Human Body." Applied Mechanics Reviews, Vol. 17, No. 12, December 1964.

25. Walker, L. B., Jr., et al., Mass Volume, Center of Mass Moment of Inertia of Head and Neck of the Human Body. Final Rept. to Dept. of Navy, AD-762 581, 1973 .

26. Young, J. W., Fisher, R. G., Price, G. T., and Chandler, R. F. "Experimental Trauma of Occipital Impacts," Proceedings, International Conference of Biokinetics and Kinematics, 1973.

APPENDIX A

CROSS REFERENCE TABLES FOR MEASUREMENT CODE NAMES

Tables A.1 through A.4 provide a cross reference for the abbreviated measurement names used in the tables of statistical results in Chapter 2 and in the tables of measurement results by subject in Appendix B.

TABLE A.1 ANTHROPOMETRY CODE NAME CROSS REFERENCE

CODE NAME	MEASUREMENT
WT(KG)	Weight in kg
WT(LB)	Weight in lb
STAT(CM)	Stature
PONDINDX	Ponderal Index
ERSITHT	Erect Sitting Height
HEADCIR	Head Circumference
HEADELPS	Bennett Ellipse Circumference
BITRGDI	Bitragion Diameter
HEADBR	Head Breadth
HEADLG	Head Length
SAGARC	Sagittal Arc Length
CORARC	Coronal Arc Length
BITRGGLB	Bitragion-Glabella Arc Length
BITRGMEN	Bitragion-Menton Arc Length
BITRGINA	Bitragion-Inion Arc Length
FACEHT	Facial Height
LATNKBR	Lateral Neck Breadth
APNKBR	Anterior-Posterior Neck Breadth
SUPNKCIR	Superior Neck Circumference
INFNKCIR	Inferior Neck Circumference
POSTNKLG	Posterior Neck Length
BIACRBR	Biacromial Breadth
BIDELTBR	Shoulder Breadth (Bideltoid)
CHESTHT	Chest Height
CHESTBR	Chest Breadth
CHESTCIR	Chest Circumference
WAISTHT	Waist Height
WAISTBR	Waist Breadth
WAISTCIR	Waist Circumference
HIPHT	Hip Height
HIPBRSTD	Hip Breadth (Standing Erect)
HIPCIR	Hip Circumference
ACCRRADLG	Acromion-Radiale Length
ARMCIRAX	Upper Arm Circ. (at Axilla)
ARMCIREL	Upper Arm Circ. (above Elbow)
BICFLCIR	Biceps Flexed Circumference
RADSTYLG	Radiale-Stylion Length
FRARMCIR	Forearm Circumference
WRISTCIR	Wrist Circumference
HANDLG	Hand Length
TRCFEMLG	Trochanter-Femoral Condyle Length
UPTHICIR	Upper Thigh Circumference
LWTHICIR	Lower Thigh Circumference
FIBULALG	Fibula Length
FIBULAHT	Fibula Height

TABLE A.1 (continued)

CODE NAME	MEASUREMENT
CALFCIR	Calf Circumference
ANKLECIR	Ankle Circumference
FOOTLG	Foot Length
FOOTBR	Ball-of-Foot Breadth
HUMDIA	Humeral Biepicondylar Dia.
FEMDIA	Femoral Biepicondylar Dia.
TRICPSF	Triceps Skinfold (mm)
SUBSCPSF	Subscapular Skinfold (mm)
SUPILSF	Suprailiac Skinfold (mm)
LTIL-SYM	Left Asis to Symphysion
RTIL-SYM	Right Asis to Symphysion
ASISBR	Anterior Superior Iliac Spine (Asis) Breadth
NRMSITHT	Normal Sitting Height (re SRP)
TRAGHTS	Tragion Height (re SRP)
TRAGDPS	Tragion Depth (re SRP)
GLABHTS	Glabella Height (re SRP)
BLABDPS	Glabella Depth (re SRP)
EYELPHTS	Eye Ellipse Point Height (re SRP)
EYELPDPS	Eye Ellipse Point Depth (re SRP)
EYELPWDG	Eye Ellipse Point Width (re Glabella)
C7HTS	Cervicale Height (re SRP)
C7DPS	Cervicale Depth (re SRP)
SSTRNHTS	Suprasternale Height (re SRP)
SSTRNDPS	Suprasternale Depth (re SRP)
SHLDRHTS	Shoulder Height (re SRP)
SHLDRDPS	Shoulder Depth (re SRP)
SHLDRBR	Shoulder Breadth
ILCSPHTS	Anterior Superior Iliac Spine Ht (re SRP)
ILCSPDPS	Anterior Superior Iliac Spine Depth (re SRP)
BISPNBR	Bispinous Breadth
TRCHHTS	Trochanter Height (re SRP)
TRCHDPS	Trochanter Depth (re SRP)
BITRCHDI	Bitrochanter Diameter
HIPBRSIT	Hip Breadth (Seated Erect)
ORBHTT	Infraorbitrale Height (re Tragion)
ORBDPT	Infraorbitrale Depth (re Tragion)
TRAGHTC7	Tragion Height (re Cervicale)
TRAGDPC7	Tragion Depth (re Cervicale)
GLABHTT	Glabella Height (re Tragion)
GLABDPT	Glabella Depth (re Tragion)
EYELPHTT	Eye Ellipse Point Ht (re Tragion)
EYELPDPT	Eye Ellipse Point Depth (re Tragion)
ECTCNATT	Ectocanthus Height (re Tragion)
ECTCNDPT	Ectocanthus Depth (re Tragion)

TABLE A.2 UPPER TORSO AND HEAD LANDMARK CODE NAME CROSS REFERENCE

CODE NAME	MEASUREMENT	
SHLDRSX	Shoulder Point	-X Direction
SHLDRSY	Shoulder Point	-Y Direction
SHLDRSZ	Shoulder Point	-Z Direction
C7 SX	Cervicale	-Y Direction
C7 SY	Cervicale	-Y Direction
C7 SZ	Cervicale	-Z Direction
SSTRNSX	Suprasternale	-X Direction
SSTRNSY	Suprasternale	-Y Direction
SSTRNSZ	Suprasternale	-Z Direction
TRAG SX	Tragion	-X Direction
TRAG SY	Tragion	-Y Direction
Trag SZ	Tragion	-Z Direction
ORBITSX	Infraorbitale	-X Direction
ORBITSY	Infraorbitale	-Y Direction
ORBITSZ	Infraorbitale	-Z Direction
GLAB SX	Glabella	-X Direction
GLAB SY	Glabella	-Y Direction
GLAB SZ	Glabella	-Z Direction
EYELPSX	Eye Ellipse Point	-X Direction
EYELPSY	Eye Ellipse Point	-Y Direction
EYELPSZ	Eye Ellipse Point	-Z Direction
ECCANSX	Ectocanthus	-X Direction
ECCANSY	Ectocanthus	-Y Direction
ECCANSZ	Ectocanthus	-Z Direction

TABLE A.3 RANGE-OF-MOTION CODE NAME CROSS REFERENCE

CODE NAME	MEASUREMENT
P2NEUTY	Photo 2--Neutral Head Position--Yaw
P2NEUTP	Photo 2--Neutral Head Position--Pitch
P2NEUTR	Photo 2--Neutral Head Position--Roll
P3EXTY	Photo 3--Extension--Yaw
P3EXTP	Photo 3--Extension--Pitch
P3EXTR	Photo 3--Extension--Roll
P4FLEXY	Photo 4--Flexion--Yaw
P4FLEXP	Photo 4--Flexion--Pitch
P4FLEXR	Photo 4--Flexion-Roll
P5RTROTY	Photo 5--Right Rotation--Yaw
P5RTROTP	Photo 5--Right Rotation--Pitch
P5RTROTR	Photo 5--Right Rotation--Roll
P6LTROTY	Photo 6--Left Rotation--Yaw
P6LTROTP	Photo 6--Left Rotation--Pitch
P6LTROTR	Photo 6--Left Rotation--Roll
P7RLBNDY	Photo 7--Right Lateral Bend--Yaw
P7RLBNDP	Photo 7--Right Lateral Bend--Pitch
P7RLBNDR	Photo 7--Right Lateral Bend--Roll
P8LLBNDY	Photo 8--Left Lateral Bend-Yaw
P8LLBNDP	Photo 8--Left Lateral Bend--Pitch
P8LLBNDR	Photo 8--Left Lateral Bend--Roll
P9LROFLY	Photo 9--Left Rotation + Flexion--Yaw
P9LROFLP	Photo 9--Left Rotation + Flexion--Pitch
P9LROFLR	Photo 9--Left Rotation + Flexion--Roll
P10LROBY	Photo 10--Left Rotation + Left Lateral Bend--Yaw
P10LROBP	Photo 10--Left Rotation + Left Lateral Bend--Pitch
P10LROBR	Photo 10--Left Rotation + Left Lateral Bend--Roll
P11RROXY	Photo 11--Right Rotation + Extension--Yaw
P11RROXP	Photo 11--Right Rotation + Extension--Pitch
P11RROXR	Photo 11--Right Rotation + Extension--Roll
PSAGROM	Sagittal Range of Motion from Photogrammetry (P3EXTP + P4FLEXP)
PROTROM	Rotational Range of Motion from Photogrammetry (P5RTROTY + P6LTROTY)
PLATROM	Lateral Bend Range of Motion from Photogrammetry (P7RLBNDR + P8LLBNOR)

TABLE A.4 REFLEX TIMES AND STRENGTH CODE NAME CROSS REFERENCE

CODE NAME	MEASUREMENT
RFL LAT	Reflex Time In Lateral Flexion
RFL PLXR	Reflex Time of Flexor Muscles
RFL EXTR	Reflex Time of Extensor Muscles
RFL AV	Average of All Reflex Times
STR RTL	Pull Force From Right Lateral Flexors
STR LTL	Pull Force From Left Lateral Flexors
STRLATAV	Average Pull Force From Left and Right Lateral Flexors
STR EXTR	Pull Force From Extensor Muscles
STR FLXR	Pull Force From Flexor Muscles
STRSAGAV	Average Pull Force From Extensors and Flexors
SAGLATAV	Average Pull Force From Lateral and Sagittal Tests

APPENDIX B

MEASUREMENT RESULTS BY SUBJECT

Tables B.1 through B.4 give the measurement results by individual subject for anthropometry, head and torso landmarks, range of motion, and strength and reflex time results respectively. The abbreviated measurement names may be cross referenced in the Tables of Appendix A.

TABLE B.1 ANTHROPOMETRY BY SUBJECT

SUBJECT NO	VARIABLES WT(KG)	WT(LB)	STAT(CM)	PONDINDX	ERSITHT	HEADCIR	HEADELPS	BITRGDI	HEADBR
NAM01 H-39	74.09	163.00	174.20	31.90	93.50	55.80	64.40	13.20	14.90
NAM02 H-46	105.23	231.50	176.30	28.72	93.40	60.20	70.50	14.50	14.80
NAT03 H-49	83.64	184.00	182.50	32.09	95.40	57.40	68.30	14.20	15.10
NAM04 H-42	75.45	166.00	176.80	32.18	91.90	59.10	70.00	13.90	15.20
NAM05 H-48	66.14	145.50	177.60	33.77	93.70	54.60	64.20	14.30	14.80
NAM06 H-44	65.68	144.50	175.80	33.51	92.30	54.70	62.40	13.20	14.40
NAS07 H-38	61.14	134.50	165.50	32.31	86.50	56.60	65.30	13.40	15.70
NAM08 H-32	75.45	166.00	176.00	32.03	91.80	57.10	64.40	13.00	14.60
NAM09 H-52	70.45	155.00	172.60	32.14	89.40	56.40	64.20	13.40	15.10
NAM10 H-47	77.27	170.00	172.20	31.09	85.00	54.70	66.10	13.80	14.90
NAT11 H-51	66.36	146.00	183.50	34.85	93.50	57.80	65.10	14.40	15.90
NAM12 H-50	69.09	152.00	175.60	32.91	90.40	55.60	63.50	13.40	14.90
NAM13 H-53	97.73	215.00	176.00	29.38	96.30	56.20	64.00	14.10	15.10
NAT14 H-43	64.09	141.00	179.00	34.40	94.50	56.00	62.20	14.00	14.70
NAT15 H-35	89.55	197.00	184.40	31.70	99.80	57.60	65.90	13.50	14.70
NAM16 H-33	95.00	209.00	177.30	29.88	96.90	57.40	67.00	14.80	14.80
NAT17 H-40	72.95	160.50	179.00	32.94	93.80	56.40	65.70	13.60	15.10
NAT18 H-37	74.09	163.00	181.70	33.27	94.90	61.60	68.00	14.80	15.00

TABLE B.1 (continued)

SUBJECT NO		VARIABLES HEADLG	SAGARC	CORARC	BITRGGLB	BITRGMEN	BITRGINA	FACEHT	LATNKBR	APNKBR
NAM01	H-39	19.10	34.30	34.30	29.40	31.20	29.20	13.30	12.50	11.10
NAM02	H-46	20.30	35.00	36.70	31.30	34.50	30.30	14.60	13.60	12.80
NAT03	H-49	20.20	35.50	35.70	30.70	34.20	27.60	13.90	13.10	11.30
NAM04	H-42	20.80	M.D.	35.70	31.00	33.20	27.20	14.10	11.60	11.70
NAM05	H-48	18.00	37.60	35.80	28.40	30.90	25.70	13.00	11.40	11.20
NAM06	H-44	19.20	32.10	35.10	28.90	29.90	24.80	13.80	11.30	10.40
NAS07	H-38	18.80	34.20	36.50	28.80	29.40	26.70	12.50	11.50	10.60
NAM08	H-32	20.20	35.10	35.00	29.70	30.80	28.50	11.90	12.90	11.10
NAM09	H-52	19.30	35.80	34.40	27.70	29.40	32.30	12.30	12.10	10.50
NAM10	H-47	19.10	35.10	35.50	28.90	31.20	29.40	14.20	12.40	11.70
NAT11	H-51	19.90	34.20	35.30	30.40	31.30	30.30	12.80	11.70	11.80
NAM12	H-50	19.60	34.30	34.30	29.00	30.50	29.30	13.20	11.70	10.50
NAM13	H-53	18.10	33.50	33.00	29.60	32.40	29.40	11.60	12.70	12.10
NAT14	H-43	19.90	35.80	34.20	29.30	30.40	27.30	13.00	11.80	10.90
NAT15	H-35	20.20	36.40	35.90	30.50	32.90	29.80	13.40	13.80	12.70
NAM16	H-33	19.80	35.30	35.20	29.80	31.90	30.20	12.30	12.60	12.90
NAT17	H-40	19.20	35.10	35.20	28.40	30.70	31.20	13.50	11.90	11.00
NAT18	H-37	20.30	37.10	36.60	30.30	31.40	31.10	13.50	12.10	10.80

TABLE B.1 (continued)

SUBJECT NO	VARIABLES SUPNKCIR	INFNKCIR	POSTNKLG	BIACRBR	BIDELTBR	CHESTHT	CHESTBR	CHESTCIR	WAISTHT
NAM01 H-39	37.90	38.40	19.50	39.70	48.00	127.90	32.30	91.50	102.60
NAM02 H-46	44.30	43.90	18.50	39.70	54.20	131.80	34.70	99.40	104.40
NAT03 H-49	40.50	39.20	17.10	40.30	46.90	136.50	30.60	97.40	108.70
NAM04 H-42	38.70	39.30	16.30	39.00	49.20	131.70	32.60	101.50	105.10
NAM05 H-48	36.10	37.50	17.60	40.50	46.90	131.70	30.20	93.00	107.50
NAM06 H-44	35.40	36.50	16.50	40.30	46.30	132.10	28.70	91.30	106.20
NAS07 H-38	36.00	36.30	15.70	39.00	46.30	122.10	29.30	91.30	99.80
NAM08 H-32	36.90	37.30	18.20	41.20	47.10	134.50	29.60	94.60	108.10
NAM09 H-52	34.90	35.60	16.80	38.20	45.80	131.10	28.80	89.50	107.00
NAM10 H-47	36.70	38.00	14.90	41.10	47.70	131.20	28.60	93.80	106.20
NAT11 H-51	37.60	39.80	16.90	42.40	47.00	138.30	29.80	91.40	111.00
NAM12 H-50	35.60	39.20	15.10	41.20	47.10	131.20	28.80	91.90	107.90
NAM13 H-53	40.80	42.20	15.20	44.90	52.70	131.40	33.70	104.50	105.50
NAT14 H-43	34.90	36.30	16.20	40.60	45.30	132.70	30.20	88.20	107.90
NAT15 H-35	42.30	43.50	17.60	43.20	51.60	136.80	34.20	101.50	108.70
NAM16 H-33	40.90	42.20	17.00	39.10	51.50	129.10	33.80	111.80	105.10
NAT17 H-40	36.00	37.60	16.20	41.10	49.30	132.10	30.50	93.30	107.80
NAT18 H-37	37.30	38.70	14.90	42.10	48.60	137.20	31.00	94.80	111.50

TABLE B.1 (continued)

SUBJECT NO	VARIABLES WAISTBR	WAISTCIR	HIPHT	HIPBRSTD	HIPCIR	ACRRADLG	ARMCIRAX	ARMCIREL	BICFLCIR
NAM01 H-39	30.60	90.80	88.40	32.90	95.70	30.50	33.00	26.70	33.60
NAM02 H-46	37.60	98.50	92.90	37.40	112.30	35.20	39.50	32.40	39.80
NAT03 H-49	30.10	83.50	94.50	35.00	99.60	35.80	31.80	28.20	33.60
NAM04 H-42	31.30	85.40	93.70	31.50	93.50	31.90	31.60	26.40	32.00
NAM05 H-48	26.70	74.80	92.90	32.90	92.20	32.30	29.70	14.80	29.80
NAM06 H-44	26.50	74.90	92.50	32.50	91.50	31.80	30.90	23.80	30.00
NAS07 H-38	28.10	76.60	86.60	31.70	91.20	30.20	30.10	24.00	31.90
NAM08 H-32	28.30	82.30	92.80	32.40	94.80	32.10	33.00	25.80	33.20
NAM09 H-52	27.90	79.00	88.80	34.00	96.80	32.60	33.30	27.20	32.20
NAM10 H-47	29.40	83.50	94.30	32.50	98.20	32.80	32.90	26.90	34.10
NAT11 H-51	27.90	75.80	95.50	31.90	90.40	34.20	31.10	24.80	30.80
NAM12 H-50	27.80	78.50	94.00	32.30	92.50	32.20	33.10	25.90	34.10
NAM13 H-53	35.20	100.00	91.00	36.00	109.20	31.30	37.80	29.50	35.80
NAT14 H-43	26.80	73.80	93.40	31.20	89.20	33.00	27.80	24.30	27.80
NAT15 H-35	32.90	94.20	95.60	35.90	103.20	34.80	34.10	27.70	35.30
NAM16 H-33	35.00	94.20	89.80	37.50	98.90	31.30	39.60	31.40	39.80
NAT17 H-40	29.50	82.80	94.60	32.90	94.10	34.80	34.00	26.40	33.80
NAT18 H-37	27.50	82.20	96.70	34.20	94.00	34.10	29.30	24.10	29.10

TABLE B.1 (continued)

SUBJECT NO	VARIABLES RADSTYLG	FRARMCIR	WRISTCIR	HANDLG	TRCFEMLG	UPTHICIR	LWTHICIR	FIBULALG	FIBULAHT
NAM01 H-39	25.20	28.20	17.50	18.30	39.00	56.70	39.20	39.50	44.50
NAM02 H-46	25.70	32.20	19.30	19.40	43.20	66.50	46.90	39.50	46.30
NAT03 H-49	25.50	30.10	18.30	19.30	41.20	60.90	42.70	41.10	46.10
NAM04 H-42	26.10	27.60	17.40	18.40	40.60	55.10	38.10	39.90	44.40
NAM05 H-48	25.10	27.20	16.90	18.90	39.30	51.00	35.80	38.10	44.40
NAM06 H-44	24.90	26.70	17.20	18.70	40.00	51.90	35.70	40.00	44.50
NAS07 H-38	26.10	27.20	16.70	19.10	38.40	51.80	34.10	38.00	41.60
NAM08 H-32	26.10	27.70	16.60	19.10	41.20	59.30	39.30	40.80	45.90
NAM09 H-52	25.30	27.10	16.70	18.80	41.70	57.10	39.30	40.20	45.00
NAM10 H-47	26.70	29.10	17.40	19.20	43.40	62.20	42.80	43.30	46.50
NAT11 H-51	28.20	27.40	17.30	19.00	43.40	48.30	34.30	42.50	47.80
NAM12 H-50	27.70	27.10	17.70	18.90	41.50	55.20	38.40	42.20	46.20
NAM13 H-53	25.90	29.90	17.20	19.30	39.60	69.20	43.20	39.40	44.50
NAT14 H-43	25.70	26.20	16.30	18.60	40.50	50.50	36.00	40.30	46.60
NAT15 H-35	26.50	29.90	18.20	18.90	42.60	59.70	40.90	42.20	48.20
NAM16 H-33	25.40	32.40	18.70	18.10	42.00	66.20	45.20	39.20	45.00
NAT17 H-40	26.80	28.00	17.50	18.90	40.70	58.90	37.80	40.70	45.80
NAT18 H-37	26.70	26.90	16.80	19.90	42.80	55.40	37.10	43.20	49.60

TABLE B.1 (continued)

SUBJECT NO	VARIABLES CALFCIR	ANKLECIR	FOOTLG	FOOTBR	HUMDIA	FEMDIA	TRICPSF	SUBSCPSF	SUPILSF
NAM01 H-39	35.20	22.10	26.00	9.90	7.10	9.40	10.40	10.40	16.20
NAM02 H-46	44.00	24.00	26.90	10.50	7.10	11.20	29.70	39.30	38.30
NAT03 H-49	39.90	24.70	27.70	11.00	7.50	10.80	24.30	10.00	14.20
NAM04 H-42	36.60	21.70	26.70	10.30	6.80	9.60	12.80	12.70	15.30
NAM05 H-48	36.30	21.80	27.40	9.10	6.80	9.70	14.50	15.20	12.50
NAM06 H-44	30.00	22.90	25.70	9.40	6.50	9.50	17.80	7.00	9.30
NAS07 H-38	35.70	19.60	25.20	9.50	6.90	9.30	15.70	11.10	9.80
NAM08 H-32	34.90	20.70	26.20	10.40	7.00	9.50	18.50	13.30	14.30
NAM09 H-52	37.40	22.30	27.10	10.60	7.10	10.00	15.30	18.00	18.00
NAM10 H-47	36.30	21.50	26.30	10.70	7.00	10.10	6.30	15.00	22.30
NAT11 H-51	33.30	21.60	27.20	9.70	7.50	10.00	5.70	9.00	6.00
NAM12 H-50	36.40	21.80	26.20	10.60	7.50	10.10	6.70	13.70	10.30
NAM13 H-53	40.50	24.70	28.20	11.10	7.50	9.40	11.70	27.30	27.70
NAT14 H-43	32.00	22.60	26.60	10.40	6.80	9.70	6.80	8.00	8.00
NAT15 H-35	37.50	23.60	27.10	10.40	7.20	9.40	9.00	18.50	19.00
NAM16 H-33	42.40	25.10	26.90	10.80	7.50	10.00	20.70	29.30	29.00
NAT17 H-40	35.70	22.50	26.40	10.10	7.40	9.90	30.50	17.80	16.00
NAT18 H-37	36.20	22.50	25.00	10.60	7.20	9.50	6.20	9.80	11.70

TABLE B.1 (continued)

SUBJECT NO.	VARIABLES NRMSITHT	TRAGHT S	TRAGDP S	GLABLHTS	GLABLDPS	EYELPHTS	EYELPDPS	EYELPWDG	C7HT S
NAM01 H-39	91.40	77.80	-4.70	82.40	6.50	79.70	4.80	3.00	64.10
NAM02 H-46	90.80	76.00	2.70	80.70	13.70	78.50	11.50	3.10	66.20
NAT03 H-49	93.70	79.60	-2.30	84.50	8.40	81.60	6.60	3.00	68.40
NAM04 H-42	87.70	73.90	-0.40	78.30	10.30	75.90	8.30	3.50	63.10
NAM05 H-48	90.80	77.60	-2.90	80.20	7.50	78.30	5.30	3.30	65.50
NAM06 H-44	89.10	76.10	-4.90	79.60	5.00	77.00	3.40	2.80	63.50
NAS07 H-38	84.20	70.50	0.30	73.90	9.40	72.10	8.00	3.80	60.90
NAM08 H-32	88.80	75.60	1.40	79.70	11.50	77.10	10.00	3.10	67.30
NAM09 H-52	85.70	74.20	-0.30	78.40	9.20	75.60	7.80	3.10	62.80
NAM10 H-47	82.50	70.50	-0.70	74.30	8.60	72.00	7.30	3.40	60.20
NAT11 H-51	89.90	77.50	3.60	80.40	14.20	78.40	12.00	3.50	66.80
NAM12 H-50	85.20	73.40	0.40	77.20	10.10	74.80	8.60	3.20	63.40
NAM13 H-53	91.70	80.30	0.70	83.80	10.00	82.10	8.50	3.60	69.40
NAT14 H-43	92.90	78.40	-2.40	83.50	7.80	80.90	6.10	2.80	67.60
NAT15 H-35	97.00	82.30	-1.30	86.10	11.40	83.50	9.70	3.10	70.30
NAM16 H-33	92.60	78.90	-2.20	83.20	7.40	80.80	5.90	3.40	66.70
NAT17 H-40	91.00	77.40	-2.40	80.90	7.10	78.30	5.50	3.40	64.70
NAT18 H-37	90.70	75.70	2.50	78.60	12.10	76.90	10.50	3.50	65.00

TABLE B.1 (continued)

SUBJECT NO		VARIABLES C7DP S	SSTENHTS	SSTRNDPS	SHLDRHTS	SHLDRDPS	SHLDRBR	ILCSPHTS	ILCSPDPS	BISPNBR
NAM01	H-39	-11.40	58.20	1.00	55.80	-6.30	41.10	19.40	10.30	24.40
NAM02	H-46	-8.10	58.50	5.10	60.30	-2.40	40.70	20.40	10.40	23.70
NAT03	H-49	-10.20	59.60	1.30	59.00	-4.40	40.70	18.20	9.30	28.20
NAM04	H-42	-7.40	55.10	4.90	56.40	-5.70	39.40	19.90	10.40	27.00
NAM05	H-48	-10.70	57.40	1.90	57.00	-5.40	40.70	20.00	10.30	25.60
NAM06	H-44	-12.60	56.70	-1.70	55.20	-8.60	42.50	19.10	10.30	27.30
NAS07	H-38	-7.90	53.00	2.80	52.20	-3.30	40.30	18.30	9.60	26.30
NAM08	H-32	-7.60	57.80	3.20	58.30	-4.70	40.30	19.50	9.50	23.20
NAM09	H-52	-8.40	56.40	3.50	56.80	-4.10	M.D.	18.30	11.20	24.00
NAM10	H-47	-8.80	52.30	2.70	53.30	-4.50	42.40	18.60	9.80	24.10
NAT11	H-51	-7.40	57.60	3.10	57.10	-7.00	36.80	19.80	9.70	24.90
NAM12	H-50	-7.90	55.00	2.50	52.60	-1.20	41.70	18.60	9.80	24.40
NAM13	H-53	-8.30	60.70	5.20	61.00	-4.80	47.00	19.60	12.90	23.50
NAT14	H-43	-9.20	58.70	0.40	58.60	-4.10	40.90	19.20	9.90	26.70
NAT15	H-35	-9.50	60.20	3.10	61.30	-1.80	44.50	20.80	12.20	25.00
NAM16	H-33	-11.10	59.50	2.60	58.50	-5.50	41.20	20.50	11.80	25.80
NAT17	H-40	-11.10	57.40	-0.40	55.90	-6.60	42.00	19.40	11.20	25.70
NAT18	H-37	-7.10	54.40	2.40	55.20	-3.60	41.90	21.20	11.10	26.50

TABLE B.1 (continued)

SUBJECT NO	VARIABLES TROCHHTS	TROCHDPS	BITRCHDI	HIPBRSIT	ORBHT T	ORBDP T	TRAGHTC7	TRAGDPC7	GLABLHTT
NAM01 H-39	10.00	11.50	30.50	33.70	0.80	9.50	13.70	6.70	4.60
NAM02 H-46	9.90	7.80	33.20	42.40	0.70	8.70	9.70	10.80	4.80
NAT03 H-49	7.40	9.20	33.50	38.20	1.00	8.70	11.20	7.90	4.90
NAM04 H-42	8.90	11.40	31.00	36.60	0.70	8.90	10.80	7.00	4.40
NAM05 H-48	8.90	10.70	32.50	34.80	-0.70	7.90	12.00	7.90	2.60
NAM06 H-44	9.40	10.00	31.80	35.90	-0.20	8.00	12.60	7.70	3.50
NAS07 H-38	7.10	10.00	30.00	34.30	0.70	7.40	9.60	8.20	3.40
NAM08 H-32	9.10	9.40	31.80	36.50	-0.20	8.10	8.30	9.00	4.10
NAM09 H-52	7.70	10.30	29.30	38.50	0.20	7.90	11.40	8.10	4.20
NAM10 H-47	9.40	10.60	32.80	35.80	-0.20	7.90	10.30	8.10	3.80
NAT11 H-51	9.00	9.60	32.30	38.10	1.00	8.00	10.70	11.10	2.90
NAM12 H-50	8.50	8.70	31.90	35.10	0.20	7.90	9.90	8.30	3.80
NAM13 H-53	7.40	11.80	34.20	46.00	-0.10	7.40	10.80	9.00	3.50
NAT14 H-43	9.70	10.30	31.30	35.20	0.80	8.10	10.80	6.80	5.10
NAT15 H-35	11.70	12.50	33.70	39.90	-0.10	10.70	12.10	8.20	3.80
NAM16 H-33	11.30	12.60	32.50	42.50	0.80	7.90	12.20	8.80	4.20
NAT17 H-40	9.20	12.00	32.40	40.20	0.00	7.80	12.60	8.70	3.50
NAT18 H-37	10.80	13.10	32.40	35.00	0.20	7.70	10.70	9.60	2.90

TABLE B.1 (continued)

SUBJECT NO	VARIABLES GLABLDPT	EYELPHTT	EYELPDPT	ECTCNHTT	ECTCNDPT	LTIL-SYM	RTIL-SYM	ASISBB
NAM01 H-39	11.20	1.90	9.50	1.90	8.30	12.80	12.00	21.00
NAM02 H-46	11.00	2.50	8.80	2.50	7.80	11.50	12.70	20.50
NAT03 H-49	10.70	2.00	8.80	2.00	7.80	13.80	13.70	23.70
NAM04 H-42	10.70	2.00	8.80	1.60	7.30	13.00	13.40	21.10
NAM05 H-48	10.40	0.80	8.20	0.90	7.30	12.90	13.60	21.10
NAM06 H-44	9.90	0.90	8.30	1.10	7.20	13.70	14.70	23.00
NAS07 H-38	9.10	1.60	7.70	1.60	6.70	14.70	14.00	23.10
NAM08 H-32	10.10	1.50	8.60	1.40	7.40	12.20	12.40	19.90
NAM09 H-52	9.60	1.40	8.10	1.40	7.00	13.90	12.60	21.70
NAM10 H-47	9.30	1.50	8.00	1.50	7.10	12.20	12.60	18.00
NAT11 H-51	10.50	0.90	8.40	1.00	7.50	14.00	14.90	22.50
NAM12 H-50	9.70	1.40	8.20	1.40	7.40	12.30	13.10	18.80
NAM13 H-53	9.20	1.80	7.70	1.70	6.80	11.40	11.70	19.20
NAT14 H-43	10.20	2.50	8.50	2.50	7.30	13.90	14.30	22.60
NAT15 H-35	12.70	1.10	11.00	1.00	10.00	12.90	14.10	21.20
NAM16 H-33	9.60	1.80	8.10	1.80	7.10	14.20	14.60	23.90
NAT17 H-40	9.50	0.90	7.90	0.80	6.60	13.20	13.30	21.50
NAT18 H-37	9.70	1.20	8.10	1.30	6.90	13.70	14.60	23.60

TABLE B.2 THREE SPACE LOCATIONS OF UPPER TORSO AND HEAD LANDMARKS BY SUBJECT

SUBJECT NO	VARIABLES SHLDRSX	SHLDRSY	SHLDRSZ	C7 SX	C7 SY	C7 SZ	SSIRNSX	SSIRNSY
NAM01 H-39	-6.30	19.20	55.80	-11.40	-1.90	64.10	1.00	-1.80
NAM02 H-46	-2.40	17.90	60.30	-8.10	-2.40	66.20	5.10	-2.30
NAT03 H-49	-4.40	19.70	59.00	-10.20	-0.80	68.40	1.30	-0.70
NAM04 H-42	-5.70	18.30	56.40	-7.40	-1.30	63.10	4.90	-1.20
NAM05 H-48	-5.40	18.30	57.00	-10.70	-2.30	65.50	1.90	-2.20
NAM06 H-44	-8.60	19.30	55.20	-12.60	-2.20	63.50	-1.70	-2.10
NAS07 H-38	-3.30	18.50	52.20	-7.90	-1.90	60.90	2.80	-1.80
NAM08 H-32	-4.70	20.70	58.30	-7.60	0.70	67.30	3.20	0.70
NAM09 H-52	-4.10	19.20	56.80	-8.40	-0.90	62.80	3.50	-0.90
NAM10 H-47	-4.50	20.60	53.30	-8.80	-0.40	60.20	2.70	-0.40
NAT11 H-51	-7.00	20.80	57.10	-7.40	-0.10	66.80	3.10	-0.10
NAM12 H-50	-1.20	20.80	52.60	-7.90	-0.30	63.40	2.50	-0.30
NAM13 H-53	-4.80	20.30	61.00	-8.30	-2.90	69.40	5.20	-2.80
NAT14 H-43	-4.10	17.30	58.60	-9.20	-3.30	67.60	0.40	-3.20
NAT15 H-35	-1.80	21.20	61.30	-9.50	-1.60	70.30	3.10	-1.50
NAM16 H-33	-5.50	14.50	58.50	-11.10	-3.10	66.70	2.60	-3.00
NAT17 H-40	-6.60	20.30	55.90	-11.10	-0.60	64.70	-0.40	-0.60
NAT18 H-37	-3.60	20.70	55.20	-7.10	-0.80	65.00	2.40	-0.80

TABLE B.2 (continued)

SUBJECT NO		VARIABLES SSTRNSZ	TRAG SX	TRAG SY	TRAG SZ	ORBITSX	ORBITSY	ORBITSZ	GLABLSX
NAM01	H-39	58.20	-4.70	5.20	77.80	4.90	1.80	78.60	6.50
NAM02	H-46	58.50	2.70	5.20	76.00	11.30	1.30	76.70	13.70
NAT03	H-49	59.60	-2.30	5.80	79.60	6.40	2.10	80.60	8.40
NAM04	H-42	55.10	-0.40	5.30	73.90	8.50	2.30	74.60	10.30
NAM05	H-48	57.40	-2.90	5.10	77.60	5.00	2.00	76.90	7.50
NAM06	H-44	56.70	-4.90	4.80	76.10	3.10	1.30	75.90	5.00
NAS07	H-38	53.00	0.30	5.60	70.50	7.70	1.80	71.20	9.40
NAM08	H-32	57.80	1.40	6.30	75.60	9.60	3.30	75.40	11.50
NAM09	H-52	56.40	-0.30	5.90	74.20	7.50	2.80	74.40	9.20
NAM10	H-47	52.30	-0.70	6.00	70.50	7.20	2.90	70.30	8.60
NAT11	H-51	57.60	3.60	5.30	77.50	11.60	3.40	78.50	14.20
NAM12	H-50	55.00	0.40	7.20	73.40	8.30	3.90	73.60	10.10
NAM13	H-53	60.70	0.70	2.70	80.30	8.20	-1.00	80.20	10.00
NAT14	H-43	58.70	-2.40	4.30	78.40	5.70	0.50	79.30	7.80
NAT15	H-35	60.20	-1.30	11.70	82.30	9.40	1.80	82.30	11.40
NAM16	H-33	59.50	-2.20	4.40	78.90	5.70	0.90	79.80	7.40
NAT17	H-40	57.40	-2.40	6.70	77.40	5.30	3.80	77.40	7.10
NAT18	H-37	54.40	2.50	6.00	75.70	10.10	2.00	75.90	12.10

TABLE B.2 (continued)

SUBJECT NO	VARIABLES GLABLSY	GLABLSZ	EYELPSX	EYELPSY	EYELPSZ	ECCANSX	ECCANSY	ECCANSZ
NAM01 H-39	-1.40	82.40	4.80	1.60	79.70	3.70	2.80	79.70
NAM02 H-46	-2.00	80.70	11.50	1.10	78.50	10.50	2.40	78.50
NAT03 H-49	-0.90	84.50	6.60	2.20	81.60	5.50	3.40	81.60
NAM04 H-42	-1.40	78.30	8.30	2.00	75.90	6.90	3.50	75.50
NAM05 H-48	-1.40	80.20	5.30	2.00	78.30	4.40	3.10	78.50
NAM06 H-44	-1.70	79.60	3.40	1.10	77.00	2.30	2.40	77.20
NAS07 H-38	-2.20	73.90	8.00	1.60	72.10	7.00	2.80	72.10
NAM08 H-32	-0.10	79.70	10.00	3.00	77.10	8.90	4.40	77.00
NAM09 H-52	-0.50	78.40	7.80	2.60	75.60	6.70	4.10	75.60
NAM10 H-47	-0.90	74.30	7.30	2.50	72.00	6.40	3.90	72.00
NAT11 H-51	-0.40	80.40	12.00	3.10	78.40	11.20	4.40	78.50
NAM12 H-50	0.60	77.20	8.60	3.70	74.80	7.80	4.90	74.80
NAM13 H-53	-4.80	83.80	8.50	-1.20	82.10	7.60	0.20	81.90
NAT14 H-43	-2.60	83.50	6.10	0.20	80.90	4.90	1.50	80.90
NAT15 H-35	-1.50	86.10	9.70	1.70	83.50	8.70	3.10	83.40
NAM16 H-33	-2.50	83.20	5.90	0.90	80.80	4.90	2.30	80.80
NAT17 H-40	0.00	80.90	5.50	3.50	78.30	4.20	4.90	78.20
NAT18 H-37	-1.60	78.60	10.50	1.90	76.90	9.40	3.10	76.90

TABLE B.3 RANGE-OF-MOTION ANGLES BY SUBJECT

SUBJECT NO	VARIABLES P2NEUTY	P2NEUTP	P2NEUTR	P3EXTY	P3EXTP	P3EXTR	P4FLEXY	P4FLEXP	P4FLEXR
NAM01 H-39	-1.60	0.80	0.20	M.D.	83.00	M.D.	-3.50	-66.00	2.20
NAM02 H-46	-2.80	4.50	-1.80	M.D.	79.00	M.D.	2.10	-63.20	-4.70
NAT03 H-49	-0.10	-5.40	1.20	M.D.	79.50	M.D.	1.90	-62.60	-6.80
NAM04 H-42	2.70	-3.10	1.30	M.D.	87.50	M.D.	3.30	-68.20	0.20
NAM05 H-48	0.00	0.50	-0.70	M.D.	82.00	M.D.	-0.80	-60.70	-3.80
NAM06 H-44	1.10	3.70	-1.90	M.D.	85.80	M.D.	2.50	-50.60	-10.30
NAS07 H-38	1.40	-5.50	-0.50	M.D.	63.00	M.D.	3.50	-55.30	-3.40
NAM08 H-32	3.50	1.80	1.10	M.D.	76.50	M.D.	2.50	-57.80	-3.30
NAM09 H-52	-1.10	-3.30	1.90	M.D.	76.00	M.D.	-10.90	-55.90	4.00
NAM10 H-47	-1.20	-1.50	-1.30	M.D.	79.00	M.D.	1.50	-54.50	-2.30
NAT11 H-51	-0.80	-3.60	1.00	M.D.	84.00	M.D.	4.00	-54.30	1.70
NAM12 H-50	-7.10	-5.40	0.10	M.D.	80.50	M.D.	11.70	-62.60	-4.80
NAM13 H-53	0.80	-4.60	-1.10	M.D.	82.00	M.D.	-1.70	-55.70	M.D.
NAT14 H-43	1.70	-6.00	0.10	M.D.	76.50	M.D.	5.10	-64.20	-6.90
NAT15 H-35	-3.90	-0.90	-0.90	M.D.	77.10	M.D.	-1.40	-65.70	M.D.
NAM16 H-33	-1.70	-2.20	0.40	M.D.	64.00	M.D.	3.60	-68.50	-3.50
NAT17 H-40	-2.20	-6.00	2.40	M.D.	85.50	M.D.	7.10	-58.20	-5.90
NAT18 H-37	-0.50	1.00	0.60	M.D.	82.00	M.D.	-9.20	-65.10	13.50

TABLE B.3 (continued)

SUBJECT NO	VARIABLES P5RTROTY	P5RTROTP	P5RTROTR	P6LTROTY	P6LTROTP	P6LTROTR	P7RLBNDY	P7RLBNDP	P7RLBNDR
NAM01 H-39	83.50	-8.60	14.60	-83.10	-0.10	-19.20	2.20	5.50	48.30
NAM02 H-46	70.20	-3.70	3.80	-68.90	-7.00	-10.00	-7.90	1.30	43.00
NAT03 H-49	71.10	-6.20	7.70	-66.70	-11.40	-7.60	-5.50	-2.50	34.90
NAM04 H-42	77.10	0.20	9.00	-81.90	-0.90	-9.90	-1.00	-1.90	51.30
NAM05 H-48	73.80	6.00	8.70	-79.70	-2.00	-8.10	10.60	0.00	44.20
NAM06 H-44	87.50	8.60	6.60	-81.60	3.30	-5.50	3.90	2.40	47.80
NAS07 H-38	66.30	-5.40	7.60	-72.60	-5.70	-15.60	6.90	3.10	37.40
NAM08 H-32	72.90	7.90	7.80	-79.00	3.30	-8.60	14.80	3.40	35.50
NAM09 H-52	78.10	-2.10	6.80	-69.00	M.D.	-2.00	1.90	3.40	45.00
NAM10 H-47	75.50	4.50	7.20	-81.40	5.30	-11.80	5.40	-2.80	43.00
NAT11 H-51	88.40	-1.20	7.80	-83.20	0.10	-9.10	20.70	10.90	67.00
NAM12 H-50	80.10	-7.70	-4.90	-79.70	-6.20	-6.00	1.40	-9.60	45.10
NAM13 H-53	73.20	2.40	7.20	-80.10	-0.60	-13.80	2.50	-3.80	37.80
NAT14 H-43	70.40	-9.90	5.00	-66.20	-11.10	-6.30	10.70	-2.20	44.20
NAT15 H-35	76.20	-3.80	-3.30	-81.40	-3.30	-8.50	4.10	-10.70	47.30
NAM16 H-33	75.30	-4.80	6.00	-81.10	-5.60	-12.80	-8.10	2.90	53.80
NAT17 H-40	73.60	-5.40	M.D.	-81.20	-1.00	-15.30	7.40	-0.80	43.40
NAT18 H-37	76.10	-8.10	3.50	-78.00	-2.50	-0.20	3.70	8.20	41.30

TABLE B.3 (continued)

SUBJECT	NC	VARIABLES P8LLBNDY	P8LLBNDP	P8LLBNDR	P9LROFLY	P9LROFLP	P9LROFLR	P10LROBY	P10LROBP	P10LROBR
NAM01	H-39	-5.60	5.10	-51.60	-64.90	-38.10	-31.60	-75.10	4.20	-55.80
NAM02	H-46	-0.20	-1.10	-53.40	-65.40	-28.50	-15.80	-63.60	6.30	-42.00
NAT03	H-49	1.80	-1.50	-41.10	-58.40	-29.90	-18.70	-66.20	7.20	-40.40
NAM04	H-42	-6.00	3.00	-50.30	-75.40	-38.10	-11.90	-74.40	13.00	-54.50
NAM05	H-48	-7.80	-2.70	-48.60	-70.20	-34.00	-10.30	-68.70	4.20	-42.50
NAM06	H-44	-0.60	-3.50	-49.90	-69.30	-26.80	-7.70	-88.60	10.50	-54.80
NAS07	H-38	-11.10	-5.70	-51.80	-72.40	-32.00	-25.30	-73.20	-3.80	-41.80
NAM08	H-32	-10.30	12.50	-35.80	-72.80	-23.50	-15.50	-80.20	6.30	-31.50
NAM09	H-52	-8.20	-0.70	-39.40	-73.10	-19.40	-4.60	-78.70	4.70	-26.80
NAM10	H-47	-8.50	-1.40	-47.70	-70.30	-28.70	-17.70	-81.30	11.70	-46.80
NAT11	H-51	-12.70	7.20	-54.40	-65.10	-26.70	-17.80	-80.60	9.80	-45.80
NAM12	H-50	-4.10	-10.60	-51.40	-81.90	-37.00	5.90	-74.10	-8.00	-35.40
NAM13	H-53	3.30	-11.90	-40.20	-82.90	-40.40	-11.70	-68.50	6.60	-36.80
NAT14	H-43	7.90	6.20	-49.50	-65.30	-31.90	-8.90	-68.90	-8.20	-24.40
NAT15	H-35	-9.00	-7.60	M.D.	-72.00	-24.60	-15.60	-74.60	5.00	-31.50
NAM16	H-33	0.80	0.00	-56.90	-71.60	-44.10	-18.00	-63.30	-10.70	-53.00
NAT17	H-40	-7.60	3.00	-40.80	-67.70	-22.50	-16.00	-80.30	9.40	-38.30
NAT18	H-37	-5.20	-2.90	-38.50	-85.50	-33.80	12.60	-69.00	-5.70	-26.80

TABLE B.3 (continued)

SUBJECT NO	VARIABLES P11RROXY	P11RROXP	P11RROXR	PSAGROM	PROTROM	PLATROM
NAM01 H-39	79.70	26.00	24.80	149.00	166.60	99.90
NAM02 H-46	78.10	24.00	12.60	142.20	139.10	96.40
NAT03 H-49	65.90	19.00	15.30	142.10	137.80	76.00
NAM04 H-42	75.30	19.50	14.90	155.70	159.00	101.60
NAM05 H-48	80.70	24.10	17.30	142.70	153.50	92.80
NAM06 H-44	89.00	26.00	11.60	136.40	169.10	97.70
NAS07 H-38	64.10	33.20	13.30	118.30	138.90	89.20
NAM08 H-32	78.90	27.70	22.50	134.30	151.90	71.30
NAM09 H-52	76.60	25.30	14.40	131.90	147.10	84.40
NAM10 H-47	72.50	40.00	11.60	133.50	156.90	90.70
NAT11 H-51	87.90	39.90	26.10	138.30	171.60	121.40
NAM12 H-50	86.10	20.80	11.50	143.10	159.80	96.50
NAM13 H-53	73.90	16.90	6.20	137.70	153.30	78.00
NAT14 H-43	73.50	10.50	17.40	140.70	136.60	93.70
NAT15 H-35	82.00	6.90	18.10	142.80	157.60	M.D.
NAM16 H-33	75.00	12.70	4.30	132.50	156.40	110.70
NAT17 H-40	73.40	33.40	13.70	143.70	154.80	84.20
NAT18 H-37	73.50	13.50	5.50	147.10	154.10	79.80

TABLE B.4 REFLEX TIME AND VOLUNTARY STRENGTH RESULTS BY SUBJECT

SUBJECT NO		VARIABLES RFL LAT	RFL FLXR	RFL EXTR	RFL AVG	STR RTL	STR LTL
NAM01	H-39	51.30	50.30	49.30	50.30	31.20	33.50
NAM02	H-46	50.70	52.00	66.00	56.20	32.30	31.30
NAT03	H-49	49.30	54.70	55.60	53.20	30.30	32.70
NAM04	H-42	54.00	68.80	66.00	62.90	49.70	53.70
NAM05	H-48	42.00	64.70	50.80	52.50	25.30	31.70
NAM06	H-44	61.30	M.D.	65.20	63.30	28.70	37.00
NAS07	H-38	42.70	44.80	55.00	47.50	22.70	19.30
NAM08	H-32	53.70	54.50	56.00	54.70	33.00	34.00
NAM09	H-52	57.00	56.30	57.30	56.90	29.30	28.30
NAM10	H-47	55.70	60.70	61.30	59.20	42.00	39.30
NAT11	H-51	70.00	61.70	60.00	63.90	41.70	44.30
NAM12	H-50	50.00	58.00	49.00	52.30	31.00	30.70
NAM13	H-53	51.70	63.70	54.70	56.70	56.00	46.70
NAT14	H-43	37.00	60.70	37.60	45.10	25.30	25.00
NAT15	H-35	55.70	43.30	42.70	47.20	28.30	34.30
NAM16	H-33	45.70	46.00	42.70	44.80	52.70	45.30
NAT17	H-40	48.30	46.00	45.70	46.70	42.00	37.70
NAT18	H-37	51.30	57.70	44.30	51.10	40.70	42.30

TABLE B.4 (continued)

SUBJECT NC		VARIABLES STIRLATAV	STR EXTR	STR FLXR	STRSAGAV	SAGLATAV
NAM01	H-39	32.30	44.70	39.30	42.00	37.20
NAM02	H-46	31.80	54.70	39.30	47.00	39.40
NAT03	H-49	31.50	32.30	41.70	37.00	34.20
NAM04	H-42	51.70	55.00	36.00	45.50	48.60
NAM05	H-48	28.50	33.70	30.00	31.90	30.20
NAM06	H-44	32.80	37.00	33.30	35.20	34.00
NAS07	H-38	21.00	33.00	16.70	24.80	22.90
NAM08	H-32	33.50	50.00	36.70	43.30	38.40
NAM09	H-52	28.80	35.30	27.00	31.20	30.00
NAM10	H-47	40.70	47.30	32.00	39.70	40.20
NAT11	H-51	43.00	57.30	38.00	47.70	45.30
NAM12	H-50	30.80	48.00	35.30	41.70	36.20
NAM13	H-53	51.30	55.30	42.00	48.70	50.00
NAT14	H-43	25.20	39.30	22.30	30.80	28.00
NAT15	H-35	31.30	40.00	36.00	38.00	34.70
NAM16	H-33	49.00	56.70	40.00	48.30	48.70
NAT17	H-40	39.80	54.00	37.70	45.80	42.80
NAT18	H-37	41.50	54.70	34.70	44.70	43.10

APPENDIX C

EXPERIMENTAL SLED TEST RESULTS

Figures C.1 through C.5 show the 6 G experimental time traces for head angular acceleration, head angular velocity, head angular position, head resultant acceleration, and T_1 resultant acceleration for the five NAMRL subjects used in the simulations of Chapter 3. The dashed line in each figure is the average of the five curves and corresponds to the solid line shown in the simulation comparisons of Chapters 4 and 5. Figures C.6 through C.10 show similar experimental curves for 15 G sled tests.

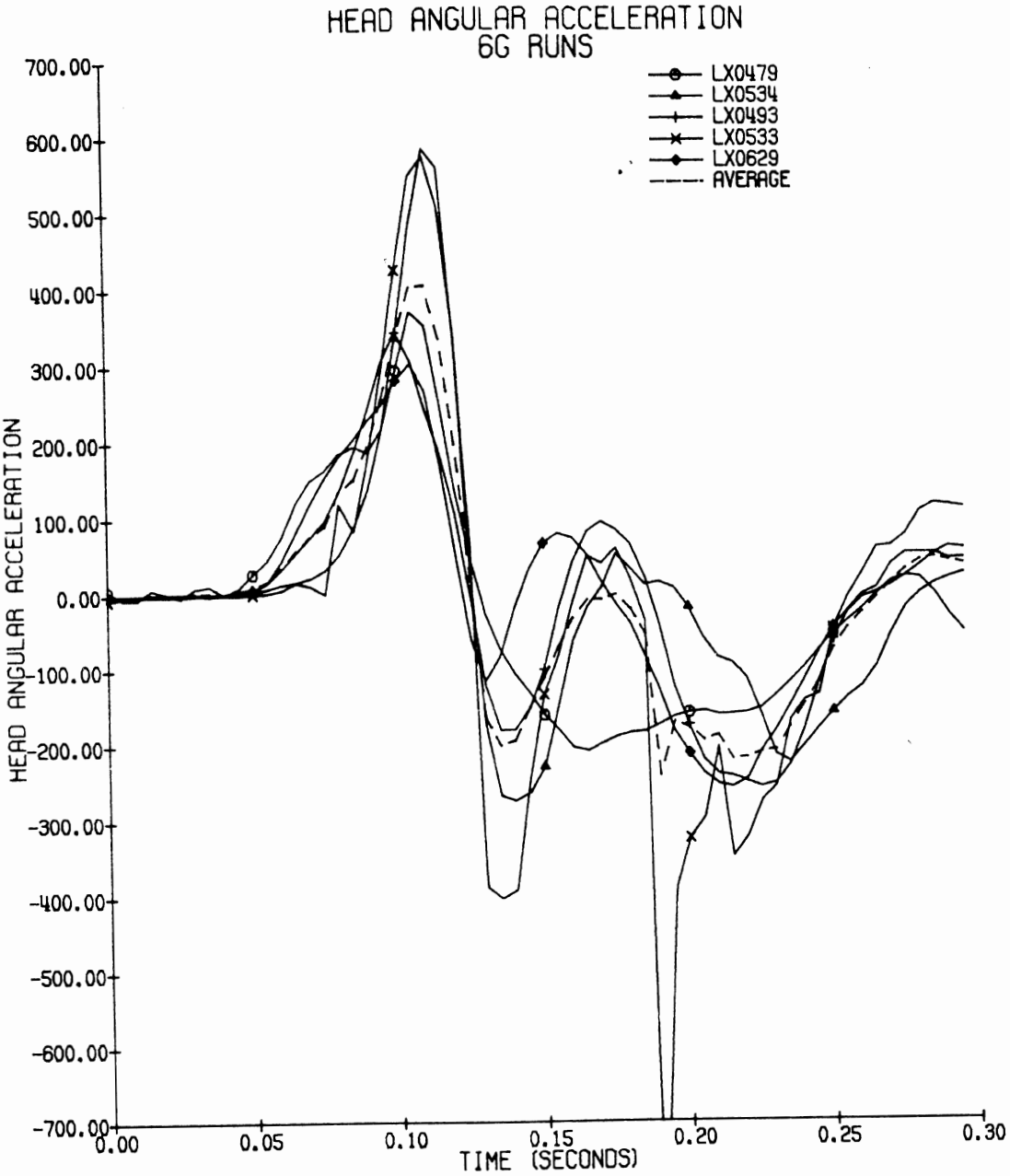

Figure C.1 6 G Experimental Head Angular Acceleration Curves for Five NAMRL Subjects. Dashed Line is Average Curve.

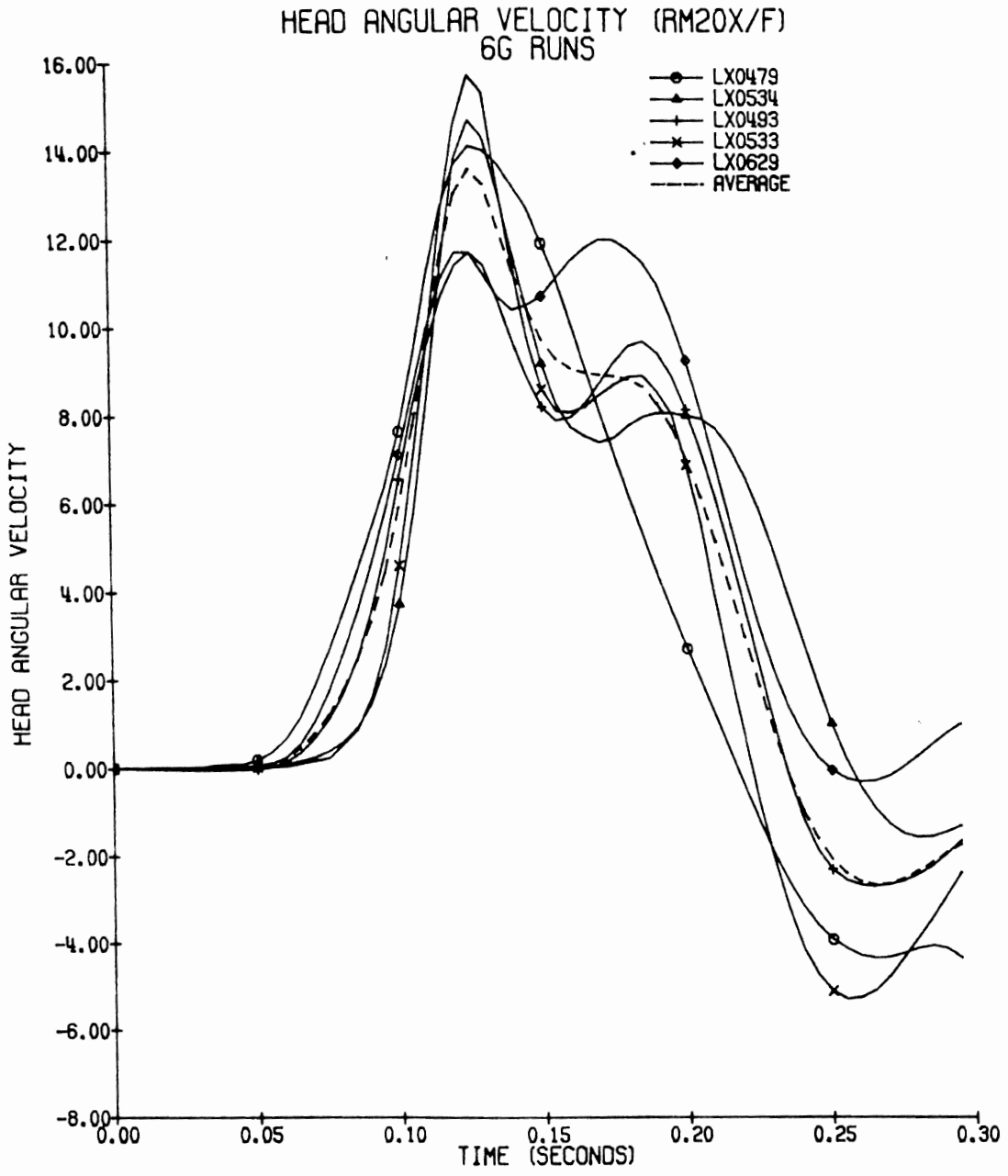

Figure C.2 6 G Experimental Head Angular Velocity Curves for Five NAMRL Subjects. Dashed Line is Average Curve.

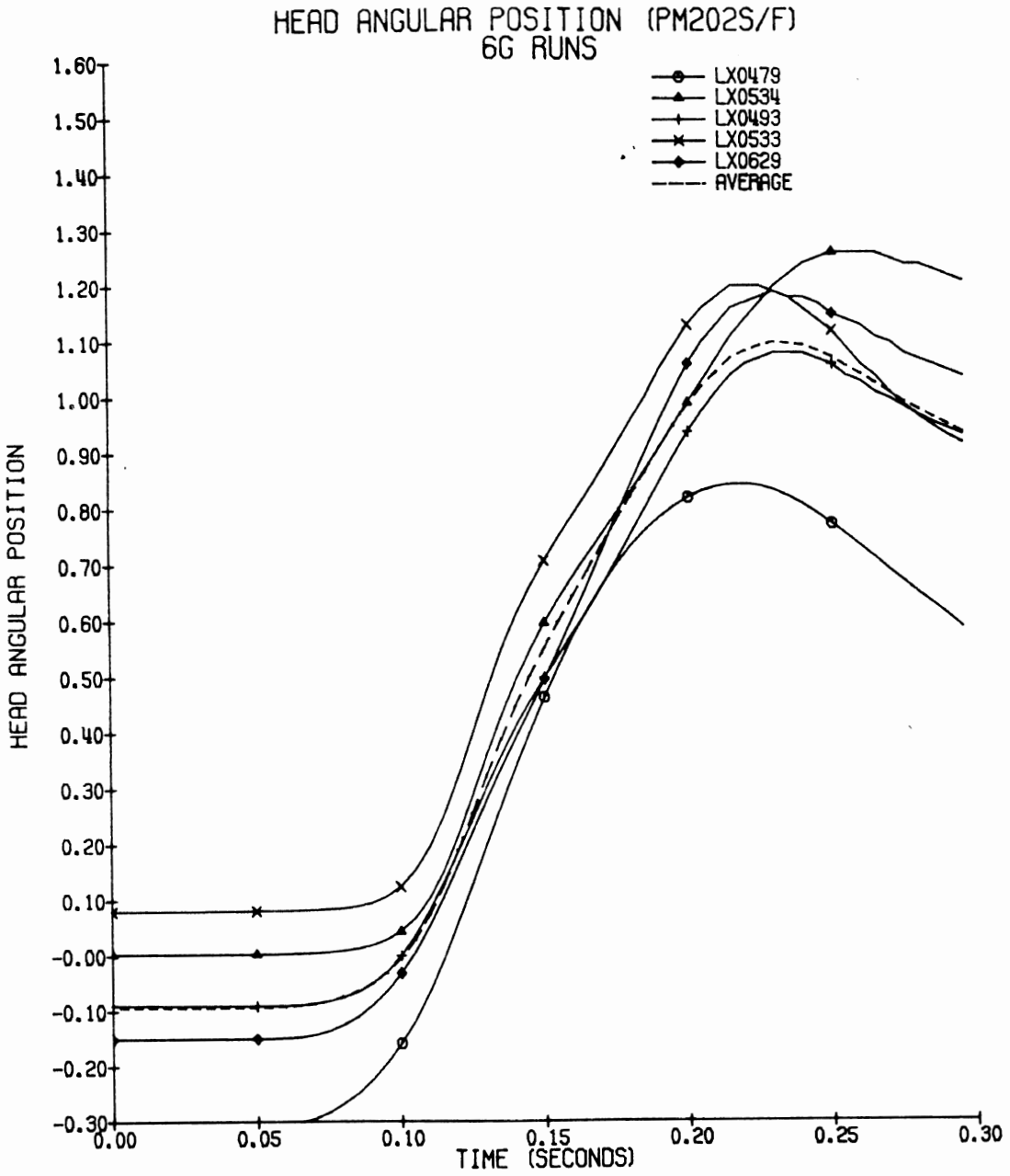

Figure C.3 6 G Experimental Head Angular Position Curves for Five NAMRL Subjects. Dashed Line is Average Curve.

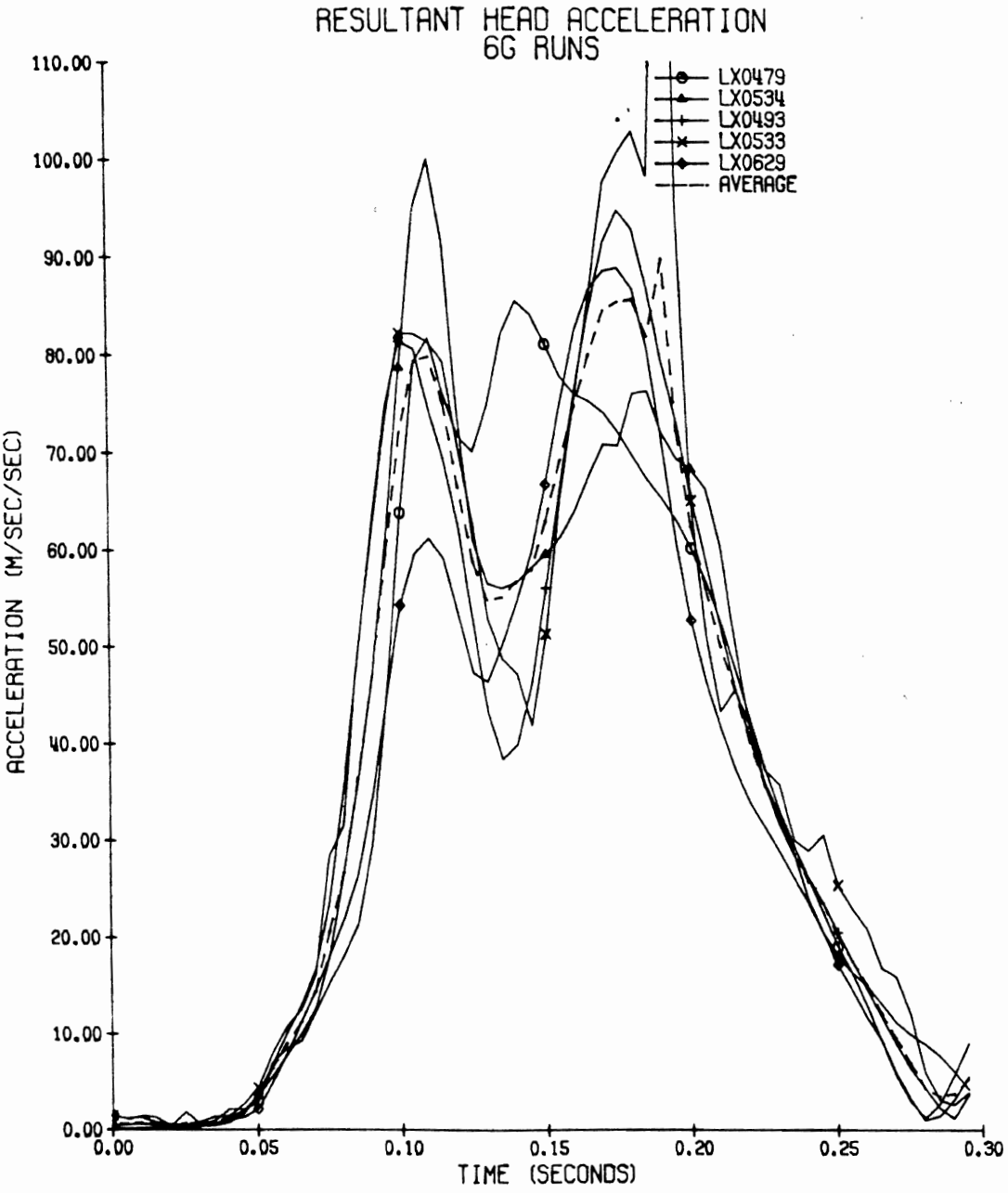

Figure C.4 6 G Experimental Head Resultant Acceleration Curves for Five NAMRL Subjects. Dashed Line is Average Curve.

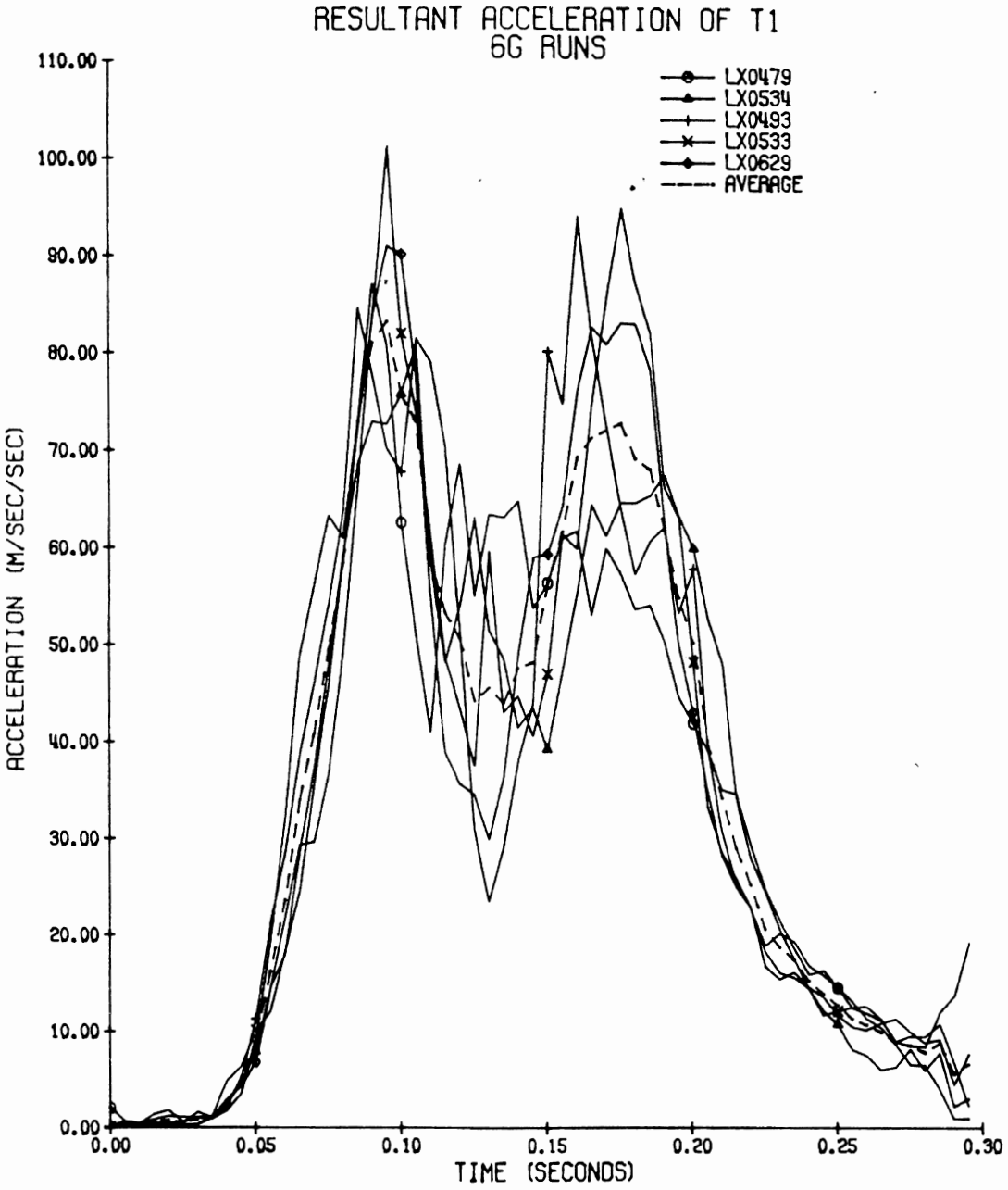

Figure C.5 6 G Experimental T_1 Resultant Acceleration Curves for Five NAMRL Subjects. Dashed Line is Average Curve.

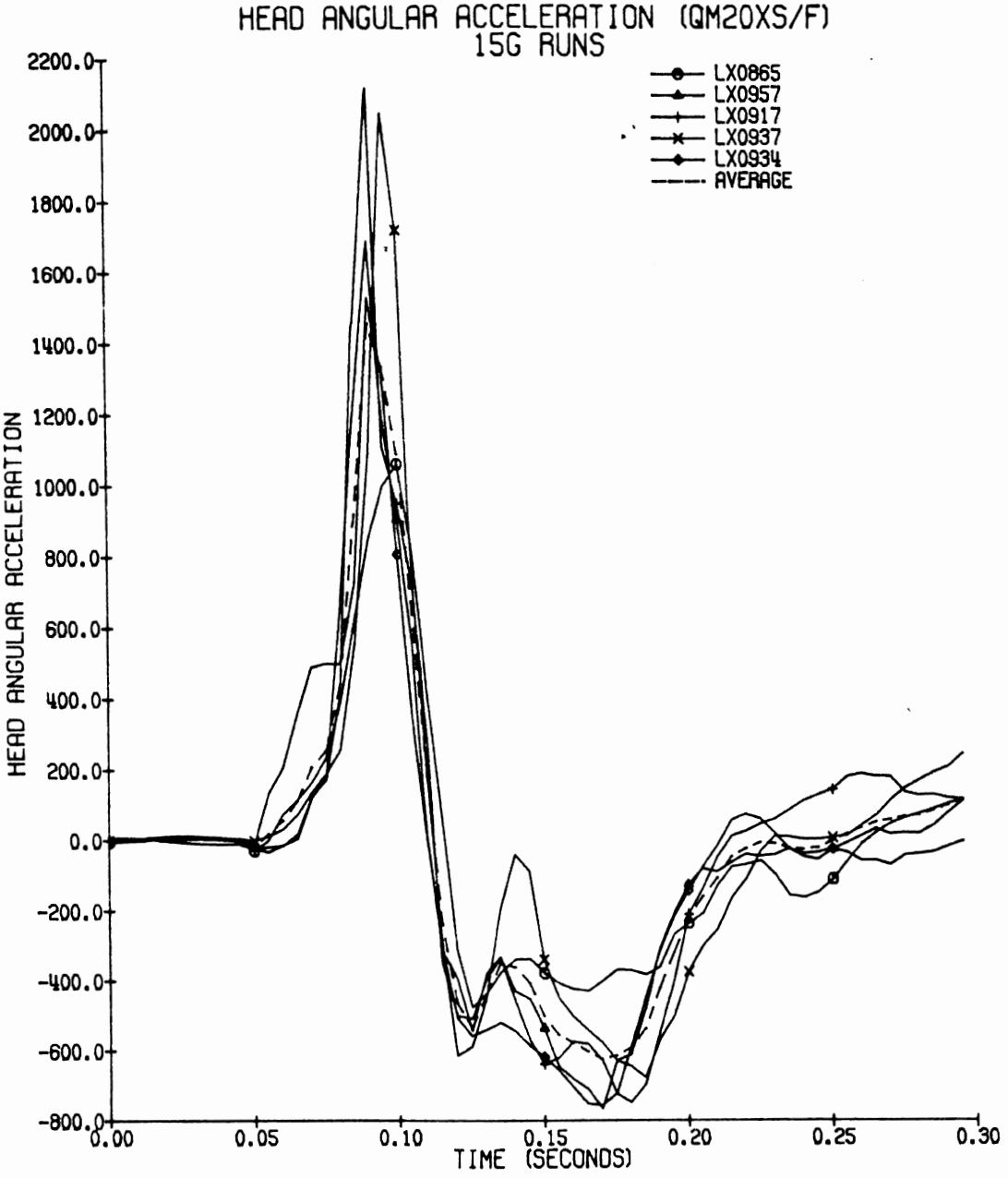

Figure C.6 15 G Experimental Head Angular Acceleration Curves for Five NAMRL Subjects. Dashed Line is Average Curve.

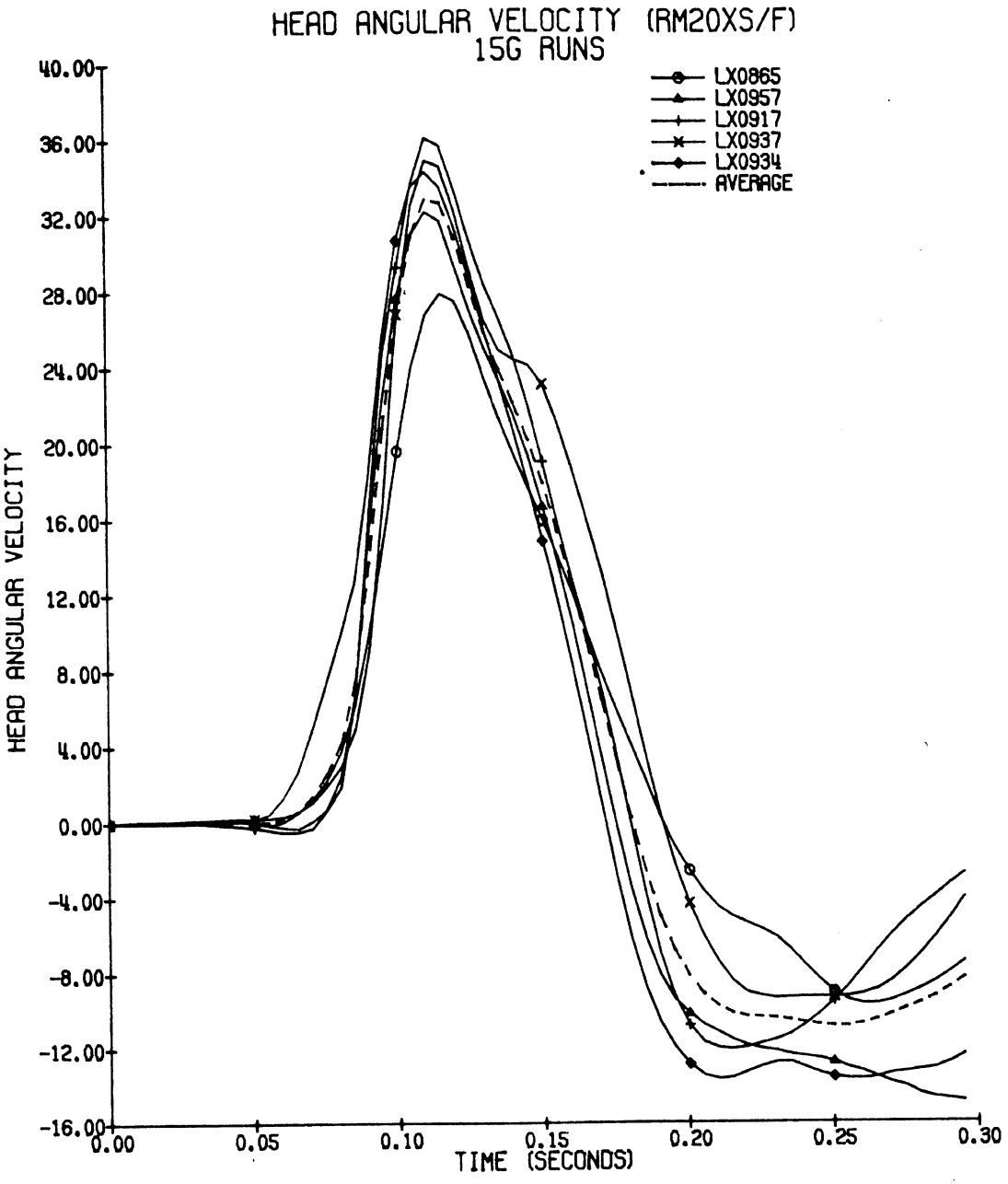

Figure C.7 15 G Experimental Head Angular Velocity Curves for Five NAMRL Subjects. Dashed Line is Average Curve.

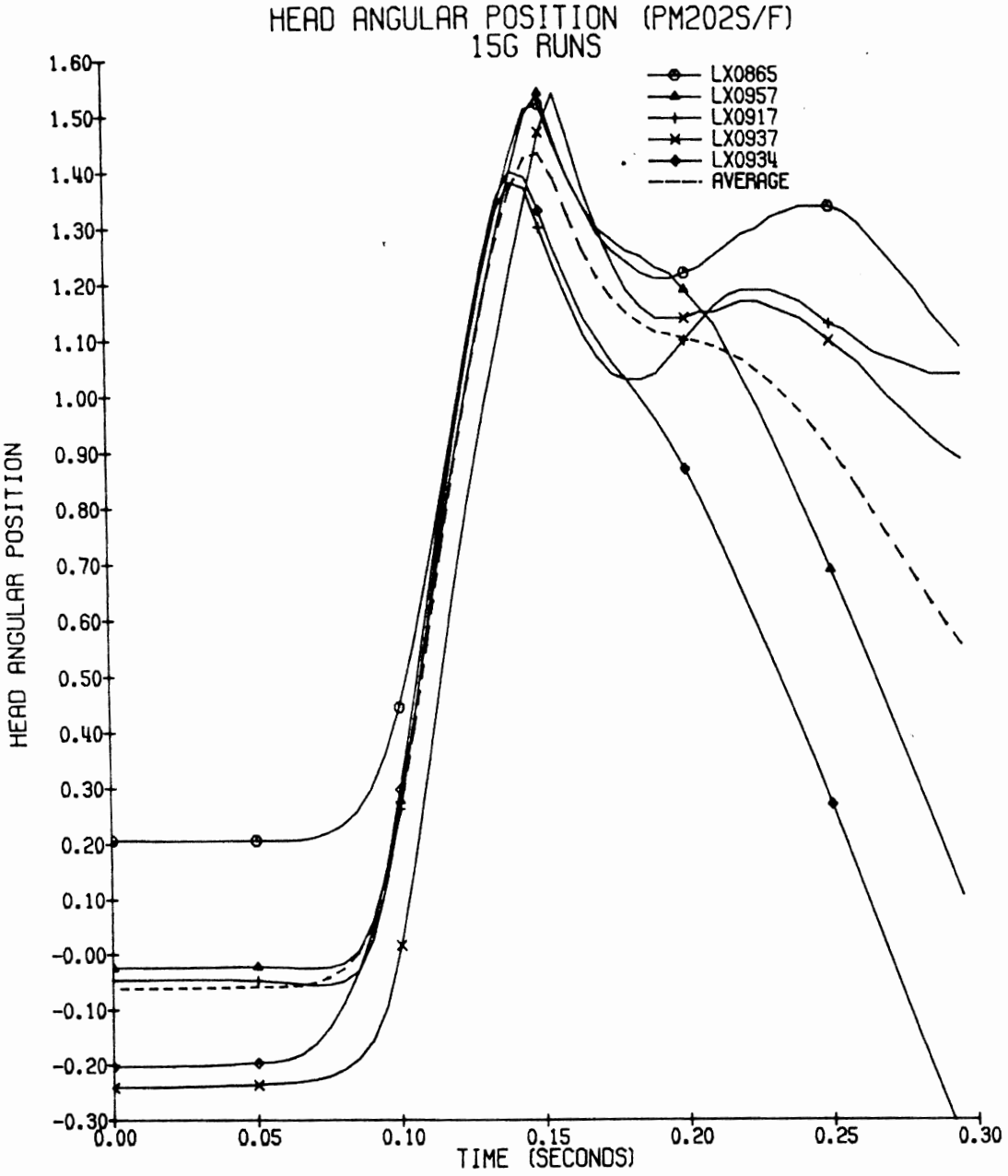

Figure C.8 15 G Experimental Head Angular Position Curves for Five NAMRL Subjects. Dashed Line is Average Curve.

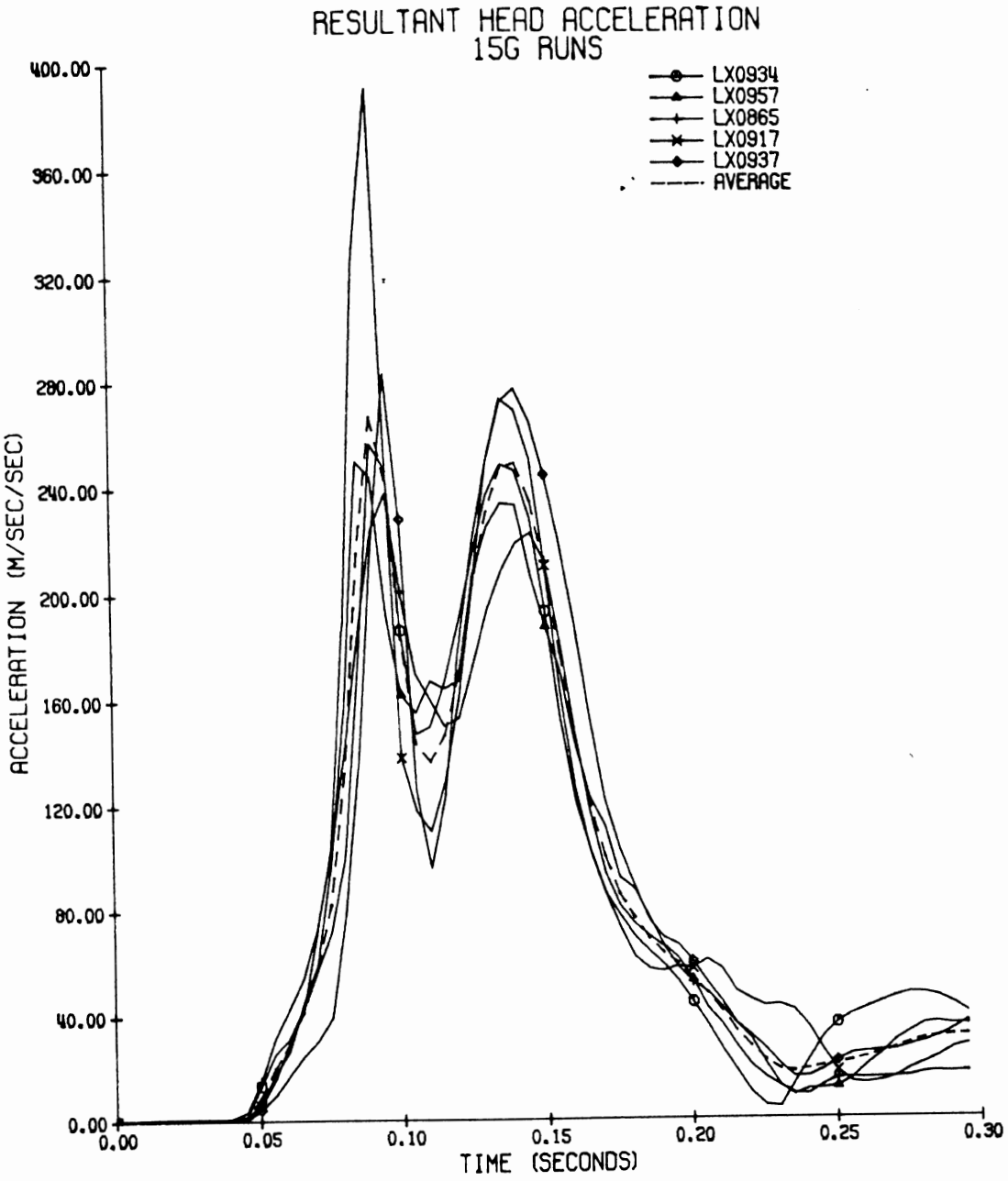

Figure C.9 15 G Experimental Head Resultant Acceleration Curves for Five NAMRL Subjects. Dashed Line is Average Curve.

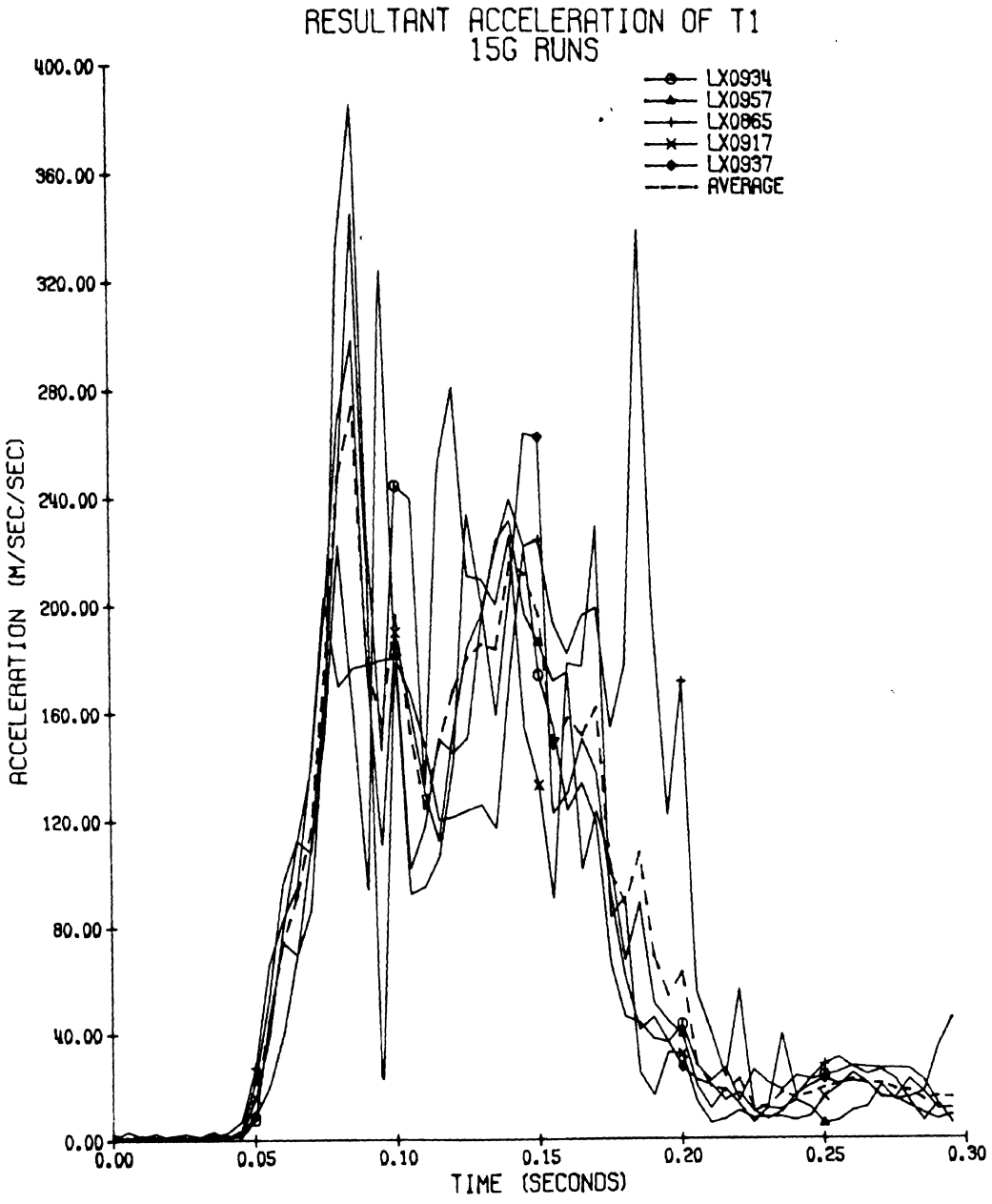

Figure C.10 15 G Experimental T_1 Resultant Acceleration Curves for Five NAMRL Subjects. Dashed Line is Average Curve.